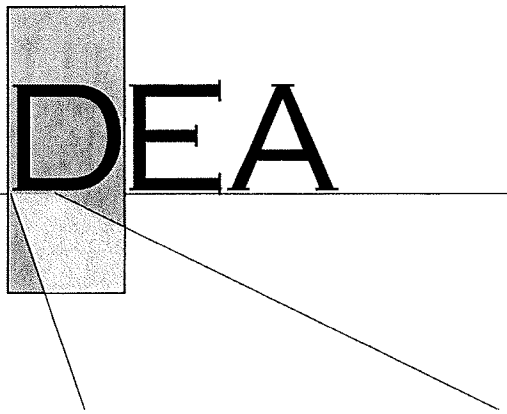

Innovations Deserving
Exploratory Analysis Programs

Highway Program

Advanced Concept Concrete Using Basalt Fiber/BF Composite Rebar Reinforcement

Final Report for Highway-IDEA Project 86

Vladimir B. Brik,
Research & Technology Corp., Madison, WI

February 2003

TRANSPORTATION RESEARCH BOARD • THE NATIONAL ACADEMIES

INNOVATIONS DESERVING EXPLORATORY ANALYSIS (IDEA) PROGRAMS
MANAGED BY THE TRANSPORTATION RESEARCH BOARD (TRB)

This NCHRP-IDEA investigation was completed as part of the National Cooperative Highway Research Program (NCHRP). The NCHRP-IDEA program is one of the four IDEA programs managed by the Transportation Research Board (TRB) to foster innovations in highway and intermodal surface transportation systems. The other three IDEA program areas are Transit-IDEA, which focuses on products and results for transit practice, in support of the Transit Cooperative Research Program (TCRP), Safety-IDEA, which focuses on motor carrier safety practice, in support of the Federal Motor Carrier Safety Administration and Federal Railroad Administration, and High Speed Rail-IDEA (HSR), which focuses on products and results for high speed rail practice, in support of the Federal Railroad Administration. The four IDEA program areas are integrated to promote the development and testing of nontraditional and innovative concepts, methods, and technologies for surface transportation systems.

For information on the IDEA Program contact IDEA Program, Transportation Research Board, 500 5th Street, N.W., Washington, D.C. 20001 (phone: 202/334-1461, fax: 202/334-3471, http://www.nationalacademies.org/trb/idea)

CONTENTS

Title Page i

Contents ii

List of Tables iv

List of Figures iv

List of Photos v

Executive Summary 1

1.0 Introduction. 2

2.0 Significance 3

3.0 Objectives 3

4. Task Description 4

4.1 Research Task 1 4

To study the bond strength between basalt rebars and cables, and concrete by conducting bond tests according to ASTM C 234.

4.1.1 Mechanism. 5

4.1.2 Specimen Preparation 5

4.1.3 Bond Test 6

4.1.4 Materials 7

4.1.5 Mix Proportions 7

4.1.6 Mixing Procedure. 7

4.1.7 Specimens 7

4.1.8 Test Results and Discussions 8

4.2 Research Task 2 9

To determine the cracking load and ultimate load of two extremely under-reinforced beams, and to determine the modes of failure of the basalt rebar reinforced concrete beams.

4.2.1 Specimens. 9

4.2.2 Mix Proportions 9
4.2.3 Basalt Bar Reinforced Concrete Beams 9

4.3 Research Task 3 11

To determine the cracking load and ultimate load of five under-reinforced beams, and to determine the mode of failure of the basalt rebar reinforced concrete beams.

4.3.1 Specimens. 11
4.3.2 Mix Proportions 11
4.3.3 Basalt Bar Reinforced Concrete Beams 12

5.0 Conclusions 14

6.0 References 15

Appendix – A

Details of Reinforcement Position and Testing Arrangement for all the Beams. . A1

Appendix – B

Photographs B1

Appendix – C

Preparation and characteristics of smart alloy barriers/anchors C1

LIST OF TABLES

Table 1: Details of Basalt Rods Used for Reinforcing Concrete Beams . . . 16

Table 2: Comparison of Calculated and Ultimate Moments. 17

LIST OF FIGURES

Figure 1: Bond stress Vs. slip for the plain basalt rebar in the lower horizontal position 18

Figure 2: Bond stress Vs. slip for the plain basalt rebar in the upper horizontal position. 18

Figure 3: Bond stress Vs. slip for the 4 – slot basalt rebar in the lower horizontal position. 19

Figure 4: Bond stress Vs. slip for the 4 – slot basalt rebar in the upper horizontal position. 19

Figure 5: Bond stress Vs. slip for the 8 – slot basalt rebar in the lower horizontal position. 20

Figure 6: Bond stress Vs. slip for the 8 – slot basalt rebar in the upper horizontal position. 20

Figure 7: Bond stress Vs. slip for the control mix specimen with the steel reinforcement in the lower horizontal position. 21

Figure 8: Bond stress Vs. slip for the control mix specimen with the steel reinforcement in the upper horizontal position. 21

Figure 9: Load Vs. Deflection Graph for Basalt Beam (BRC-1) 22

Figure 10: Load Vs. Concrete Strain for Basalt Beam (BRC-1) 22

Figure 11: Load Vs. Deflection Graph for Basalt Beam (BRC-2) 23

Figure 12: Load Vs. Concrete Strain for Basalt Beam (BRC-2) 23

Figure 13: Load Vs. Basalt Rebar Strain for Basalt Beam (BRC-2) 24

Figure 14: Load Vs. Deflection Graph for Basalt Beam (BRC-3) 24

Figure 15: Load Vs. Concrete Strain for Basalt Beam (BRC-3) 25

Figure 16: Load Vs. Basalt Rebar Strain for Basalt Beam (BRC-3) 25
Figure 17: Load Vs. Deflection Graph for Basalt Beam (BRC-4) 26
Figure 18: Load Vs. Concrete Strain for Basalt Beam (BRC-4) 26
Figure 19: Load Vs. Deflection Graph for Basalt Beam (BRC-5) 27
Figure 20: Load Vs. Concrete Strain for Basalt Beam (BRC-5) 27
Figure 21: Load Vs. Deflection Graph for Basalt Beam (BRC-6) 28
Figure 22: Load Vs. Concrete Strain for Basalt Beam (BRC-6) 28
Figure 23: Load Vs. Basalt Rebar Strain for Basalt Beam (BRC-6) 29
Figure 24: Load Vs. Deflection Graph for Basalt Beam (BRC-7) 29
Figure 25: Load Vs. Concrete Strain for Basalt Beam (BRC-7) 30
Figure 26: Load Vs. Basalt Rebar Strain for Basalt Beam (BRC-7) 30

Appendix C

Figure C1: Procedure of fixing of barrier made from Ti-Ni smart alloy . . C3
Figure C2: Procedure of cryofitting of two tubes utilizing washer made from shape memory alloy. C4

LIST OF SKETCHES

Sketch 1: Details of reinforcement position and testing arrangement (BRC–1). . A2
Sketch 2: Details of reinforcement position and testing arrangement (BRC–2). . A2
Sketch 3: Details of reinforcement position and testing arrangement (BRC–3). . A3
Sketch 4: Details of reinforcement position and testing arrangement (BRC–4). . A3
Sketch 5: Details of reinforcement position and testing arrangement (BRC–5). . A4
Sketch 6: Details of reinforcement position and testing arrangement (BRC–6). . A4
Sketch 7: Details of reinforcement position and testing arrangement (BRC–7). . A5

LIST OF PHOTOGRAPHS

Photo 1-6: Bond Test Photographs . . . . . B2 – B4
Photo 7-56: Flexure Test Photographs B5– B29

Executive Summary

This report presents the results of an experimental investigation that was carried out to evaluate the performance characteristics of modified basalt rebar reinforced concrete beams. The modified basalt rebars were supplied by Research and Technology Corporation, Madison.

The primary objective of this investigation was to determine the strength of the bond between the modified basalt rebars and concrete, and to compare the experimentally determined ultimate moment capacity of basalt rebar reinforced concrete beams, and their calculated ultimate moment capacities according to ACI-318 Building Code recommended design procedures.

Bond tests according to ASTM C 234 procedure were performed on modified basalt rebars (4 slot and 8 slot) and plain basalt rebars. Bond tests were also done on single, double and triple cables. The double and triple cables were obtained by twisting together two and three single cables respectively. The results indicated that all the modified basalt rebars and cables, had considerably higher bond strength than the plain basalt rebars. The plain basalt rebars without slots failed due to the pull-out of the basalt rebars. The basalt rebars with slots, and the cables were not pulled out, they failed due to the fracture of basalt rebars in tension.

A total of seven beams reinforced with modified basalt rebars were tested. All the seven beams were designed and cast in the Rama Materials Laboratory of South Dakota School of Mines & Technology. Deflections were measured with the help of LVDT's. Strains in the concrete and basalt rods were measured using electrical resistant strain gauges, and the readings were recorded using MEGADAC data acquisition system. The ultimate moments were much higher than the first crack moments, indicating good bond between the rebar and concrete. The beams had considerable cracking and large deflections before ultimate failure. Most of the beams failed primarily in flexure followed in shear failure. Some beams had typical flexural failure. Beams with modified basalt rebars (with slots, corrugations, and smart alloy anchors) had adequate load carrying capacity and their actual ultimate moment capacities exceeded the calculated moment values. All the modified basalt rebars tested had adequate bonding capacity with concrete and therefore they could be effectively used as reinforcement in concrete structures.

1. Introduction

Basalt fibers are manufactured in a single-stage process by melting pure raw material. They are environmentally safe and non-toxic, possess high heat stability and insulating characteristics and have an elastic structure. When used for composite materials, they provide unique mechanical properties. They can be easily processed into fabric with high reliability [1].

The tensile strength of continuous basalt fibers is about twice that of E-glass fibers and the modulus of elasticity is about 15-30% higher. Basalt fibers in an amorphous state exhibit higher chemical stability than glass fibers. When exposed to water at 70° C (158° F), basalt fibers maintain their strength for 1200 hours, whereas the glass fibers do so only for 200 hours [1].

The innovative aspect of this project is the detailed study of non-corrosive, basalt fiber composite rebar. This rebar consists of 80% fibers and has a tensile strength three times that of the steel rebar normally used in building construction. It is made by utilizing a resin (epoxy) binder [1]. Basalt fiber composite rebars have the potential to replace steel in reinforced concrete structures exposed to salt water, ocean climate, etc. wherever the corrosion problem exists. This advantage alone could warrant a sufficient argument for substitution of the basalt rebar on a large scale. Other advantages of the basalt rebar are that its weight is one-third of the weight of steel and the thermal expansion coefficient is very close to that of concrete. The high mechanical performance/price ratio of basalt fiber composite rebar, combined with corrosion resistance to alkaline attack are further reasons, for replacing steel in concrete by basalt fiber composite rebars. There is no published information available on the behavior of the basalt fiber composite rebar and therefore there is a need for this research.

The Basalt fibers have been used in Russia for some time and these fibers were investigated for their usefulness in various Civil Engineering applications in the United States. To achieve this objective, an investigation was carried out to evaluate the performance of the 3-D basalt fiber reinforced concrete and basalt fiber composite rebars under the IDEA Program of the Transportation Research Board (Contract No. NCHRP – 45, 1998) [1]. This project was conducted at South Dakota School of Mines & Technology in collaboration with Research and Technology Corporation (RTC), Madison, WI.

It was found from the investigation that the basalt bars had three times higher tensile strength compared to the steel bars. However, the bond between the bar and the concrete had to be increased to increase the load carrying capacity of the beams. To achieve this goal, a research proposal was submitted to the IDEA program of the Transportation Research Board and the project was funded. This project investigated the modified basalt rebar's (Supplied by RTC) ability to address the bond problem encountered in the earlier project.

2. Significance

One of the major problems the construction industry faces to day is corrosion of reinforcing steel, which significantly affects the life and durability of concrete structures. Basalt rebars can effectively counter this problem because they are immune for corrosion, have high tensile strength, low young's modulus, have light weight and do not conduct electricity. Currently there are many FRP rebar companies that market their products. Most of them are made of E-glass fiber and thermosetting resin. But these bars lack sufficient durability under extreme environments. The material costs of these bars are also costly, and are also not resistant to alkalis [2-3]. But basalt rebars do not possess these disadvantages and can be effectively used in various applications such as highway barriers, offshore structures and bridge decks.

3. Objectives

This investigation was undertaken to evaluate the performance of concrete beams reinforced with the modified basalt fiber composite rebars. The following were the objectives of the research.

- To determine the ultimate failing load.
- To study the load-deflection behavior.
- To observe the bond strength.
- To measure the strain in the concrete.
- To measure the strain in the basalt rebar
- To study the mode of the failure.
- To compare the calculated and actual cracking and ultimate moments.

4. Task Description

4.1 Research Task 1: To study the bond between basalt rebars and cables, and concrete by conducting bond tests according to ASTM C 234.

The earlier research [1] conducted by the investigators had revealed that the actual ultimate moments of the basalt rebar reinforced concrete beams were less than the theoretically calculated ultimate moments. This was due to the slip of the rebars in concrete during the bending test. To avoid this type of failure the Principal Investigators had developed basalt cables with corrugations, rods with slots, barriers and anchors, for improving the bond strength of the bars with the concrete. The primary task in this project was to study the bond between the basalt rebars and the concrete.

The tensile strength development of reinforced concrete depends on the compatibility of the two materials to act "together" in resisting the external load. The transfer of force across the interface between concrete and basalt reinforcing bars is called bond force. Bond stress is normally expressed as stress per unit area of bar surface.

Basalt rebar is used as reinforcing element in this experiment in order to utilize its higher tensile strength. The bond strength is controlled by the following major factors:

- Adhesion between the concrete and the reinforcing element (basalt rebar)
- Gripping effect resulting from the drying shrinkage of the surrounding concrete and the shear interlock between the bar deformations and the surrounding concrete
- Frictional resistance to sliding and interlock as the reinforcing element is subjected to tensile stress
- Effect of concrete quality and strength in tension and compression
- Mechanical anchorage effect of the ends of bars through splicing, hooks and cross bars and
- Diameter, shape, and spacing of reinforcement as they affect crack development.

There are several tests that can determine the bond quality of reinforcing element. One of these is the pullout test (See figure below). In this test, the concrete is subjected to compression and the reinforcing bar is subjected to tension, and both the bar and the surrounding concrete are subjected to the same stress.

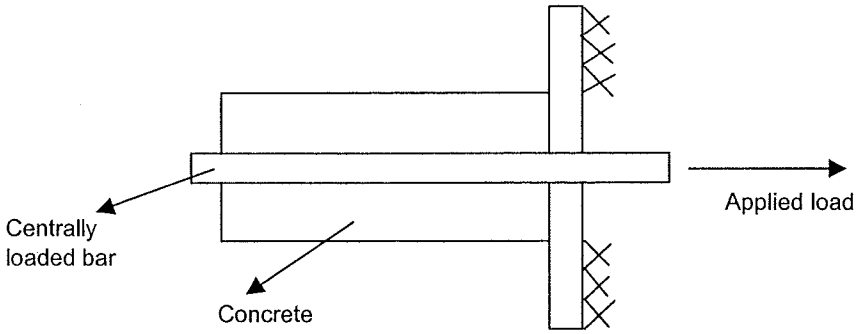

Pullout Test

4.1.1 Mechanism: The mechanism of bond consists of three main components: chemical adhesion, friction and mechanical interlock between bar deformations and concrete. Initially, for very small values of bond stress of upto 1.38 MPa (200 psi), chemical adhesion is the main resisting mechanism. Adhesion is partly microscopic interlock of paste into imperfections of the basalt rod surfaces. While the adhesion is active, no real slip occurs, and the observed slip is comprised of local deformations adjacent to the basalt surface.

The other two mechanisms, friction and rib support, go into action when adhesion fails. At this time, significant slip may be observed, as well as the formation and growth of cracks. In order to avoid permanent deformations and possible internal cracking radiating out from the ribs or slots, ASTM C234 [4] has designated the maximum slip level as 0.254 mm (0.01 inch).

4.1.2 *Specimen Preparation:* The horizontally reinforced specimen was made by placing the concrete in four layers of approximately equal thickness and rodded 25 times with the tamping rod. The horizontally embedded bar specimens, when they were between 7 and 14 days old, were broken in half in flexure to form two 152.4 mm (6-in.) cubes. To do this, the specimen was set up as a simple beam with center-point loading in accordance with ASTM C 293 [5] with two triangular grooves in the upper and lower faces of the beam at midspan. The load was applied to a 19 mm (3/4-in.) diameter bar laid in the upper groove and continued until fracture occurred, as shown in the figure below. During the operation, care was taken not to strike or disturb the reinforcing bars.

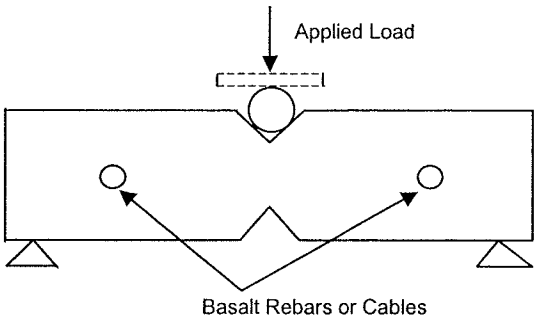

Breaking of the Horizontal Specimen

4.1.3 Bond Test: The procedure used for the bond test was according to ASTM C 234 [4], two dial gages were provided for measuring the movement of the reinforcing bar with respect to the concrete at the loaded end of the bar (Photo 1, Appendix B). The dial gages used in the test were graduated in 0.0025 mm (0.0001-in). units; a range of atleast 6.35 mm (0.25 in.) was provided. The major steps were as follows:

- The specimen was mounted in the testing machine so that the surface of the cube from which the long end of the bar project was in contact with the two bearing blocks. The projecting reinforcing bar extended through the bearing blocks, cross bar, and the support, and was gripped for tension by the jaw of the testing machine. Then the lower square yoke was fixed on the concrete cube by the screws. Two dial gages were fixed on opposite sides of the yoke, and adjusted to touch the cross bar with certain amount of movement shown in the dial gages.
- The load was applied to the reinforcing bar at a rate not greater than 22 KN/min (5000 lbf/min), or at the no-load speed of the testing machine head of not greater than 1.27 mm/min (0.05 in./min).
- The applied load and the two-dial gage readings were recorded at a sufficient number of intervals throughout the test to provide at least 15 readings by the time a slip of 0.254 mm (0.01 in.) had occurred at the load end of the bar. The dial gage readings were recorded to an estimated 0.1 of the least division of the dial.
- The loading and readings at appropriate intervals were continued until the yield point of reinforcing bar had been reached or the enclosing concrete had split, or a slippage of at least2.5mm (0.10 in.) had occurred at the loaded end.

During the bond tests, the operation of applying the load and reading and recording the two dial gages was performed by a crew of three; the machine operator, two people to read the dial gages and record the readings. The machine operator called "read" as the first 222.5 N (50 lbf) of load was applied and at each 4.45 KN (1000 lbf) increment of load was applied. On this signal the other two people observed the respective readings and recorded the values.

4.1.4 Materials: The materials consisted of ASTM Type I cement and was produced by the South Dakota Cement Plant. Coarse aggregate used was crushed limestone. The coarse aggregate had a maximum size of 19 mm (0.75 in). The fine aggregate used was natural sand. Both fine and coarse aggregates satisfied ASTM aggregate requirements. The Basalt rebars were provided by Research and Technology Corporation.

4.1.5 Mix Proportions: The basic mixture proportions used in casting the bond specimens were as follows:

Cement	388.4 kg/m^3 (655 lbs./cu.yd).
Coarse Aggregate	1022.9 kg/m^3 (1725 lbs./cu.yd).
Fine Aggregate (Sand)	652.3 kg/m^3 (1100 lbs./cu.yd).
Water	155.4 kg/m^3 (262 lbs./cu.yd).
Water/Cement ratio	0.40

4.1.6 Mixing Procedure: All mixings were done in a nine cubic feet capacity mixer. First the buffer mix was done. Then coarse aggregates were put in the mixer. Then the sand and two thirds of the water were added and mixed for one minute. Cement was then added along with the remaining one third of the water. The ingredients were mixed for three minutes, which was followed by a three-minute rest period and a final mixing was done for 2 minutes so that the concrete is uniformly mixed. Immediately after mixing, the slump and the air content of the freshly mixed concrete were determined. Seven different batches were made in 3 different days during the month of November 2001.

4.1.7 Specimens: One horizontal bar specimen was cast from each mix. The specimens for horizontally embedded bars consisted of concrete prisms 152.4mm x 152.4mm x 304.8mm (6 in. x 6 in. x 12 in.) with the longer axes vertical. Two bars were embedded in each specimen,

perpendicular to the long axis and parallel to and equidistant from the vertical sides of the prism. In the vertical direction, one bar was located with its axis 76.2 mm (3 in.) from the bottom of the prism, and the other with its axis 228.6 mm (9 in.) from the bottom. A triangular groove was formed in each of the two opposite sides of the prism parallel to the axes of the bars and at the midheight of the prism. They were used for facilitating the breaking of the prism into two test specimens at this weakened plane prior to conducting the bond test.

4.1.8 Test Results and Discussions: First the plain basalt rebar reinforced specimens were tested for the bond strength at an age of 21 days. As the load was applied the plain basalt rebars started slipping and there was no bond between the reinforcement and the concrete (Photo 2-3, Appendix B). It was also found out that the grip of the testing machine was slipping i.e., it was not holding the bar properly as the basalt fibers in the bar were crushed and powdered. There was also a slip in the anchoring end leaving a scratch mark on the bar. Therefore, the anchorage was done using a chuck, which held the specimen in its place at the anchoring end. The specimen was then tested and the plain basalt bar slipped and the marks of concrete were distinctly seen on the bar.

Then the 4-slot basalt bar was tested with both the lower and upper horizontal position of the reinforcement. The 4-slot basalt bar did not slip and hence there was no bond failure. But the basalt bar itself failed due to tension failure. The failure was brittle. The basalt fibers at the failed end can be seen clearly in the photographs shown (Photo 4-5, Appendix B). The 8-slot basalt bar also failed in a similar manner to that of 4-slot basalt bar (Photo 6, Appendix B).

The 2mm (0.08 in.) cables were also tested for the bond strength. At first a single cable was tested for the bond strength. The single cable failed in tension and there was no bond failure. The failure of the cable was brittle in nature. Similarly two cables were twisted together and were also tested for bond. The results were similar to that of the single cable test. The cables failed due to tension and not due to lack of bond. When three cables twisted together were tested, the failure mode was the same as described above for the single and two cables.

The graphs of bond stress vs. slip were plotted for all the specimens reinforced with different types of basalt bars for both the lower and the upper horizontal positions of the basalt

rebars (Figs. 1 to 6). Bond test was also done with steel rebars and graphs were also drawn for comparison purpose (Figs. 7 and 8).

All the basalt reinforced bars and cables except the plain basalt bar had good bond with concrete. The failure was due to the tensile failure of the rebars and the cables and not due to bond slip.

4.2 Research Task 2: To determine the cracking load and ultimate load of two extremely under-reinforced beams, and to determine the modes of failure of the basalt rebar reinforced concrete beams.

4.2.1 Specimens: Two beams (152.4 x 228.6 x 1117.6 mm [6 x 9 x 44 in.], and 228.6 x 457.2 x 1320.8 mm [9 x 18 x 52 in.]) reinforced with basalt rebars were tested. Research & Technology Inc supplied the rebars. The beams were designed and cast in the lab, and are referred to as BRC-1 and BRC-2.

4.2.2 Mix Proportions: The mixture proportions used for the concrete were as follows:

Cement	388.4 kg/m^3 (655 lbs./cu.yd.)
Coarse Aggregate	1022.9 kg/m^3 (1725 lbs./cu.yd.)
Fine Aggregate (Sand)	652.3 kg/m^3 (1100 lbs./cu.yd.)
Water	182.6 kg/m^3 (308 lbs./cu.yd.)
Water/Cement ratio	0.47

The slump of the mix was 146 mm (5.75 in.) and the air content was 1.2%. The average cylinder compressive strength of the mix was 47 MPa (6816 psi).

4.2.3 Basalt Bar Reinforced Concrete Beams
(Designed and cast in the Lab)

The reinforcement details of the beams BRC-1 and 2 are given in Table 1 and the testing arrangements are given in Appendix A. The basic engineering principles generally applied to the design of steel reinforced concrete can also be applied to design of FRP reinforced concrete. Stress equilibrium of the cross section, strain compatibility between reinforcement and concrete, kirchoff's hypothesis (plain sections remain plane), and Whitney's rectangular stress block (for approximating concrete stress distribution) are the principles that can be applied to FRP rebar

reinforced concrete [6-8]. Strain compatibility was assumed which required that there is good bond between the FRP rebar and concrete. These assumptions will be proven correct if the theoretical values of the ultimate moment and experimental moment match.

Two extremely under reinforced beams were tested to see whether adequate bond was developed between the rebar and concrete. The reinforcement provided for one beam was less than the minimum required according to ACI code 318. Another beam was provided with the ACI recommended minimum reinforcement. For both beams deflections were measured with the help of LVDT's. Strain readings were measured using electrical resistance strain gauges. Both strain and deflection readings were recorded by a data acquisition system (MEGADAC). Both beams were tested in flexure after the 28-day curing period. A development length of 203.2 mm (8 in.) was provided for both beams. The length between the two-point loading was 304.8 mm (12 inch). Beam BRC-1 was reinforced with basalt cables (3.25 mm [0.128 in. dia.]). Strain gauge was placed on the compression side of the beam for measuring the concrete strain. Since the rebars used for BRC-1, had more corrugations on the surface, the strain gauge could not be placed on the rod. The first crack occurred at the calculated cracking moment (Table 2). After first crack, the beam failed suddenly breaking into two pieces, because the beam was extremely under reinforced (Photos 21-22, Appendix B). The rebar broke without slipping, which indicated that there was good bond between the rebar and the concrete. The load vs. deflection and the load vs. concrete strain are shown in Figs. 9 and10 respectively.

Beam BRC-2 was under reinforced with the minimum ACI 318 recommended reinforcement. A strain gauge was placed on the compression side of the beam, and one strain gauge was placed on the 4-slot rebar (slot dia: 10.4 mm [0.41 in.]) in the tension side. The beam first had a flexural crack at 85% of the calculated cracking moment (Table 2), but ultimately the beam failed in shear (Photos 17-19, Appendix B). This was attributed to the fact that the beam was very deep. Even though the beam failed in shear, it took 88% of the calculated ultimate moment (Table 2). The beam did not fail due to slip of the rebar, which indicated that there was a good bond between the 4-slot rebar and the concrete. If the beam had failed in flexure rather than in shear the beam would have definitely carried more ultimate moment than the calculated moment. The load vs. deflection, load vs. concrete strain and basalt rebar strain are shown in

Figs. 11 to 13 respectively. The overall test results indicated that there was sufficient bond strength and the bars did not slip even after the ultimate load was reached. The measured and calculated ultimate and cracking moments are compared in Table 2. The photographs (Photos 7-22) of the test set-up and the tested beams are shown in Appendix B.

The tests indicated that it is possible to make concrete beams reinforced with basalt composite rebars. This testing gave adequate information to plan for testing other beams.

4.3 Research Task 3: To determine the cracking load and ultimate load of five under-reinforced beams, and to determine the mode of failure of the basalt rebar reinforced concrete beams

4.3.1 Specimens: A total of five beams of dimensions, 127 x 203.2 x 1346.2 mm (5 x 8 x 53 in.), 127 x 203.2 x 1625.6 mm (5 x 8 x 64 in.), 76.2 x 101.6 x 1143 mm (3x 4 x 45 in.), 152.4 x 254 x 1320.8 mm (6x 10 x 52 in.) [Fe-Mn-Ni anchors], and 152.4 x 254 x 1320.8 mm (6x 10 x 52 in) [Ti-Ni anchors], reinforced with basalt rebars were tested. Research & Technology Corp supplied the rebars and the five beams were designed and cast in the Rama materials laboratory of SDSM&T. The beams are referred to as BRC-3 to BRC-7 in the discussion. The reinforcement details of the beams BRC-3 to 7 are given in Table 1 and their testing arrangements are given in Appendix A. The main aim of the experiment was to determine the experimental cracking and ultimate moments and compare them with the calculated values. All the beams were designed as under-reinforced beams with the normal range used in construction.

4.3.2 Mix Proportions: The basic mixture proportions used are given below:

Cement	308.4 kg/m^3 (520 lbs./cu.yd.)
Coarse Aggregate	907.3 kg/m^3 (1530 lbs./cu.yd.)
Fine Aggregate (Sand)	907.3 kg/m^3 (1530 lbs./cu.yd.)
Water	179 kg/m^3 (302 lbs./cu.yd.)
Water/Cement ratio	0.58

The slump of the concrete was 88.9 mm (3.5 in.) and the air content was 2.0%. The average cylinder compressive strength of the concrete was 34.2 MPa (4959 psi). When each beam was cast, three cylinders were made along with it, to determine the respective compressive strength. This was necessary because the beams were cast on different days and eventhough the mix proportions were the same, the respective cylinder compressive strengths might be slightly different due to the temperature and humidity variations during casting. The modulus of rupture values for the beams were calculated from the compressive strength using ACI 318 formula.

4.3.3 Basalt Bar Reinforced Concrete Beams

(Designed and cast in the Lab)

The deflections for all beams were measured with the help of LVDT's. Strain readings were obtained using electrical resistance strain gauges. Both strain and deflection readings were recorded by a data acquisition system (MEGADAC). All beams were tested in flexure after a 28-day curing period. A development length of 203.2 mm (8 in.) was provided for all beams. The span between the two-point loading was 152.4 mm (6 in.) for all beams.

Beam BRC-3 was designed as a lightly under reinforced beam with one corrugated basalt rod 8.6 mm (0.34 in. dia) (Photo 23, Appendix B). Strain gauge was placed on the compression side of the beam for measuring the strain in the concrete. Strain gauge was also placed on the rod (tension side of the beam) to determine the strain in the rebar. The first crack occurred at 95% of the calculated cracking moment (Table 2). After first crack the beam took **2.7 times more** moment than the cracking moment (Table 2) indicating a very good bond strength between the rebar and the concrete. The beam failed at 98% of the calculated ultimate moment (Table 2). The load vs. deflection, the load vs. concrete strain and basalt rebar strain are shown in Figs. 14 to 16 respectively. The beam failed primarily in flexure and secondarily in shear (Photos 24-30, Appendix B).

Beam BRC-4 was also under reinforced. Two cables of 1524 mm (60 in.) length and 8 mm (0.315 in.) diameter were used as rebars (Photos 31-32, Appendix B). These cables were made in the laboratory by twisting three individual basalt wires into one. A strain gauge was placed on the compression side of the beam. A strain gauge could not be placed on the rebar,

because of the corrugations formed due to twisting the wires. The beam first had a flexural crack at 76% of the calculated cracking moment (Table 2). After first crack the beam took **4.9 times more** moment than the cracking moment (Table 2) indicating a very good bond strength between the rebar and the concrete. The beam failed at 97% of the calculated ultimate moment (Table 2). The beam failed purely in flexure (Photos 33-36, Appendix B). Overall the performance of the beam was good and the wires were split partially at failure indicating good bond strength. The cables did not slip even after the ultimate load was reached. The load vs. deflection and the loads vs. concrete strain are shown in Figs. 17-18 respectively.

Beam BRC-5 was made of three basalt cables of 1041.4 mm (41 in.) length and 3.45 mm (0.136 in.) diameter (Table 1). The beam was under-reinforced. The cables were supplied by the manufacturer (Photo 37, Appendix B), unlike the one used in beam BRC-4 that was made in the laboratory. A strain gauge was placed on the compression side of the beam, and the strain gauge could not be fixed on the rebar, because of the corrugations formed due to twisting the wires. The beam first had a flexural crack at 95% of the calculated cracking moment (Table 2). After the first crack the beam took **2.4 times more** moment (less than the other beams because it was under-reinforced, and the tensile strength of the bar was also less) than the cracking moment (Table 2) indicating a very good bond strength between the rebar and the concrete. The beam took **49% more** than the calculated ultimate moment (Table 2). The beam failed primarily in flexure and secondarily in shear (Photos 38-40, Appendix B). Overall the performance of the beam was good and the cables completely fractured at failure (Photos 41-42, Appendix B), indicating a good bond strength. The cables did not slip even after the ultimate load was reached. The load vs. deflection and the loads vs. concrete strain are shown in Figs. 19-20 respectively.

Beam BRC-6 was made with two basalt rods of 1219.2 mm (48 in.) length and 9.65 mm (0.38 in.) diameter (Table 1). The beam was lightly under-reinforced. The rods were supplied by the manufacturer and were provided with 1 Fe-Mn-Ni anchors (smart alloys) on each end of the bar to prevent slip (Photos 43,45, Appendix B). A strain gauge was placed on the compression side of the beam, and another strain gauge was also placed on the rebar on the slot to measure the strain in the rebar (Photo 44, Appendix B). The first flexural crack occurred at **4.5% more** than the calculated cracking moment (Table 2). After first crack the beam took **5.1 times more**

moment than the cracking moment (Table 2) indicating a very good bond strength between the rebar and the concrete. The beam took **12% more** than the calculated ultimate moment (Table 2). The beam failed primarily in flexure and secondarily in shear (Photos 46-50, Appendix B). Overall the performance of the beam was very good and the rods did not slip even at failure because of the anchors provided at the ends. The load vs. deflection, the loads vs. concrete strain, and the load vs. basalt rebar strain are shown in Figs. 21-23 respectively.

Beam BRC-7 was made with two basalt rods of 1219.2 mm (48 in.) length and 10.1 mm (0.399 in.) diameter (Table 1). The beam was lightly under-reinforced. The rods were supplied by the manufacturer and were provided with 2 Ti-Ni (50/50) anchors (smart alloys) on each end of the bar (Photo 51, Appendix B) to prevent slip. A strain gauge was placed on the compression side of the beam, and another strain gauge was also placed on the rebar in the slot to measure the strain in the rebar. The first flexural crack occurred at **7.3% more** than the calculated cracking moment (Table 2). After the first crack the beam took **5.9 times more** moment than the cracking moment (Table 2) indicating a very good bond strength between the rebar and the concrete. The beam took **21% more** than the calculated ultimate moment (Table 2). Of all the beams, this beam performed very well basically because of the anchors and the slots that were provided on the rebar. The beam failed primarily in flexure and secondarily in shear (Photos 52-56, Appendix B). Overall the performance of the beam was very good because of the anchors at the ends. The rods did not slip even after the ultimate load was reached. The load vs. deflection, the loads vs. concrete strain and the load vs. basalt rebar strain are shown in Figs. 24-26 respectively.

5. Conclusions

- The bond between all the modified basalt rebars and concrete was extremely good.
- The experimental ultimate moment was much higher than the first crack moment in all the beams tested, indicating a good bond between rebar and concrete.
- The deflections were considerable indicating adequate ductility.
- All the beams had primary flexural failures and a few beams had secondary shear failures.
- There was no slip of the rebars in any of the beams tested and there was no evidence of bond failure between the concrete and the modified basalt rebars and twisted cables.
- In general, the basalt rebars are suitable for use in reinforced concrete structures.

6. References

1. Vladimir Brik, V. Ramakrishnan and Neeraj Tolmare, "Performance Evaluation of 3-D Basalt Fiber Reinforced Concrete & Basalt Rod Reinforced Concrete", IDEA Program Final Report, Contract No. NCHRP-45, November 1998.
2. Ramakrishnan, V., " Recent Advancements in Concrete Fiber Composites", Concrete Lecture- 1993, American Concrete Institute, Singapore Chapter, Singapore.
3. Ramakrishnan, V., " Performance characteristics and Application of High-Performance Polyolefin Fiber Reinforced Concretes", SP-171, Proceedings of the third CANMET/ACI. International conference 'Advances in Concrete Technology', American Concrete Institute, Detroit, 1997, pp. 671-692.
4. ASTM C234-91a, "Standard Test Method for Comparing Concretes on the Basis of the Bond Developed with Reinforcing Steel", American Society of Testing of Materials, 1998.
5. ASTM C 293-94, "Standard Test Method for Flexural Strength of Concrete (Using Simple Beam With Center-Point Loading)", American Society of Testing of Materials, 1998.
6. ACI Committee 440, "Guide for the Design and Construction of Concrete Reinforced with FRP Bars", ACI Report 440.1R-01 American Concrete Institute, Detroit, 2001, pp. 1-41.
7. ACI Committee 440, "State-of-the-Art Report on Fiber Reinforced Plastic Reinforcement for Concrete Structures", ACI Report 440 R-96 American Concrete Institute, Detroit, 1996, pp. 1-65.
8. ACI Committee 318, "Building Code Requirements for Structural Concrete and Commentary", ACI 318 R-99 American Concrete Institute, Detroit, 2000, pp. 1-65.

Table 1: Details of Basalt Rods Used for Reinforcing the Concrete Beams

Beam No.	Size of Beam mm (Inches)	No. of Bars	Description of bars
BRC-1	152.4 x 228.6 x 1117.6 mm (6 x 9 x 44 in.)	2	Two basalt cables of 1016 mm (40 in.) length and 3.25 mm (0.128 in.) in diameter. Two basalt wires were sprirally wound to form a cable and were supplied by the manufacturer.
BRC-2	228.6 x 457.2 x 1320.8 mm (9 x 18 x 52 in.)	2	Two basalt rods of 1219 mm (48 in.) length and 10.4 mm (0.41 in.) in diameter. Each rebar was provided with 4 slots for improving the bond.
BRC-3	127 x 203.2 x 1346.2 mm (5 x 8 x 53 in.)	1	One basalt rod of 1245 mm (49 in.) length and 8.6 mm (0.34 in.) diameter. The basalt rod had a corrugated surface. This ribbed or corrugated surface was obtained by pultrusion.
BRC-4	127 x 203.2 x 1625.6 mm (5 x 8 x 64 in.)	2	Two cables of 1524 mm (60 in.) length and 8 mm (0.315 in.) diameter. Each cable was made by twisting three individual basalt wires of 4.8 mm (0.19 in.) in diameter, in the laboratory.
BRC-5	76.2 x 101.6 x 1143 mm (3 x 4 x 45 in.)	3	Three basalt cables of 1041 mm (41 in.) length and 3.45 mm (0.136 in.) in diameter. Two basalt wires were spirally wound to form a cable and were supplied by the manufacturer.
BRC-6	152.4 x 254 x 1320.8 mm (6 x 10 x 52 in.)	2	Two basalt rods of 1219 mm (48 in.) length and 9.65 mm (0.38 in.) in diameter. Each rebar was provided with 2 slots for improving the bond. The rods were also provided with 1 Fe-Mn-Ni anchors (smart alloys) on each end of the bar to prevent slip.
BRC-7	152.4 x 254 x 1320.8 mm (6 x 10 x 52 in.)	2	Two basalt rods of 1245 mm (49 in.) length and 10.1 mm (0.399 in.) in diameter. Each rebar was provided with 2 slots for improving the bond. The rods were also provided with 2 TiNi (50/50) anchors (smart alloys) on each end of the bar to prevent slip.

Table 2: Comparison of Calculated and Actual Moments

Beam No.	Actual Moments		Calculated Moments		Type of Failure
	Ultimate N-m (lb-in)	Cracking N-m (lb-in.)	Ultimate N-m (lb-in.)	Cracking N-m (lb-in.)	
BRC-1	5038 (44588)	4992 (44180)	4997 (44218)	4997 (44218)	Flexural failure. Beam failed by splitting into two pieces due to the complete fracture of the rebars.
BRC-2	63457 (561570)	23691 (209658)	72340 (640179)	28116 (248815)	First flexural cracking followed by failure in shear.
BRC-3	8407 (74400)	3107 (27497)	8619 (76273)	3260 (28852)	Primary flexural failure and secondary shear failure.
BRC-4	12577 (111300)	2551 (22575)	12983 (114895)	3376 (29879)	Typical flexural failure with partial fracture of strands
BRC-5	1137 (10063)	481 (4261)	765 (6772)	505 (4471)	Beam failed primarily in flexure by splitting into two pieces after fracture of rebar
BRC-6	33184 (293663)	6475 (57300)	29685 (262701)	6199 (54855)	Primary flexural failure and secondary shear failure.
BRC-7	38724 (342690)	6610 (58500)	32047 (283605)	6160 (54513)	Primary flexural failure and secondary shear failure.

Note: In all the beams, the rebars did not slip or pull out, and there was no bond failure.

Conversion Factor:
25.4mm = 1in.
1 in-lb = 0.113 Nm

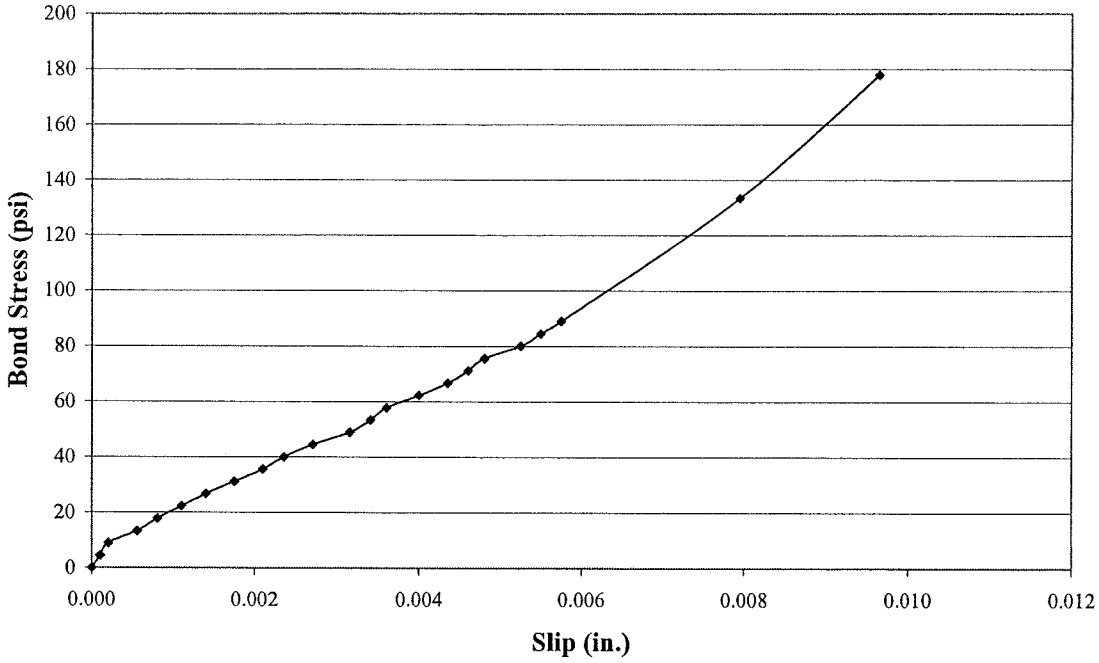

Fig. 1: Bond stress Vs. slip for the plain basalt rebar in the lower horizontal position.

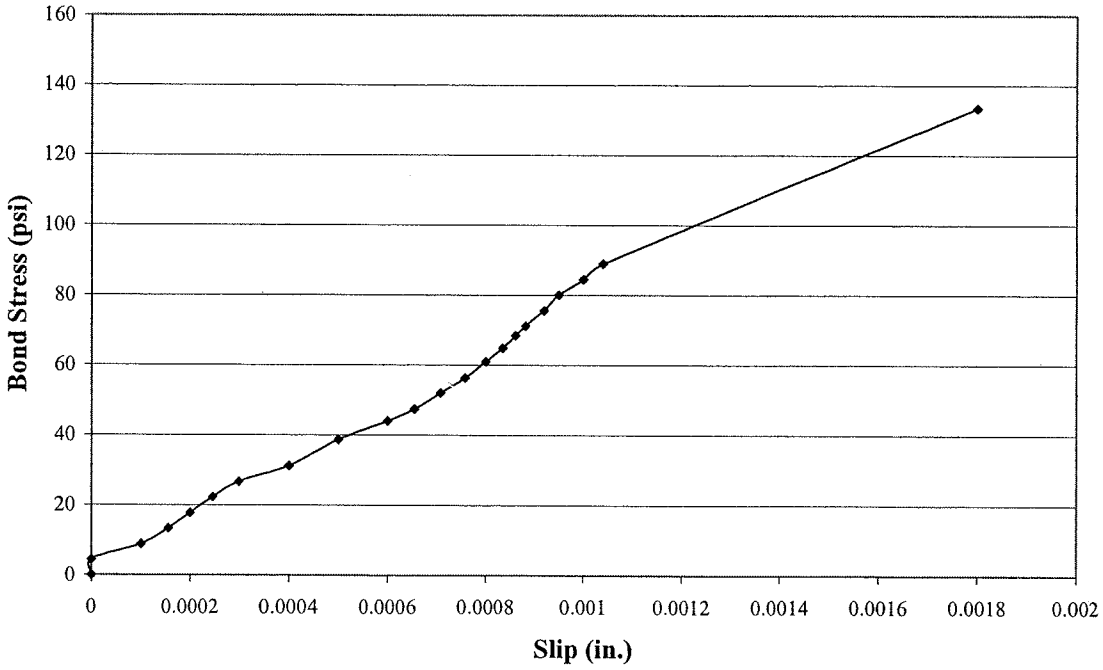

Fig. 2: Bond stress Vs. slip for the plain basalt rebar in the upper horizontal position.

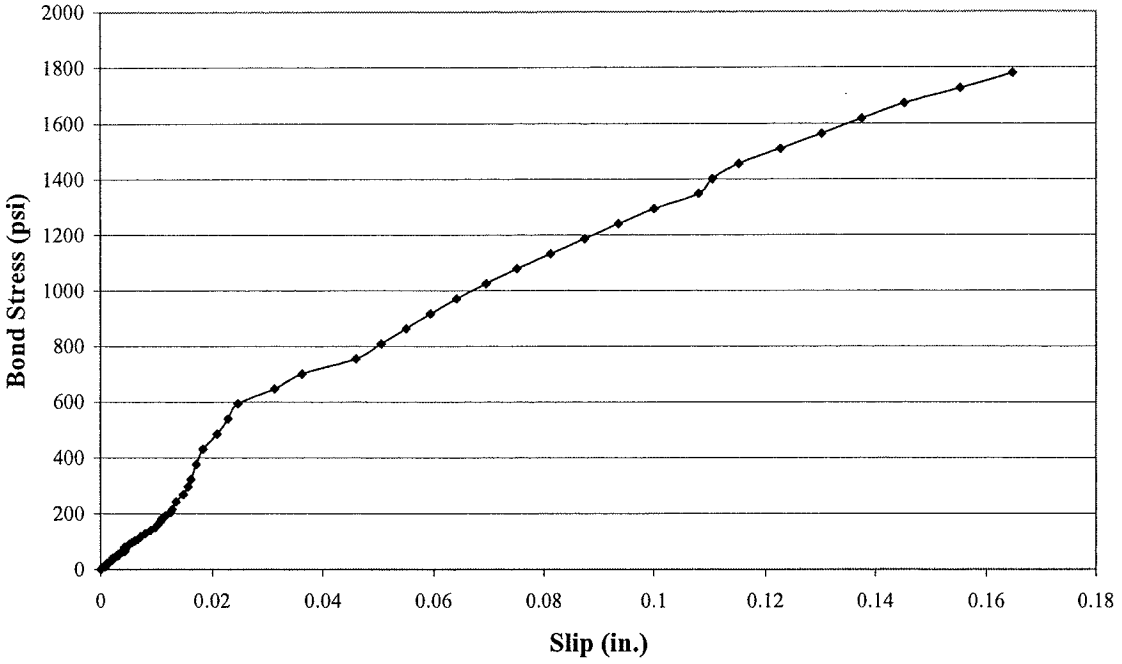

Fig. 3: Bond stress Vs. slip for the 4 - slot basalt rebar in the lower horizontal position.

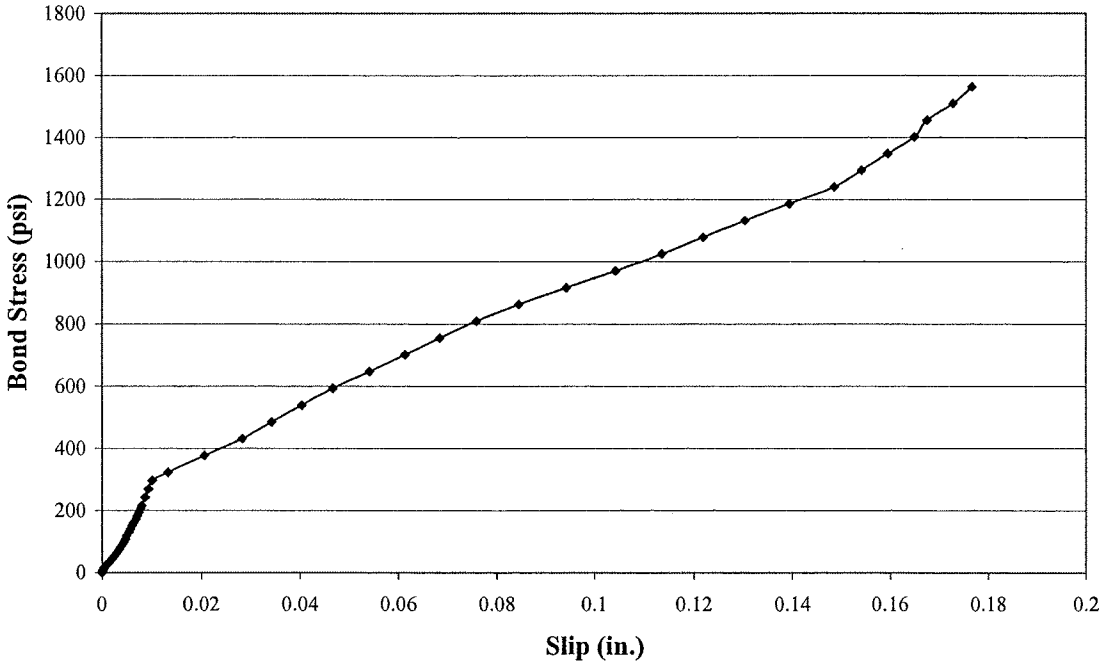

Fig. 4: Bond stress Vs. slip for the 4 - slot basalt rebar in the upper horizontal position.

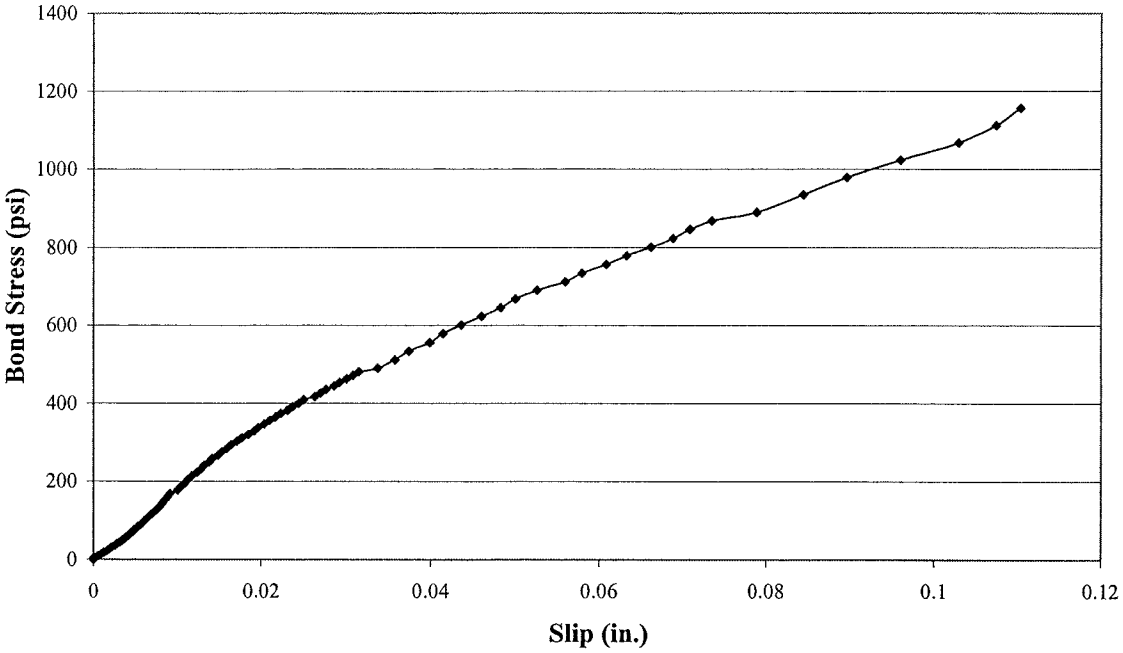

Fig. 5: Bond stress Vs. slip for the 8 - slot basalt rebar in the lower horizontal position.

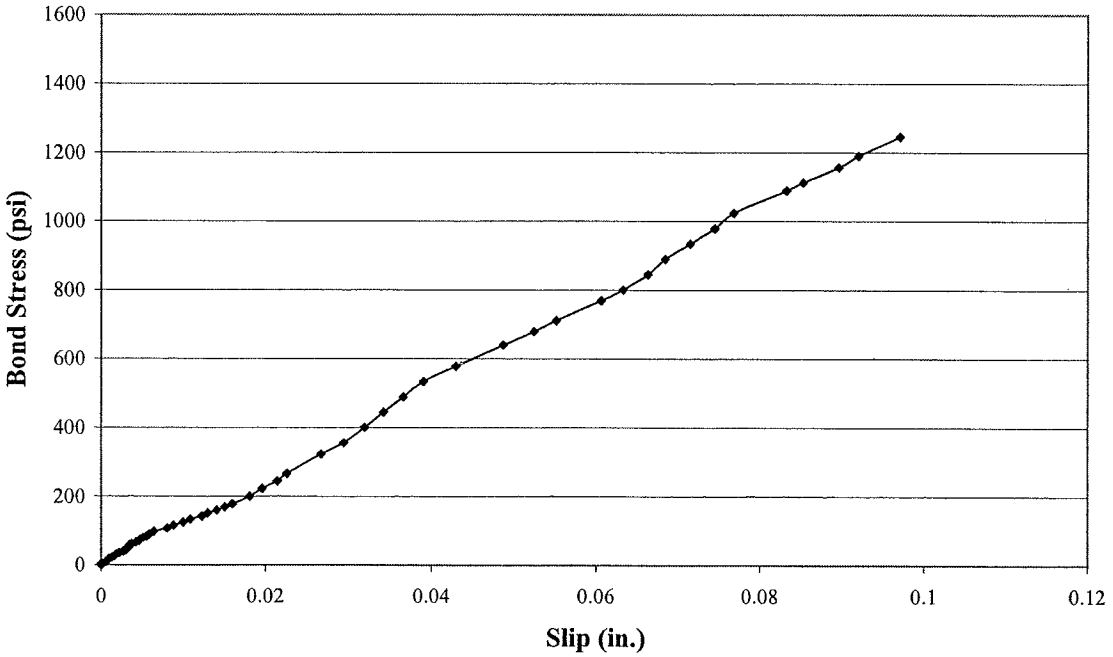

Fig. 6: Bond stress Vs. slip for the 8 - slot basalt rebar in the upper horizontal position.

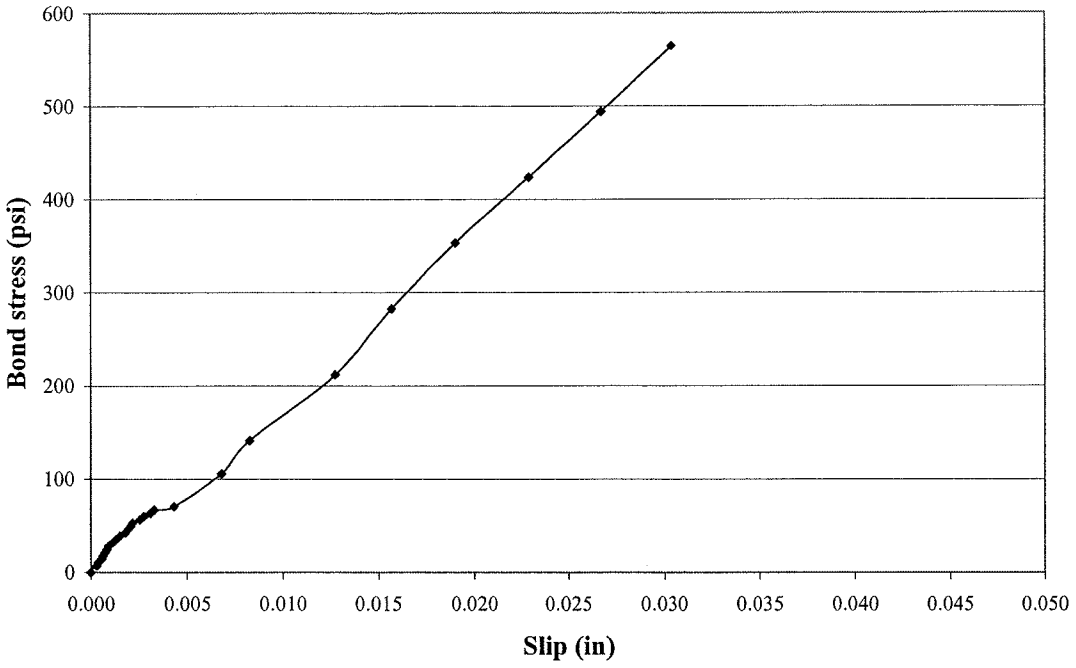

Fig. 7: Bond stress Vs. slip for the control mix specimen with the steel reinforcement in the lower horizontal position.

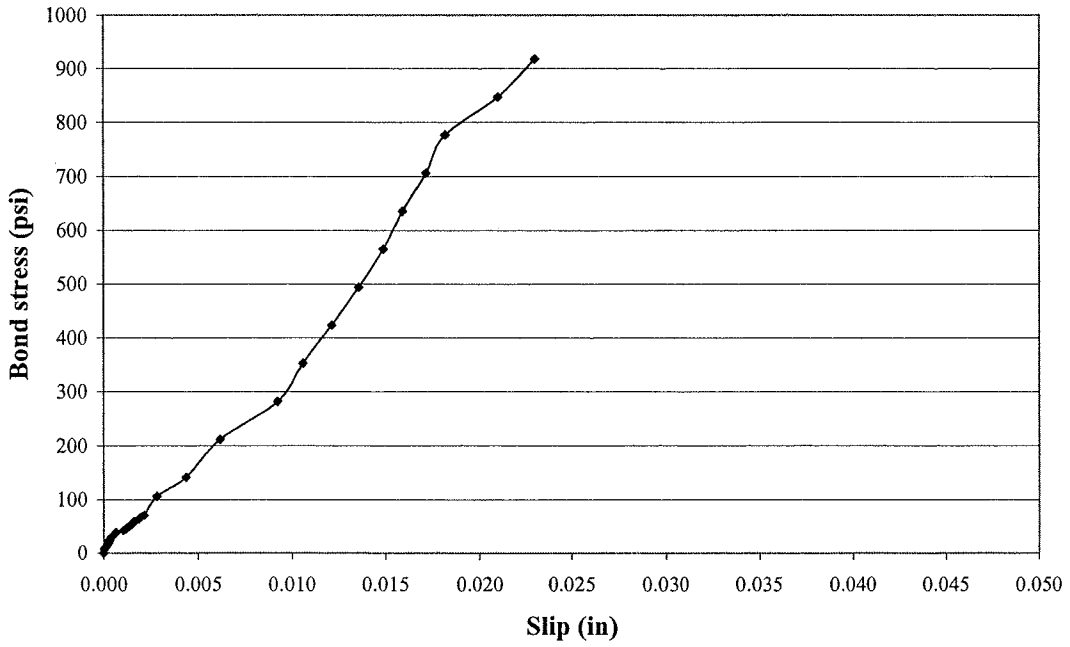

Fig. 8: Bond stress Vs. slip for the control mix specimen with the steel reinforcement in the upper horizontal position.

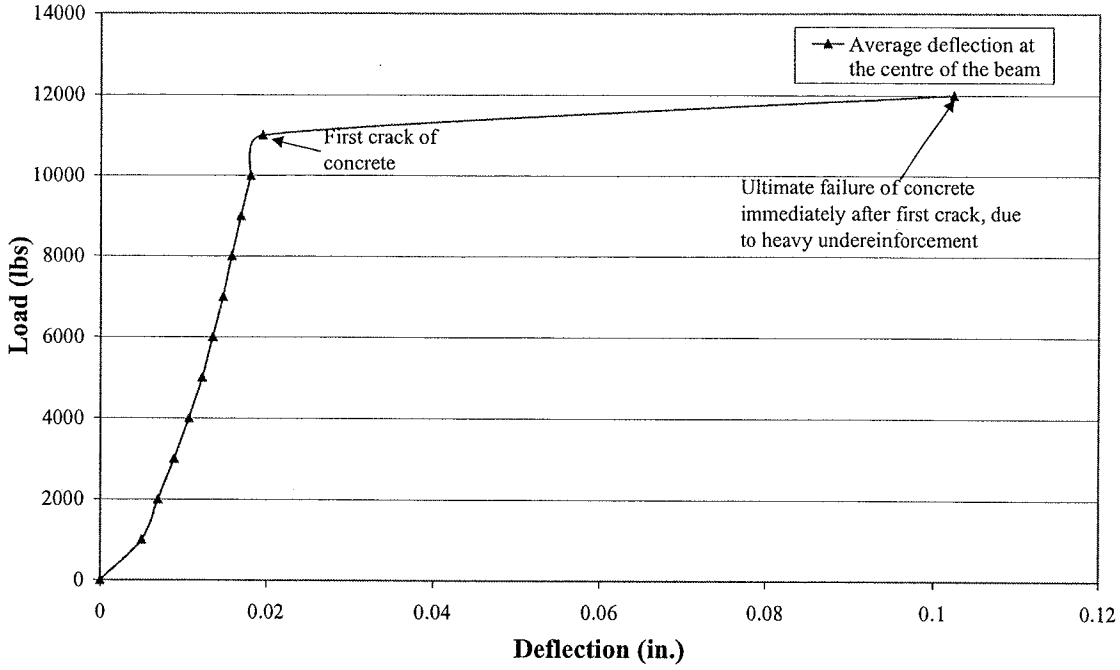

Fig. 9: Load Vs. Deflection Graph for Basalt Beam (BRC-1).

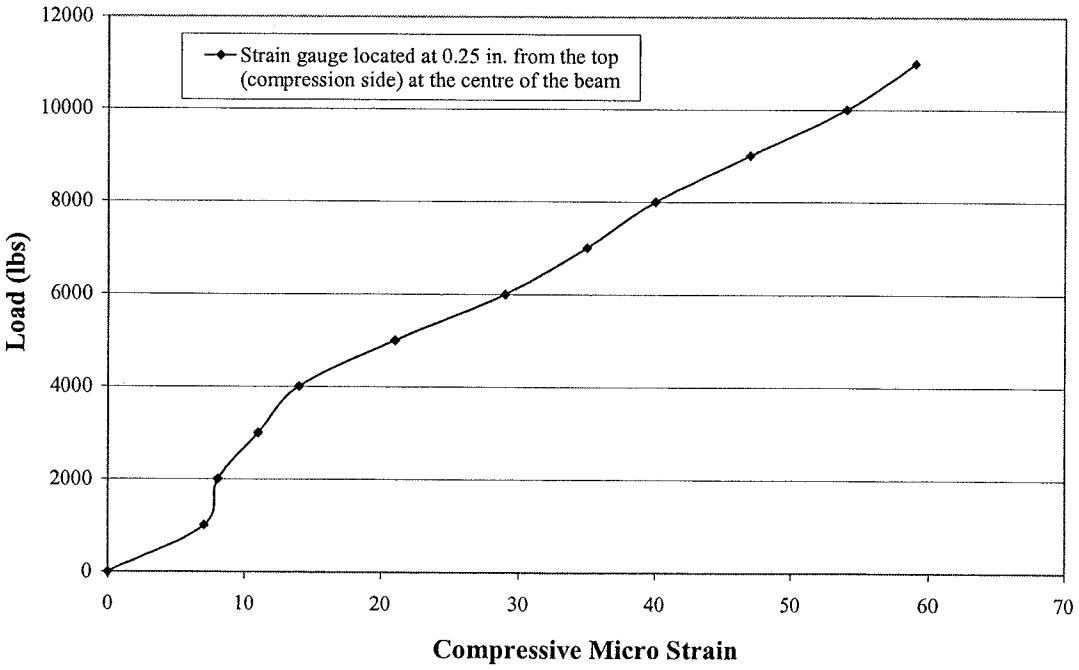

Fig. 10: Load Vs. Concrete Strain for Basalt Beam (BRC-1).

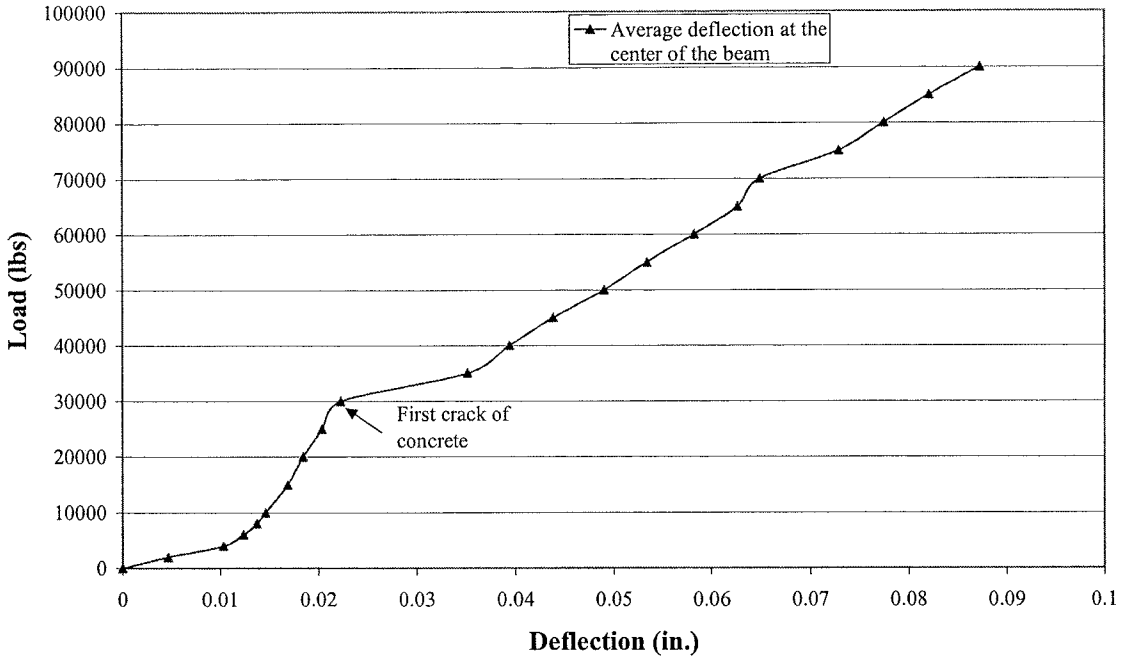

Fig. 11: Load Vs. Deflection Graph for Basalt Beam (BRC-2).

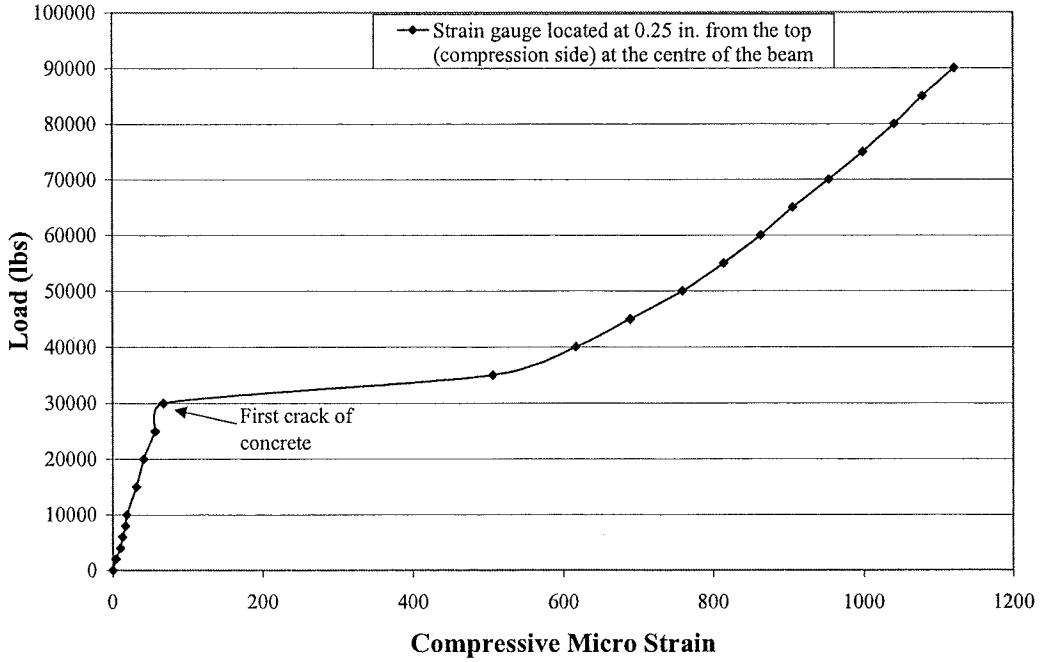

Fig. 12: Load Vs. Concrete Strain for Basalt Beam (BRC-2).

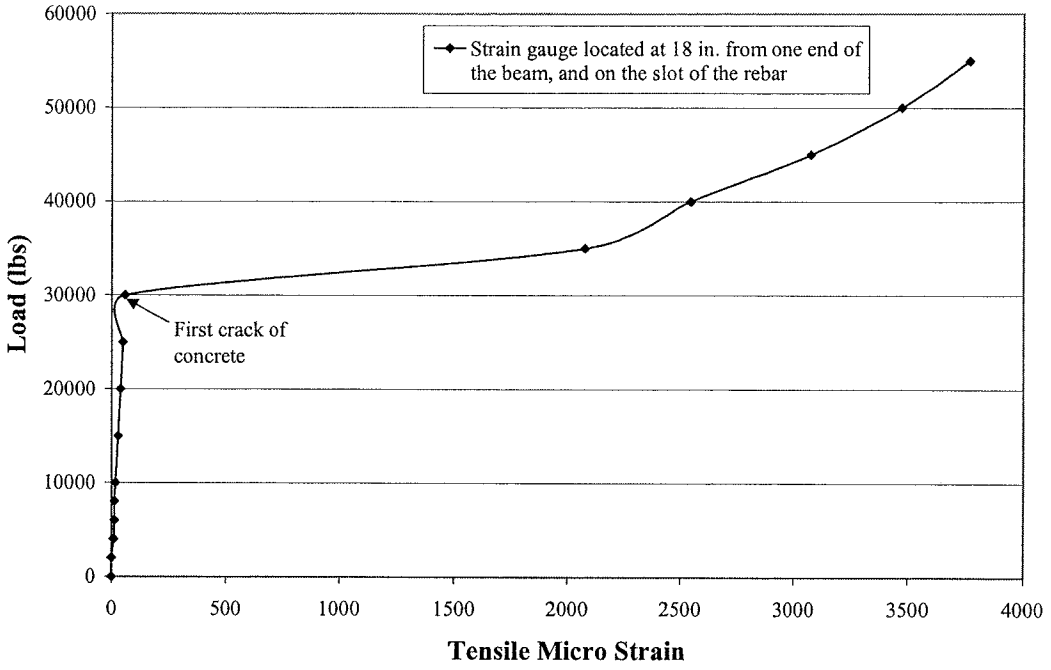

Fig. 13: Load Vs. Basalt Rebar Strain for Basalt Beam (BRC-2).

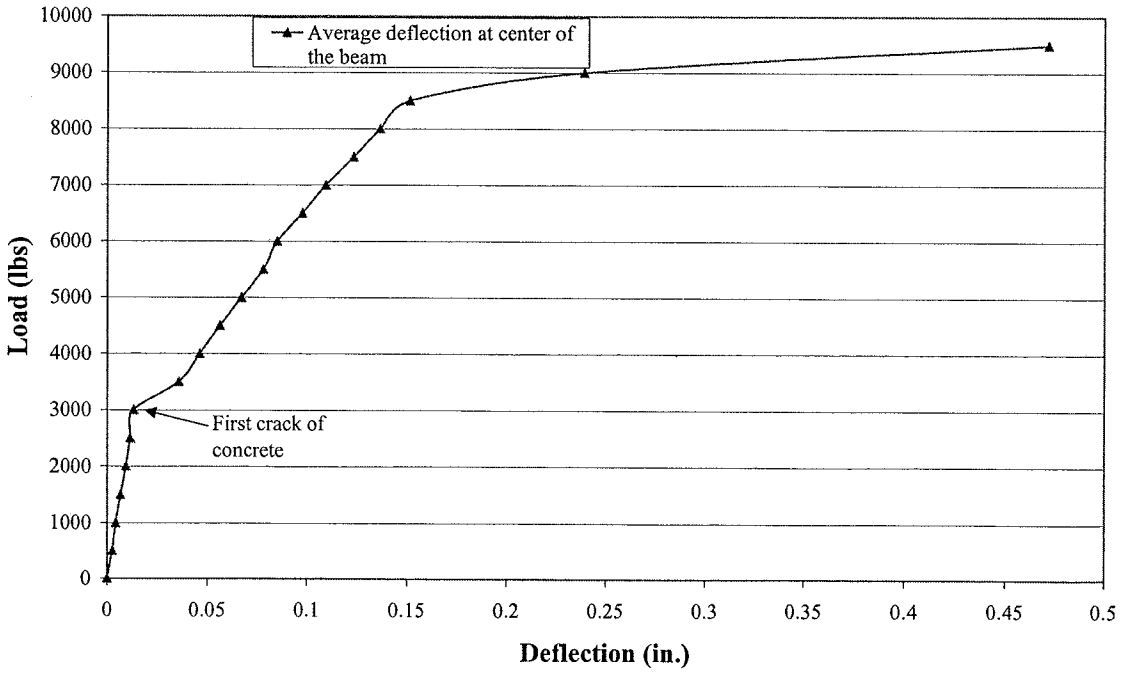

Fig. 14: Load Vs. Deflection Graph for Basalt Beam (BRC-3).

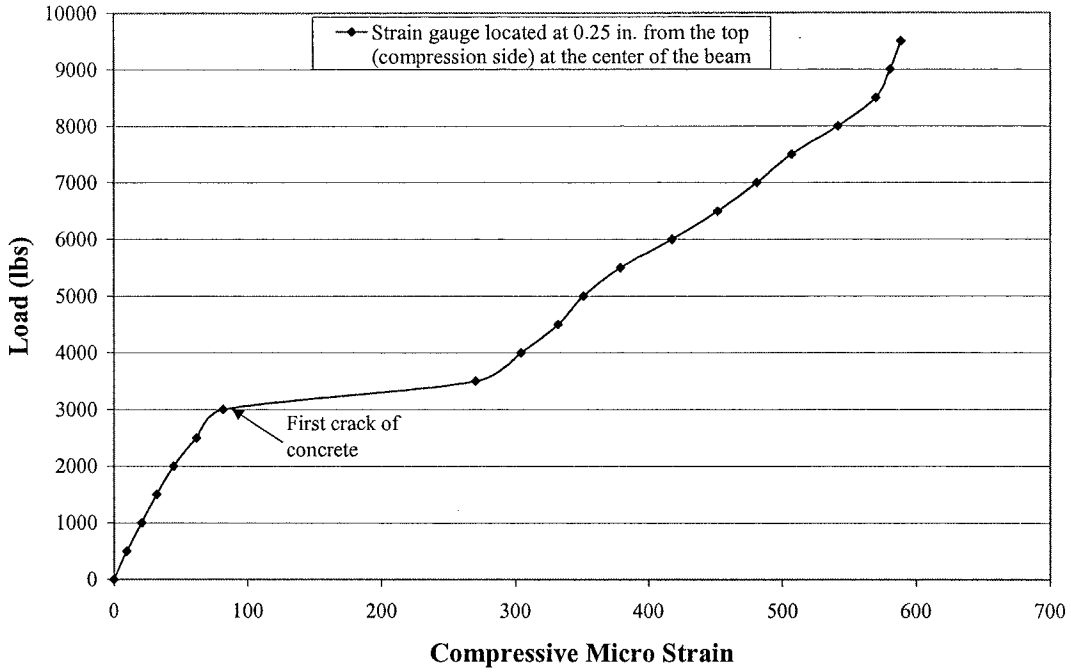

Fig. 15: Load Vs. Concrete Strain for Basalt Beam (BRC-3).

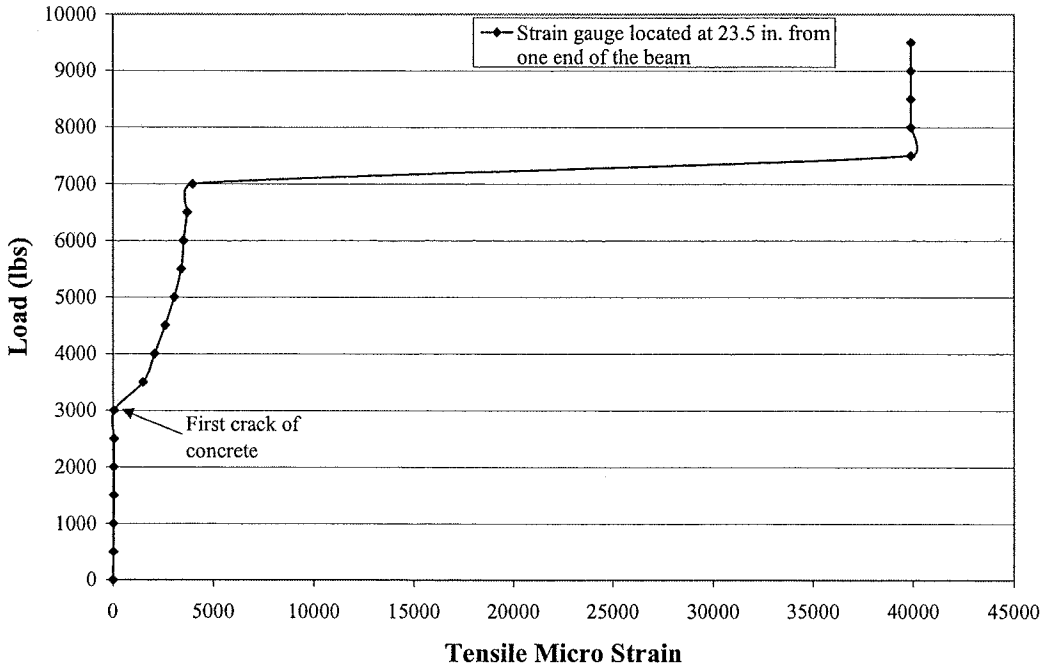

Fig. 16: Load Vs. Basalt Rebar Strain for Basalt Beam (BRC-3).

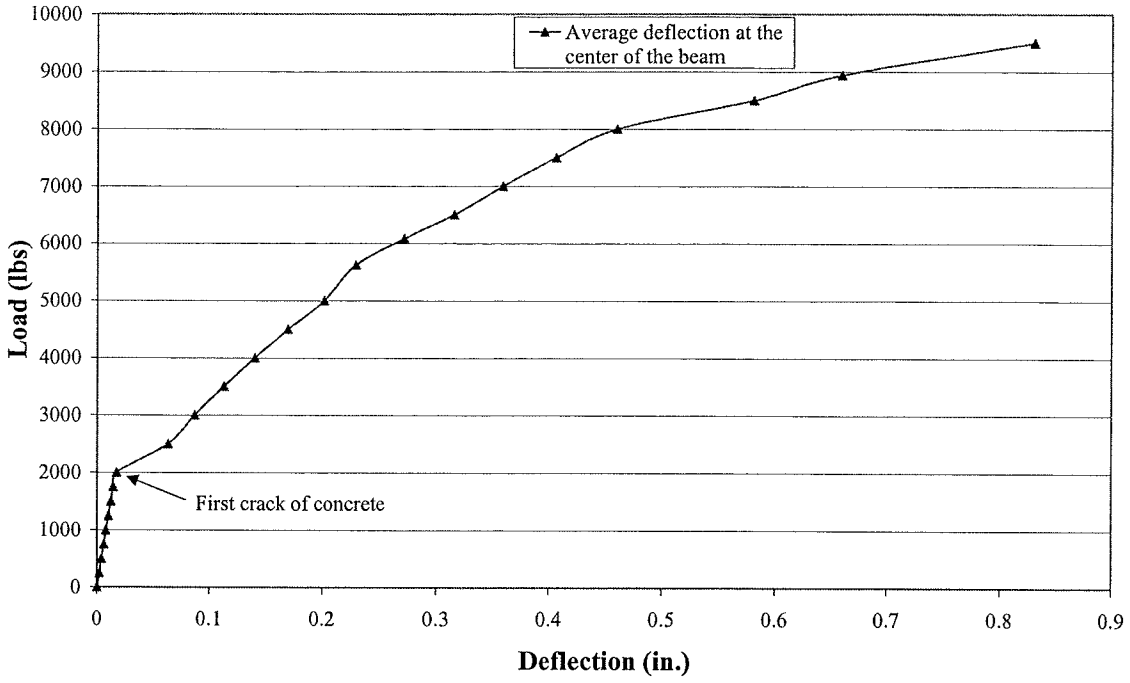

Fig. 17: Load Vs. Deflection Graph for Basalt Beam (BRC-4).

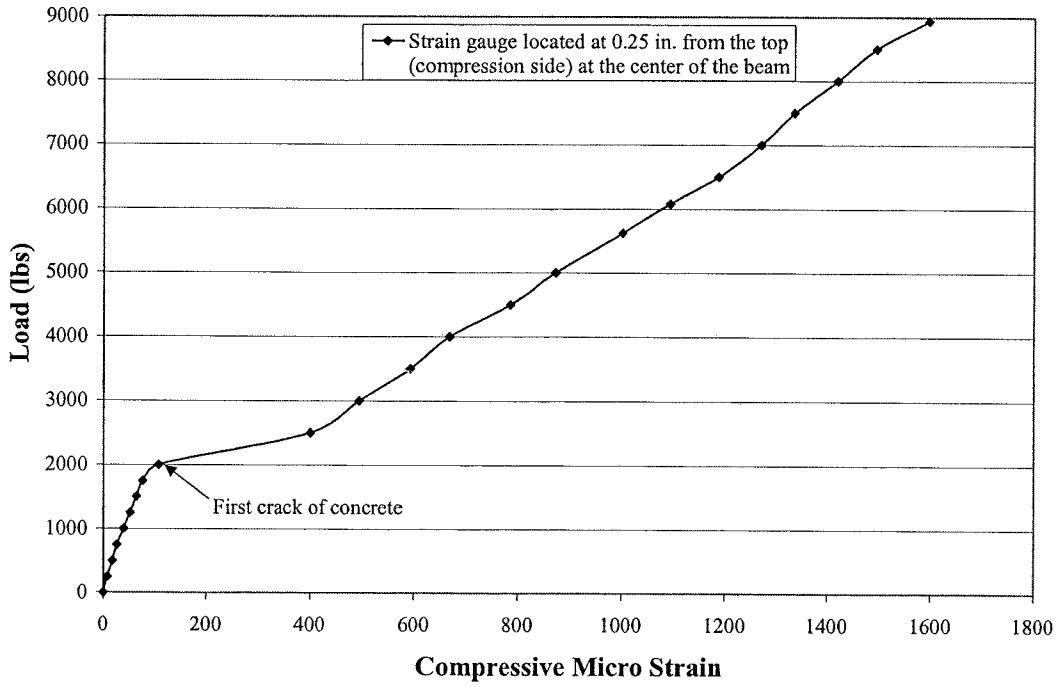

Fig. 18: Load Vs. Concrete Strain for Basalt Beam (BRC-4).

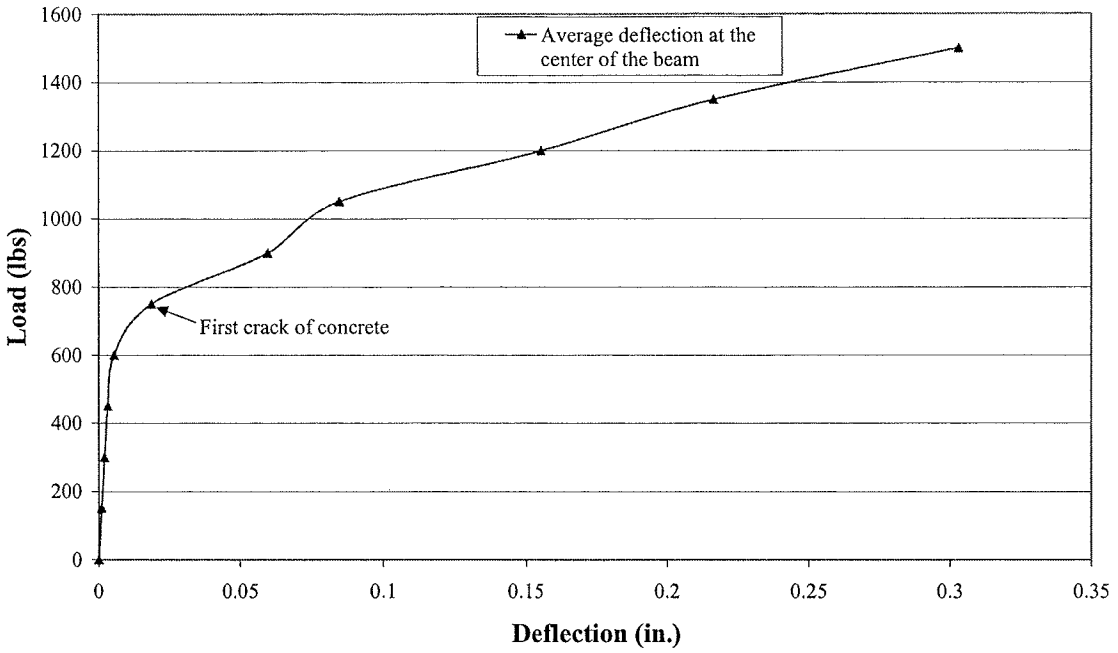

Fig. 19: Load Vs. Deflection Graph for Basalt Beam (BRC-5).

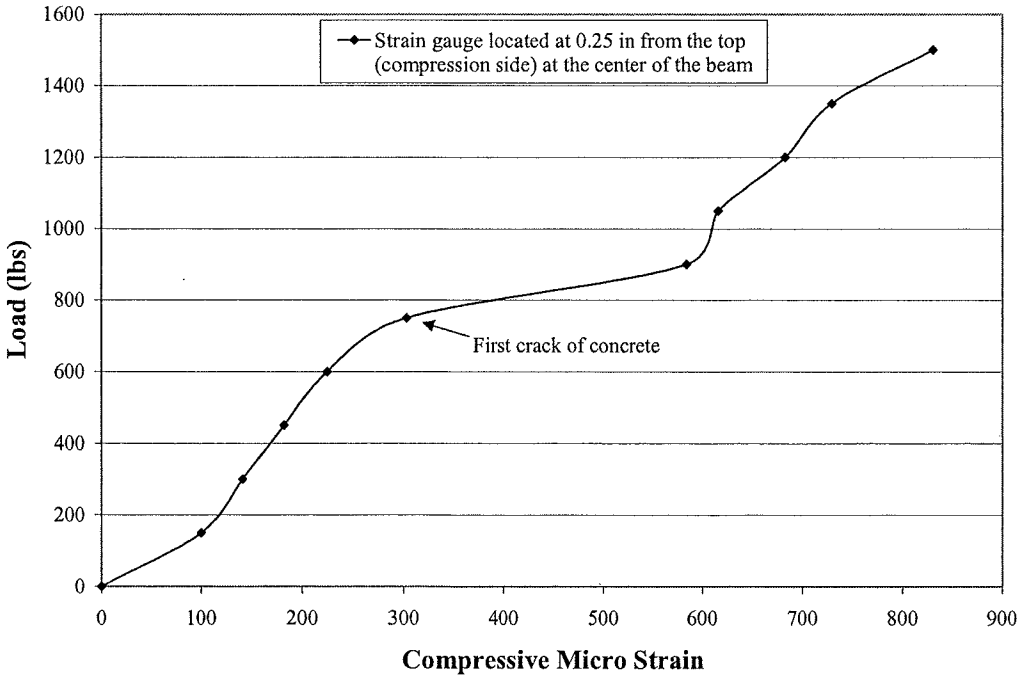

Fig. 20: Load Vs. Concrete Strain for Basalt Beam (BRC-5).

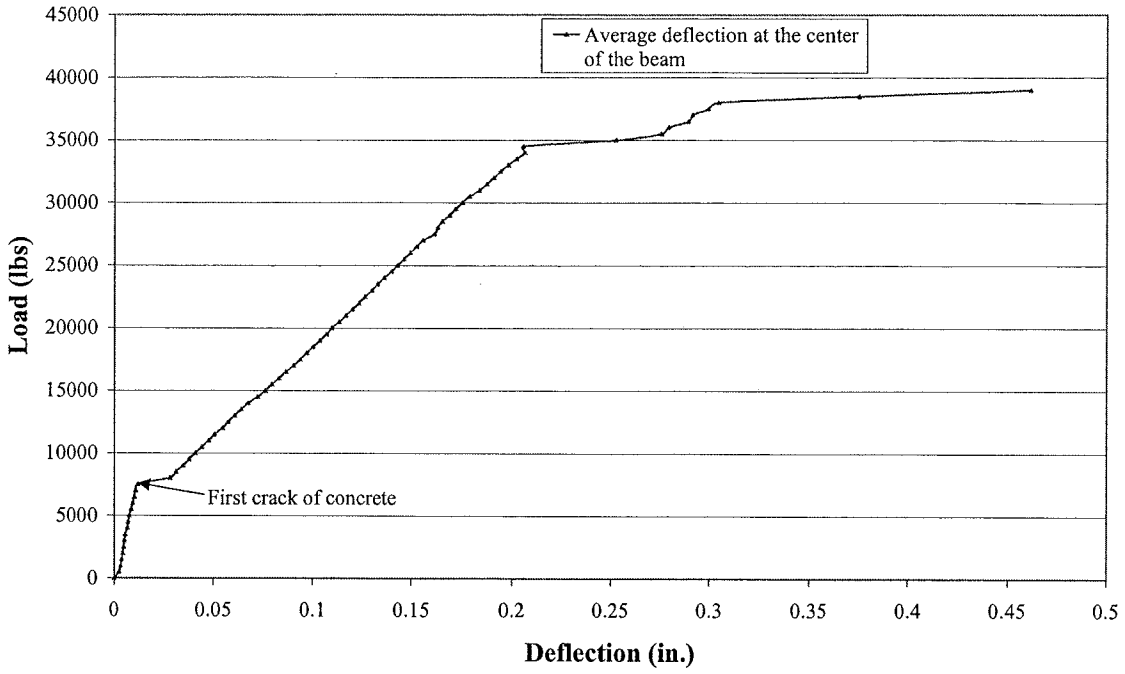

Fig. 21: Load Vs. Deflection Graph for Basalt Beam (BRC-6).

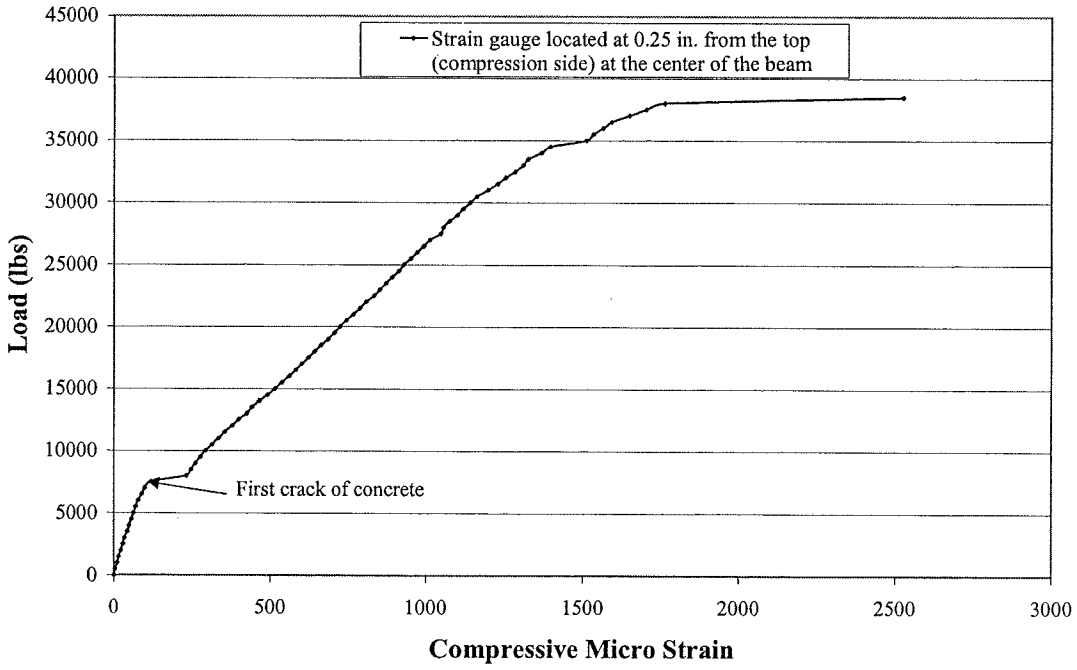

Fig. 22: Load Vs. Concrete Strain for Basalt Beam (BRC-6).

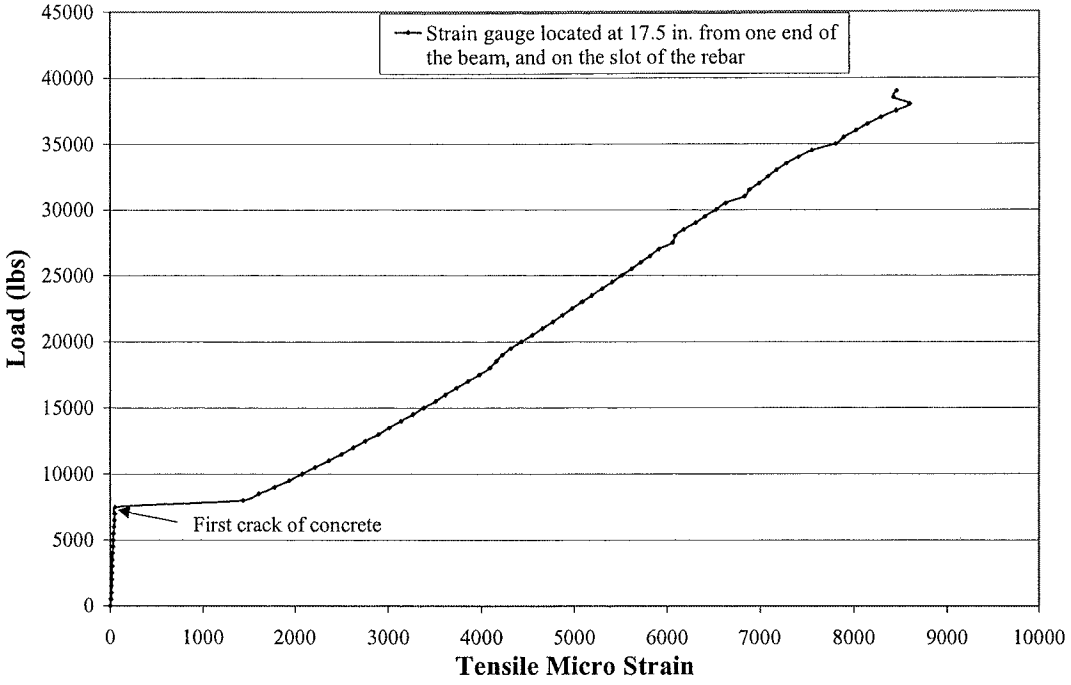

Fig. 23: Load Vs. Basalt Rebar Strain for Basalt Beam (BRC-6).

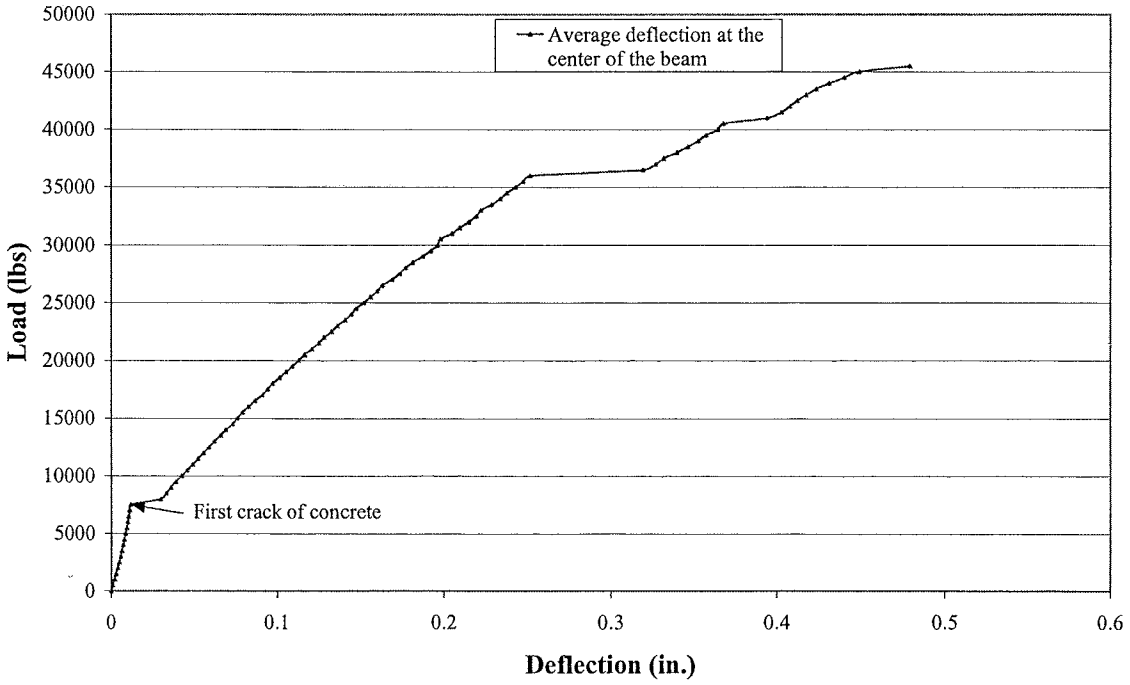

Fig. 24: Load Vs. Deflection Graph for Basalt Beam (BRC-7).

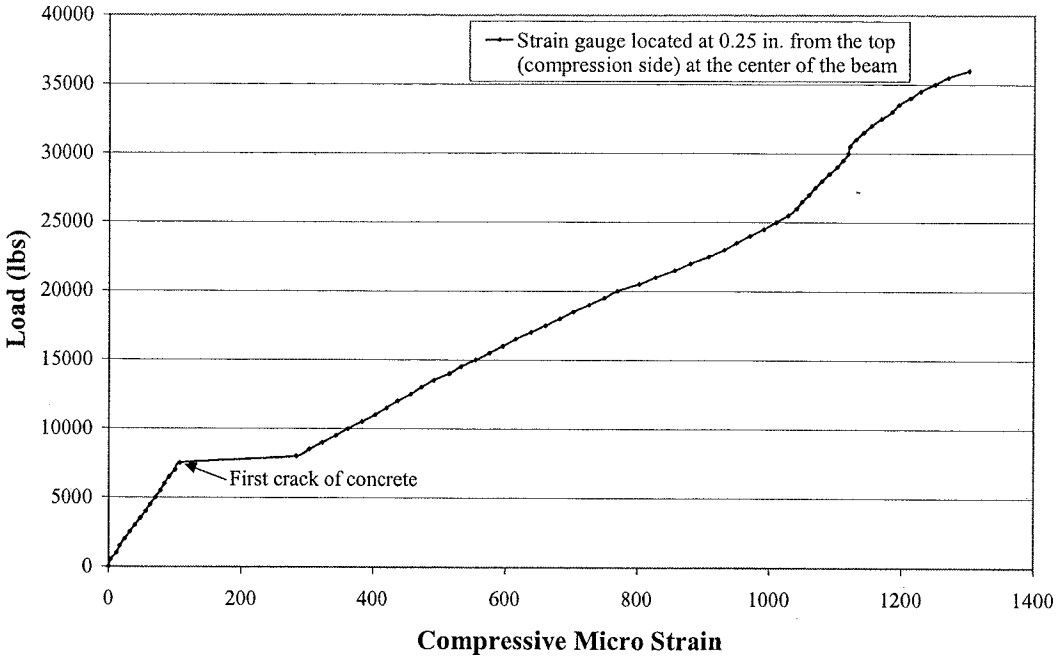

Fig. 25: Load Vs. Concrete Strain for Basalt Beam (BRC-7).

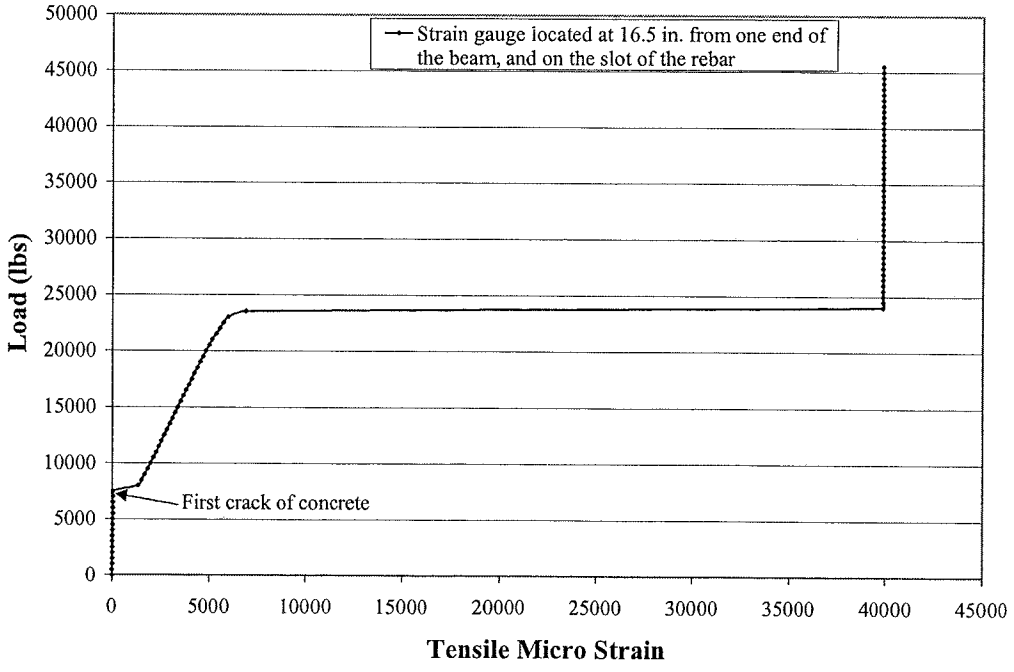

Fig. 26: Load Vs. Basalt Rebar Strain for Basalt Beam (BRC-7).

APPENDIX A

Details Of Reinforcement Position And Testing Arrangement For All The Beams

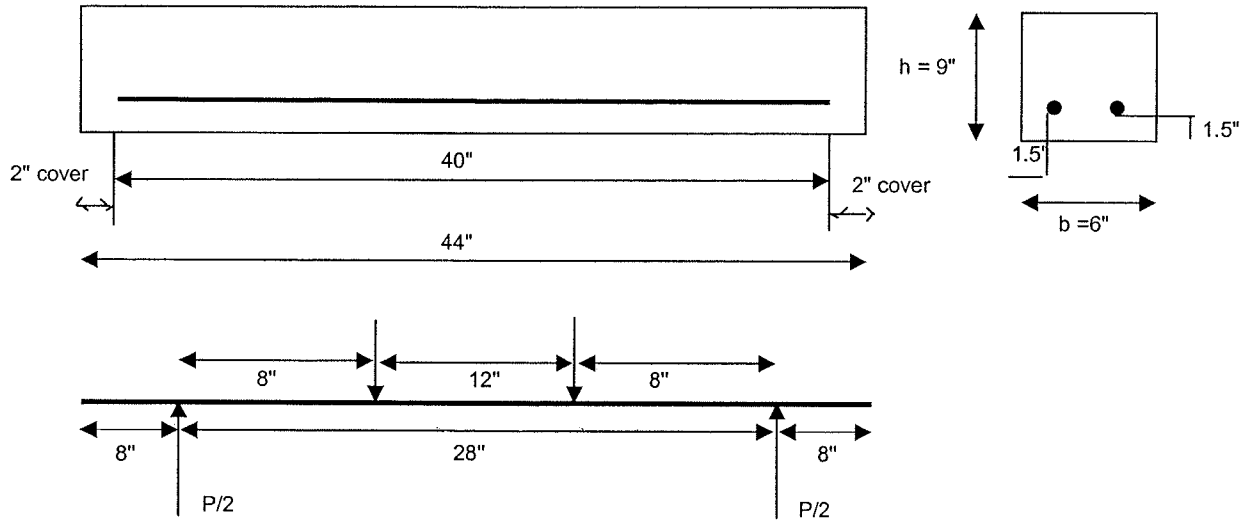

Sketch 1 – Details of reinforcement position and testing arrangement (BRC–1).

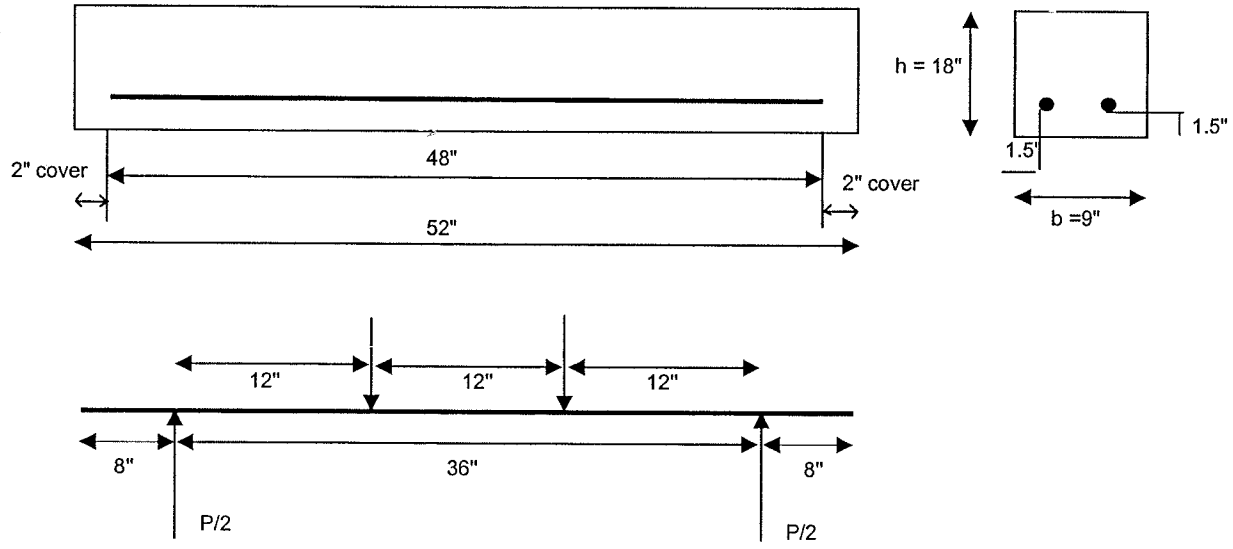

Sketch 2 – Details of reinforcement position and testing arrangement (BRC–2).

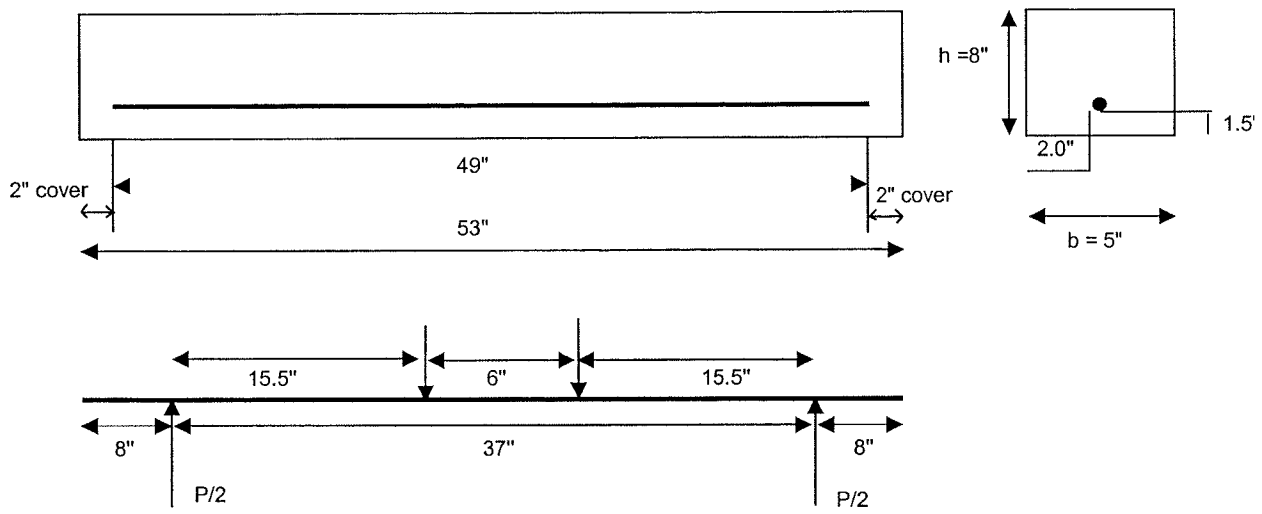

Sketch 3 – Details of reinforcement position and testing arrangement (BRC–3).

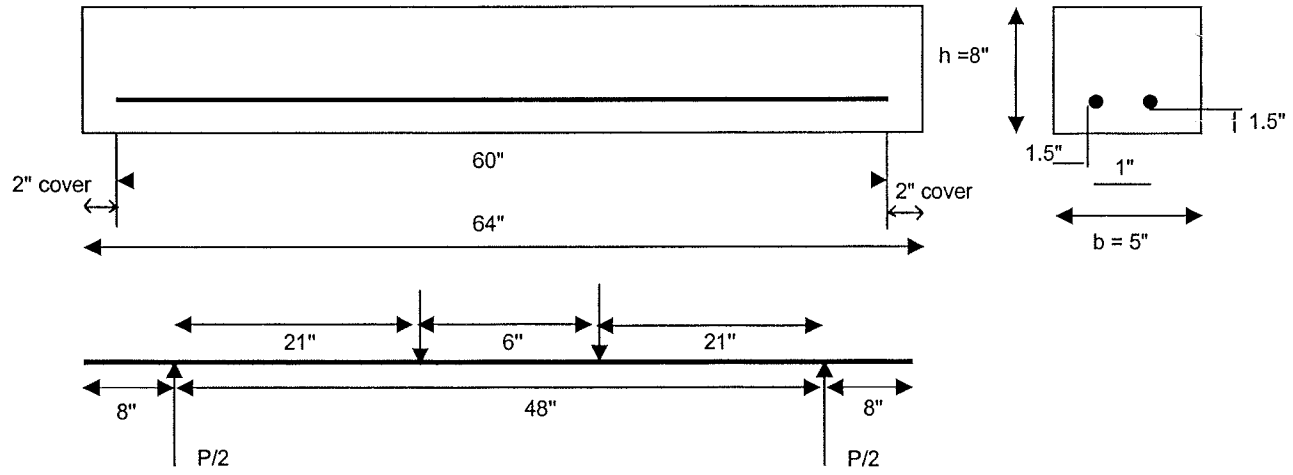

Sketch 4 – Details of reinforcement position and testing arrangement (BRC–4).

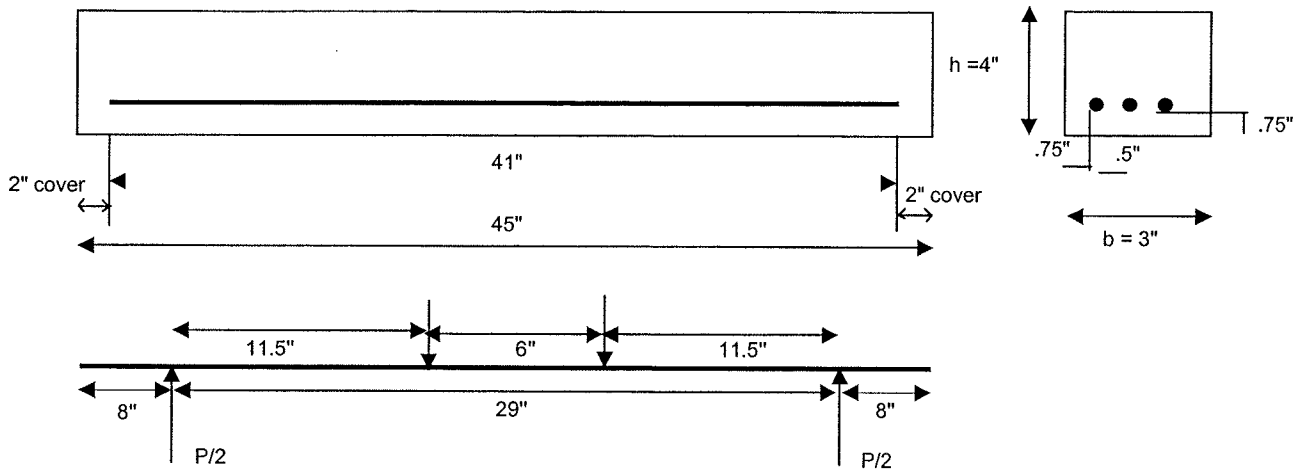

Sketch 5 – Details of reinforcement position and testing arrangement (BRC–5).

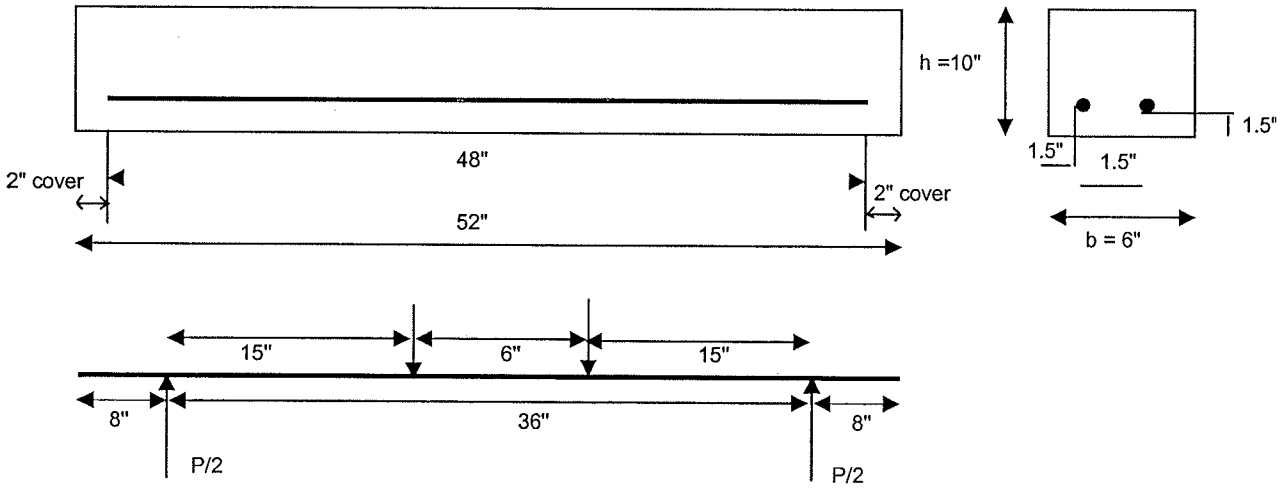

Sketch 6 – Details of reinforcement position and testing arrangement (BRC–6).

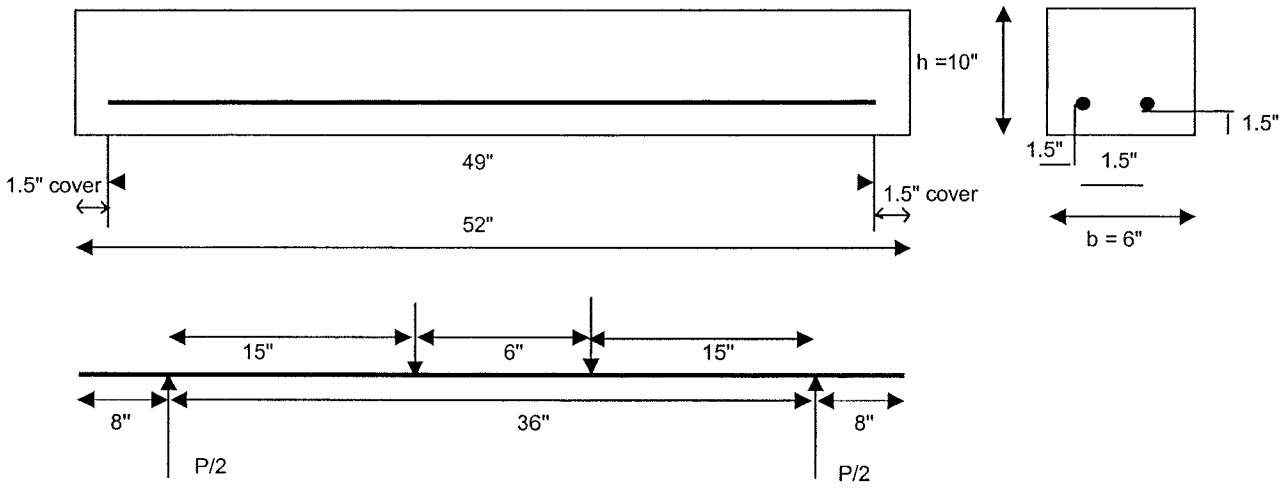

Sketch 7 – Details of reinforcement position and testing arrangement (BRC–7).

APPENDIX B

PHOTOGRAPHS

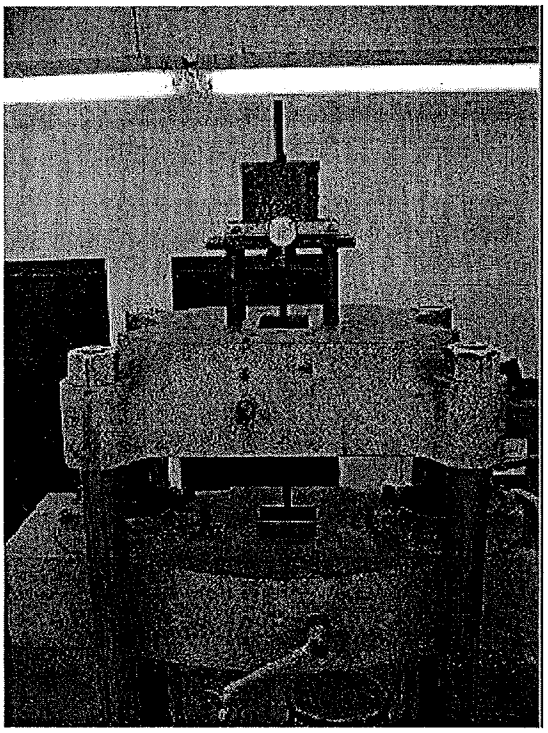

Photo 1: The test set-up for bond test.

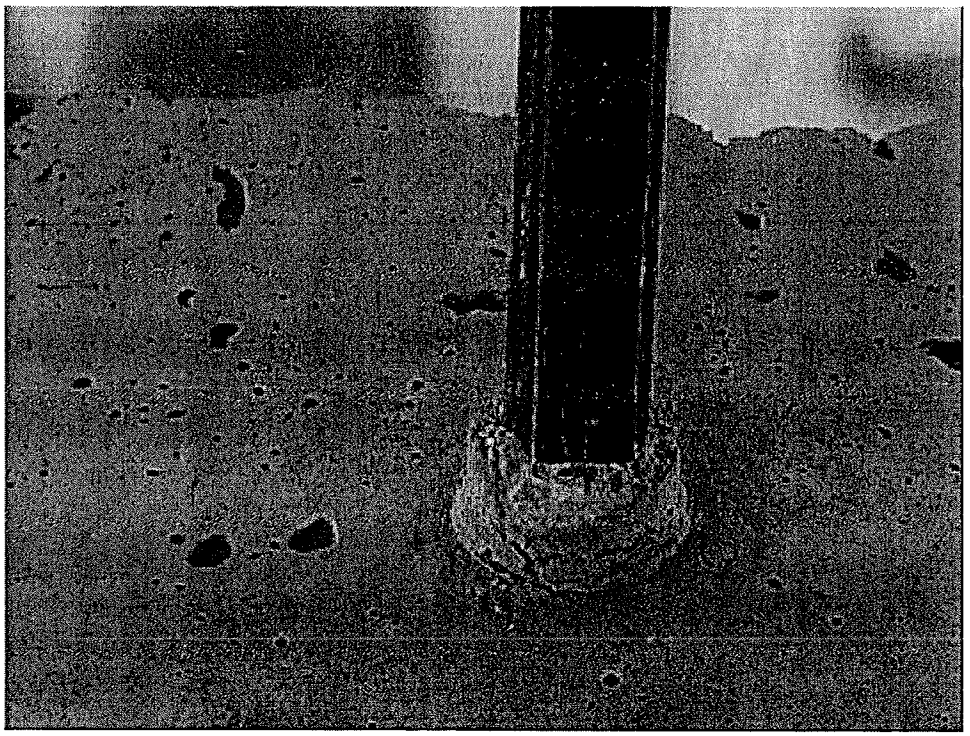

Photo 2: The bond failure due to the slip in plain basalt rebar.

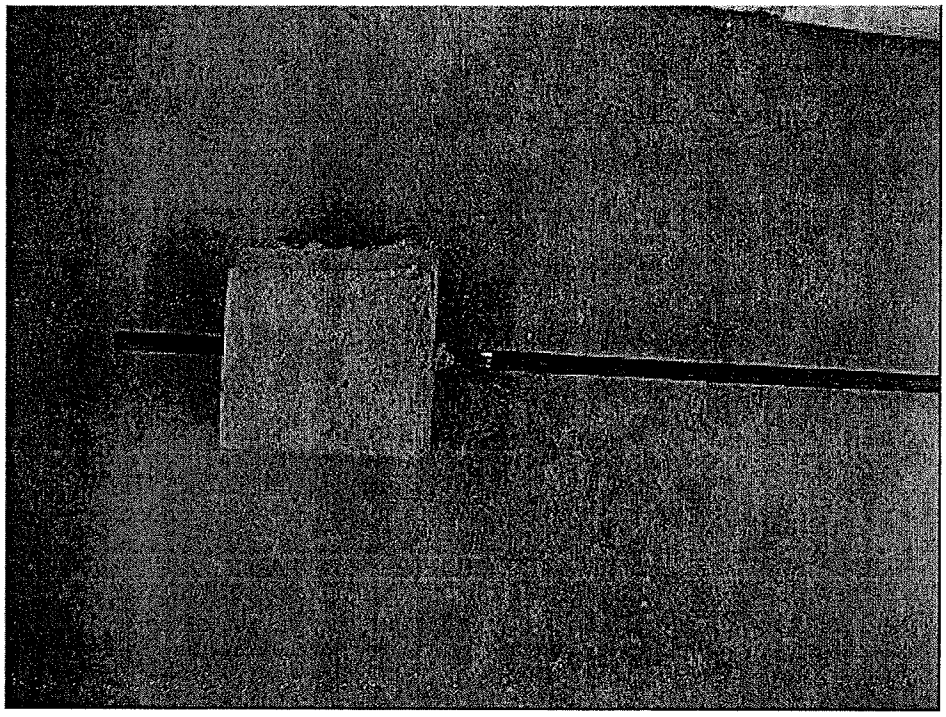

Photo 3: The bond failure of plain basalt rebar reinforced specimen due to slip. The slip can be clearly seen in this photo due to the mark of concrete on rebar.

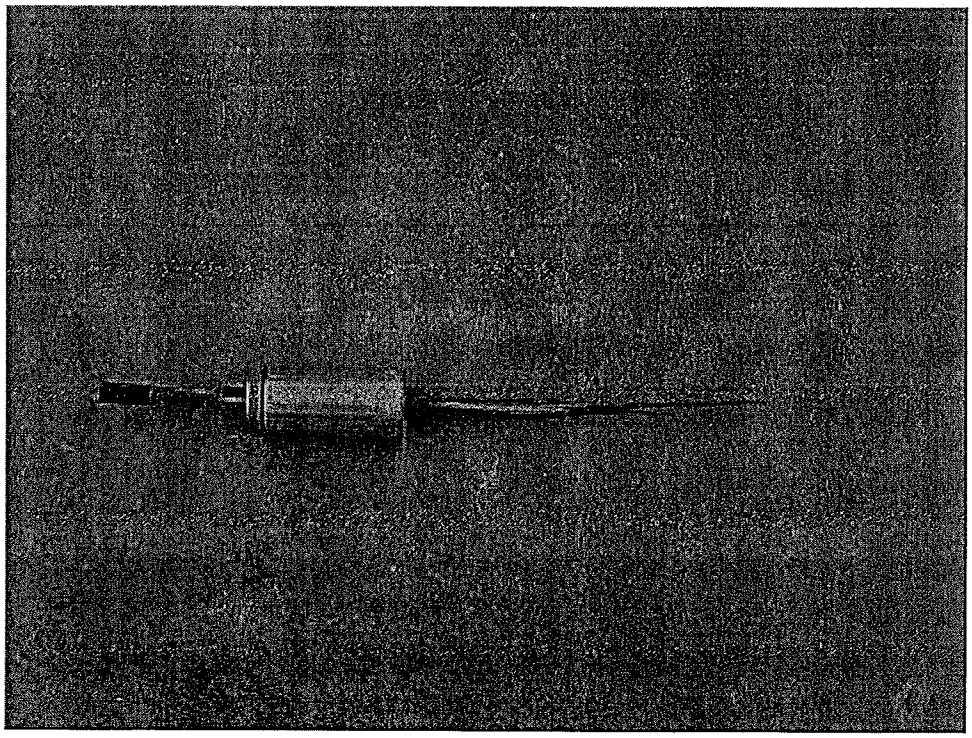

Photo 4: The chuck used to anchor the rebar along with the broken rebar.

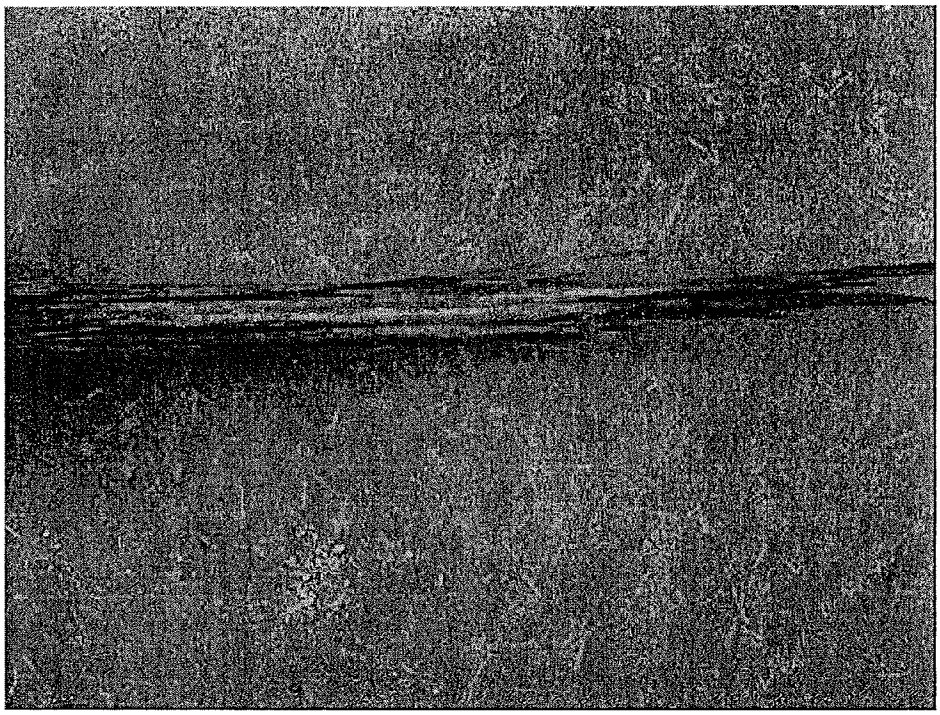

Photo 5: The failed basalt rebar in close up. The splitted basalt fibers of rebar can be seen clearly.

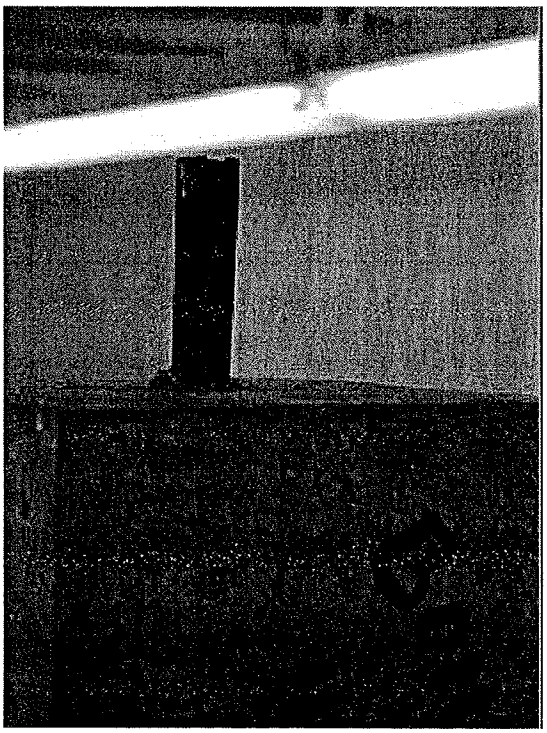

Photo 6: The failed 8 – slot basalt rebar in close up. The splitted rebar along with the slip can be seen clearly here.

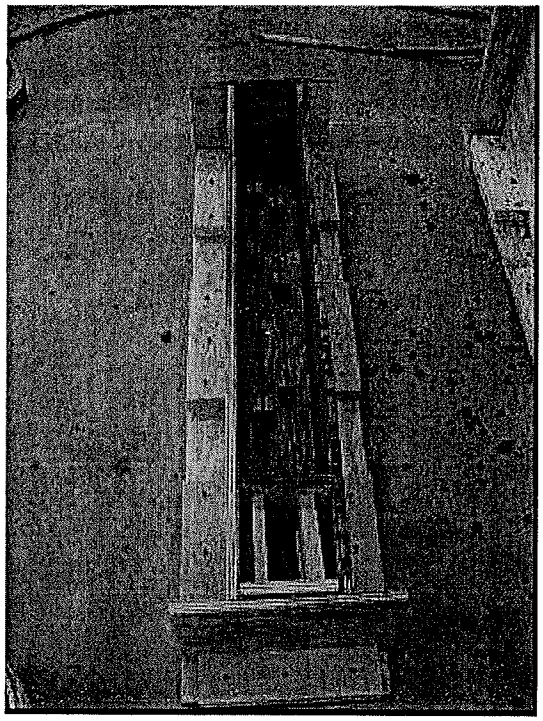

Photo 7: BRC-1 beam with the basalt cables with the cover blocks.

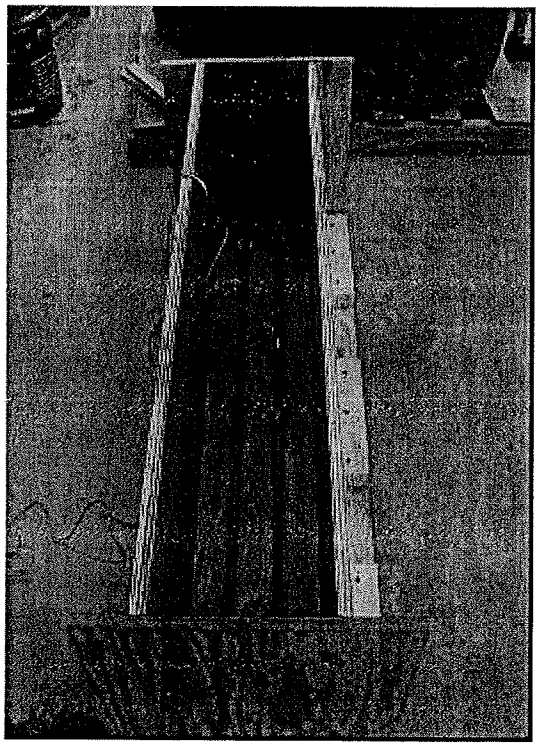

Photo 8: BRC-2 beam with the 4-slot basalt rebar with the strain gage and cover blocks.

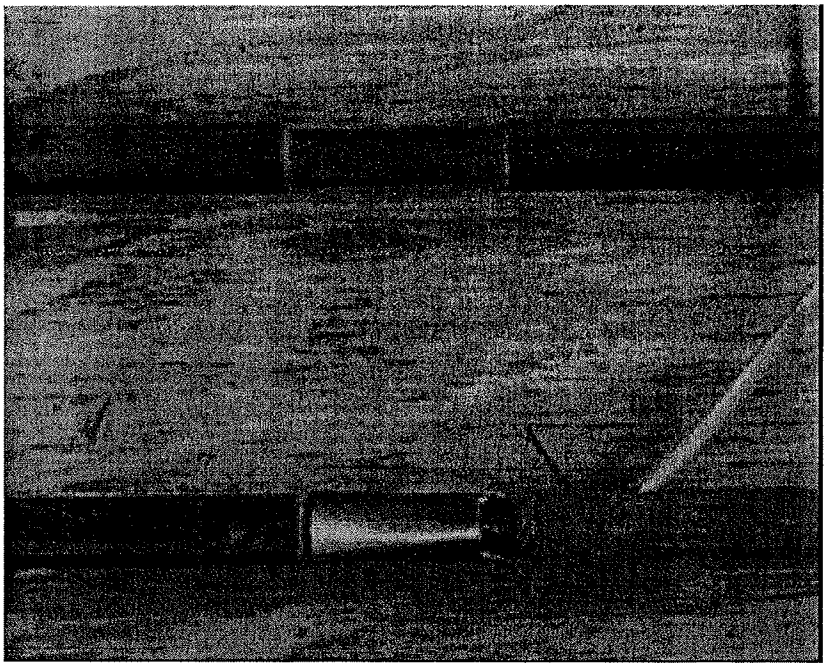

Photo 9: 4-slot basalt rebar with the strain gage (on the slot) in the BRC-2 beam.

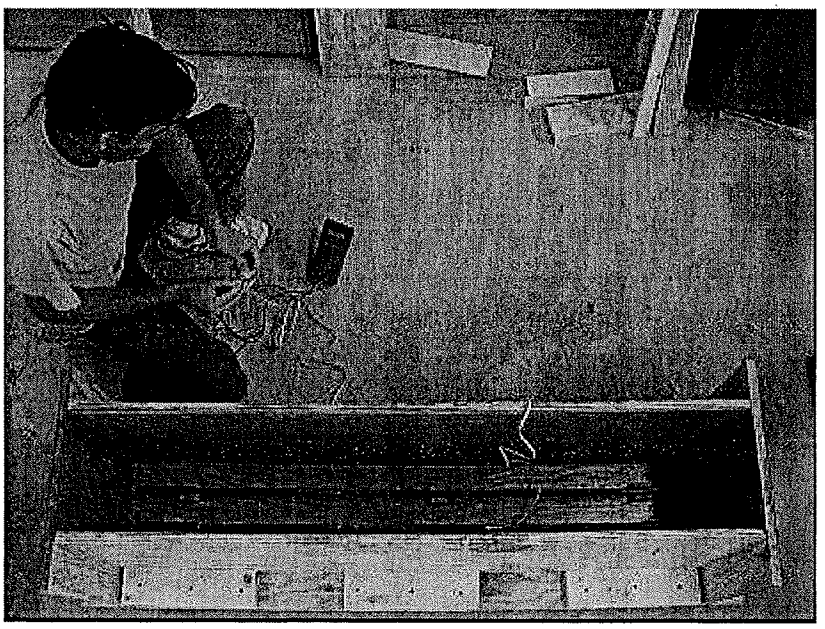

Photo 10: Strain gage is being tested before the pouring of concrete.

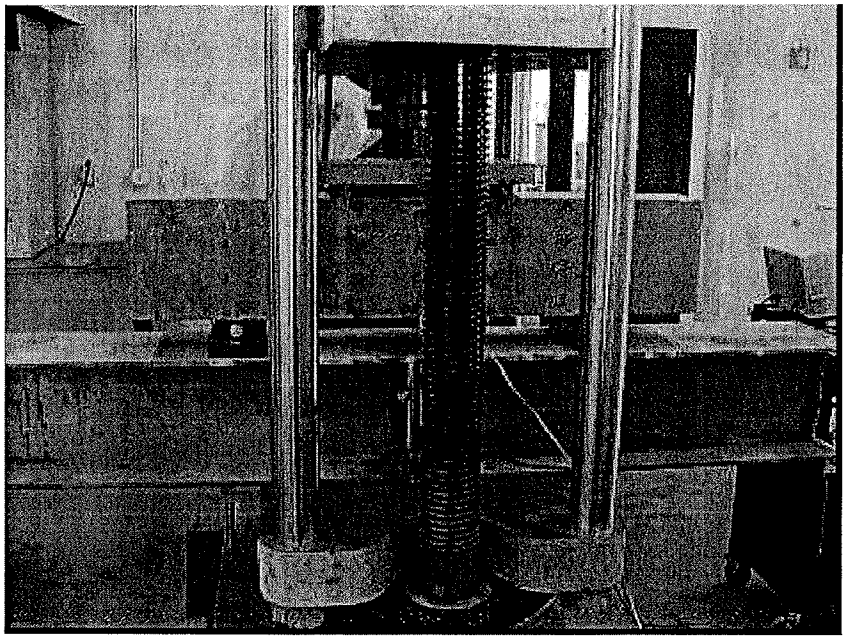

Photo 11: BRC-1 beam is placed on the UTM for testing.

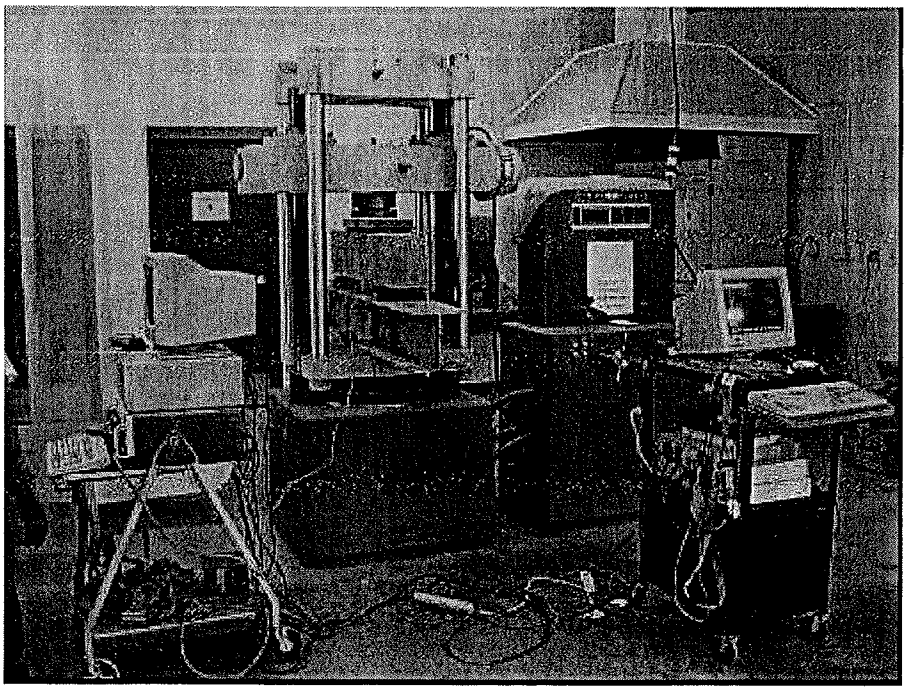

Photo 12: The test set up with the LVDT and the strain gage measuring devices.

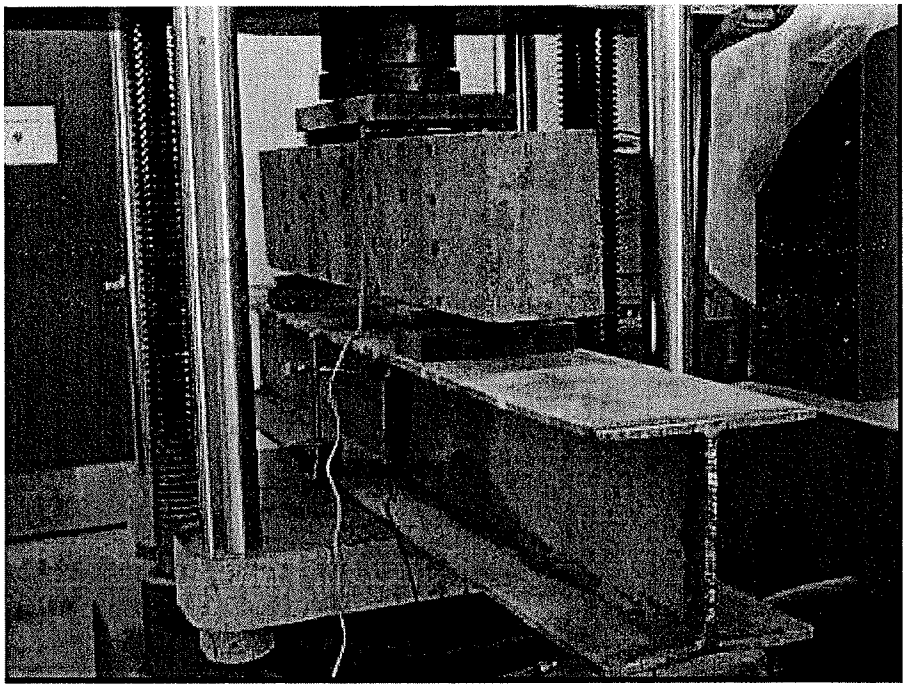

Photo 13: This photo shows the support, dial gage measuring the deflections, strain gages along with the loading system.

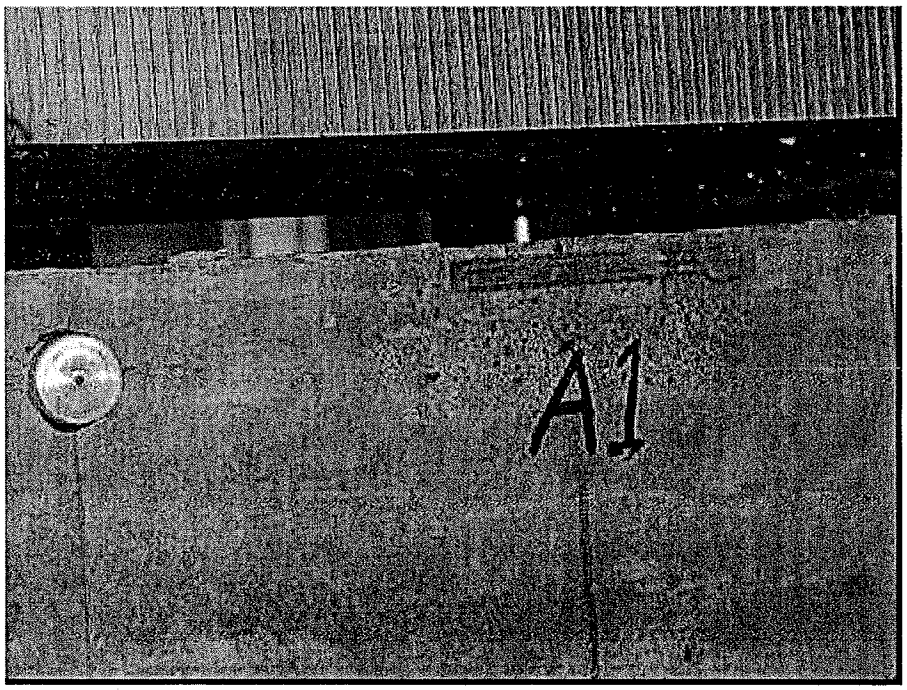

Photo 14: Close up of the strain gage fixed on the top surface of the beam.

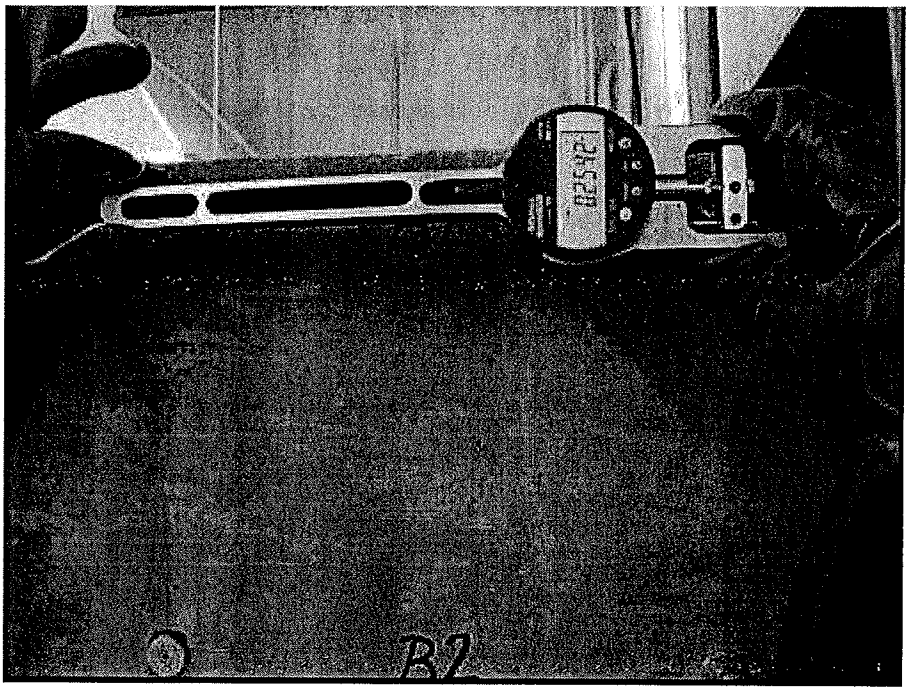

Photo 15: Strain is being measured along the longitudinal direction of the beam by mechanical strain gauge.

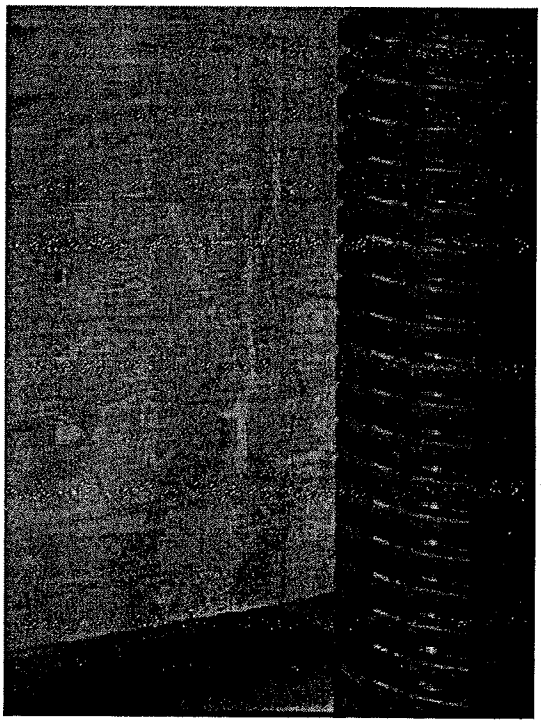

Photo 16: Crack due to flexure in the BRC-2 beam.

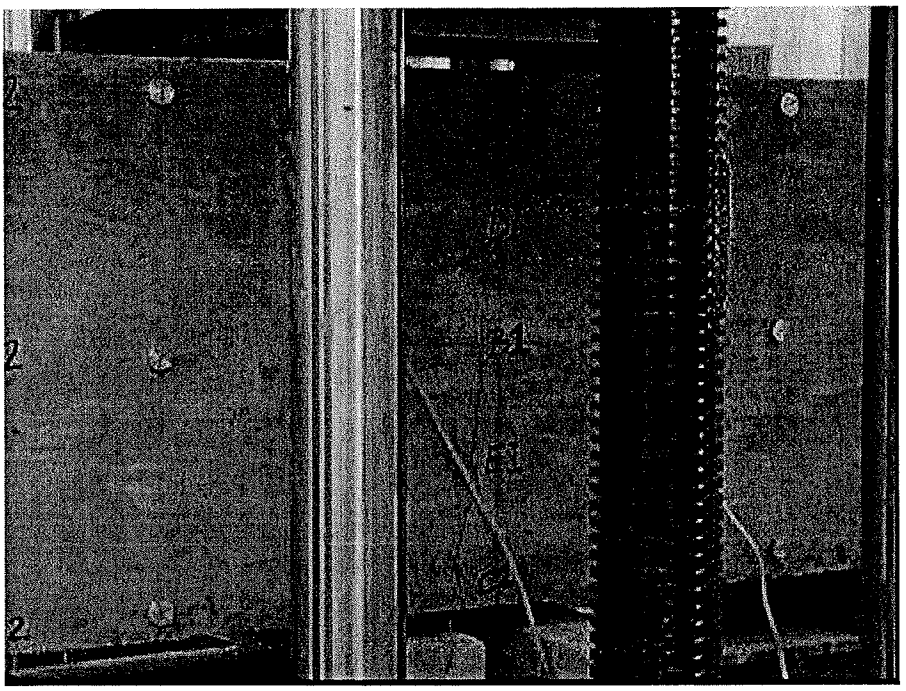

Photo 17: Crack in the center of BRC-2 beam due to flexure.

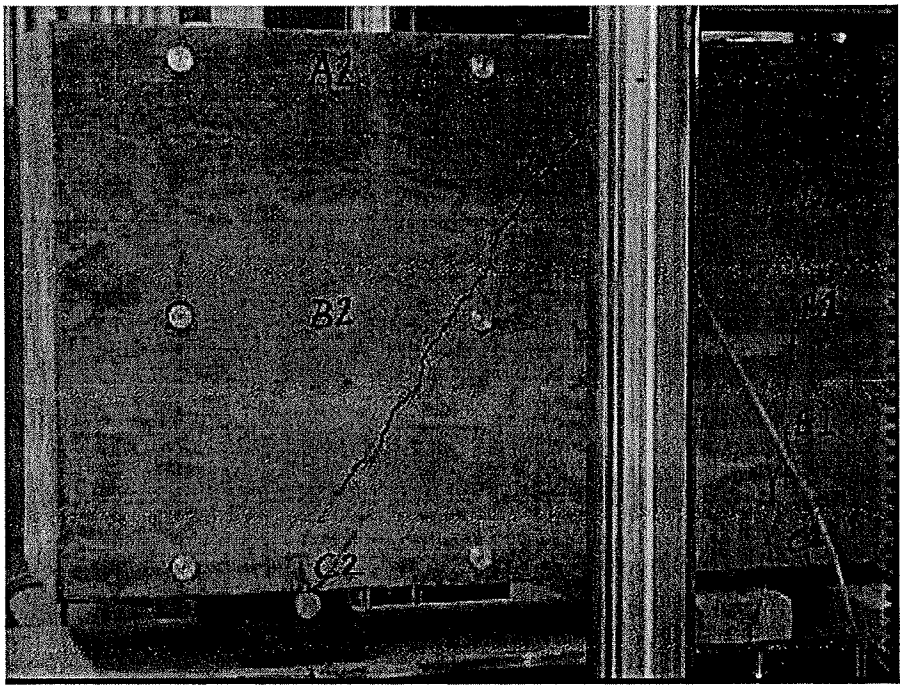

Photo 18: Failure of the BRC-2 beam due to shear crack.

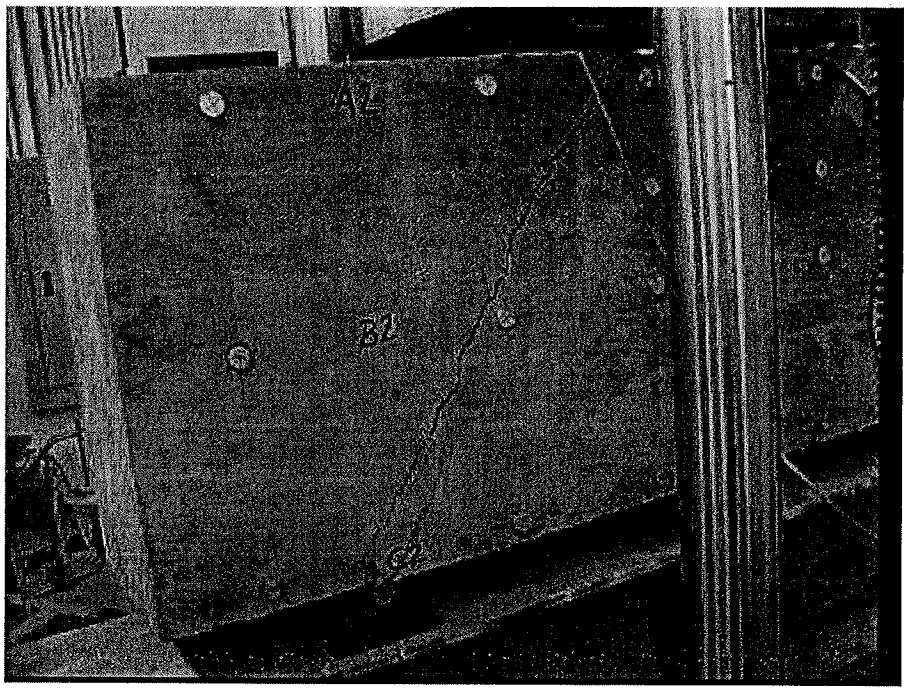

Photo 19: View of the failed BRC-2 beam.

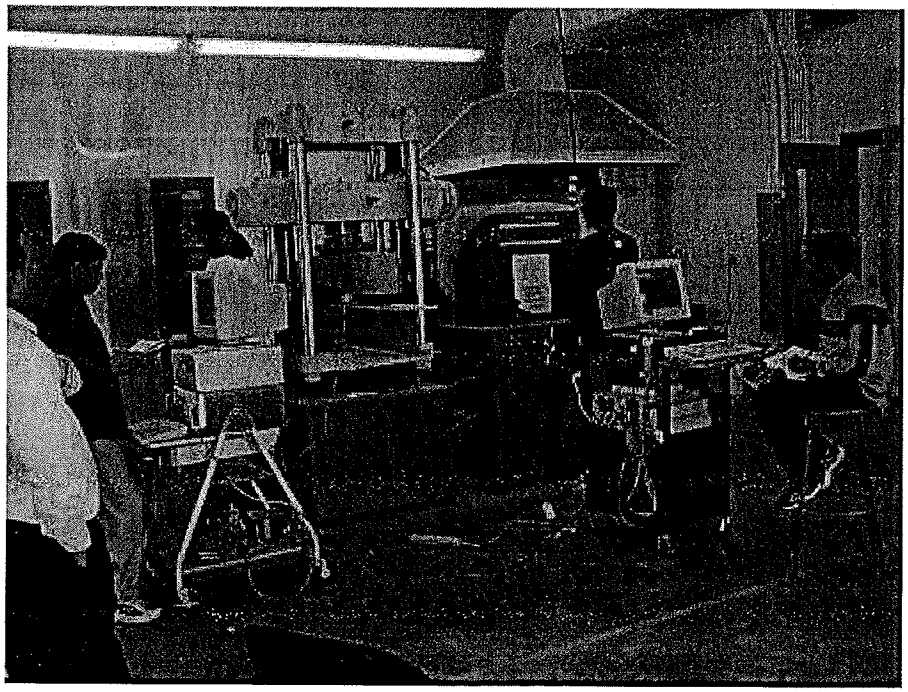

Photo 20: Testing under progress.

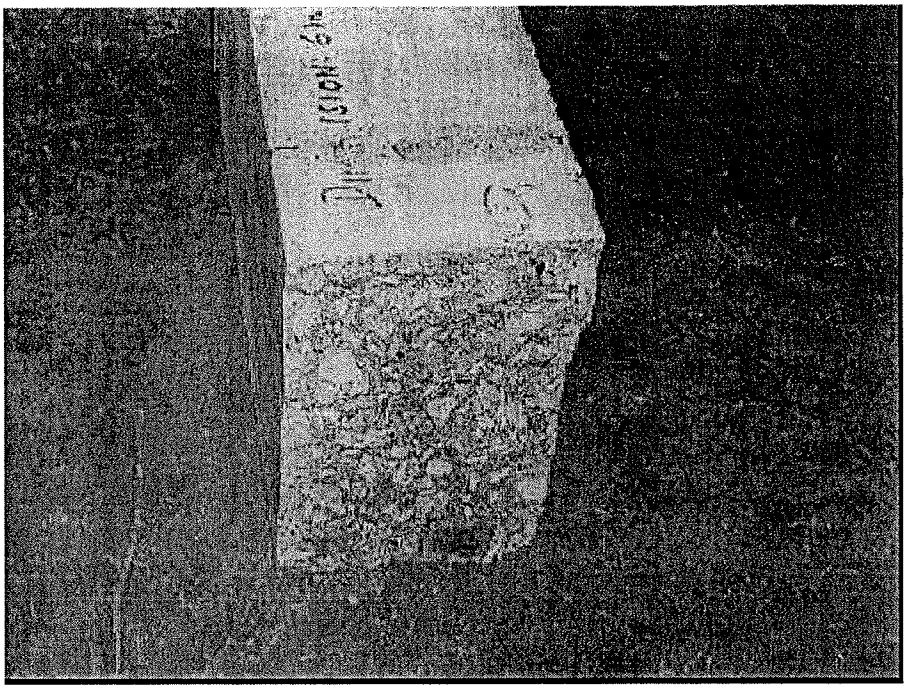

Photo 21: Failed BRC-1 beam (after testing).

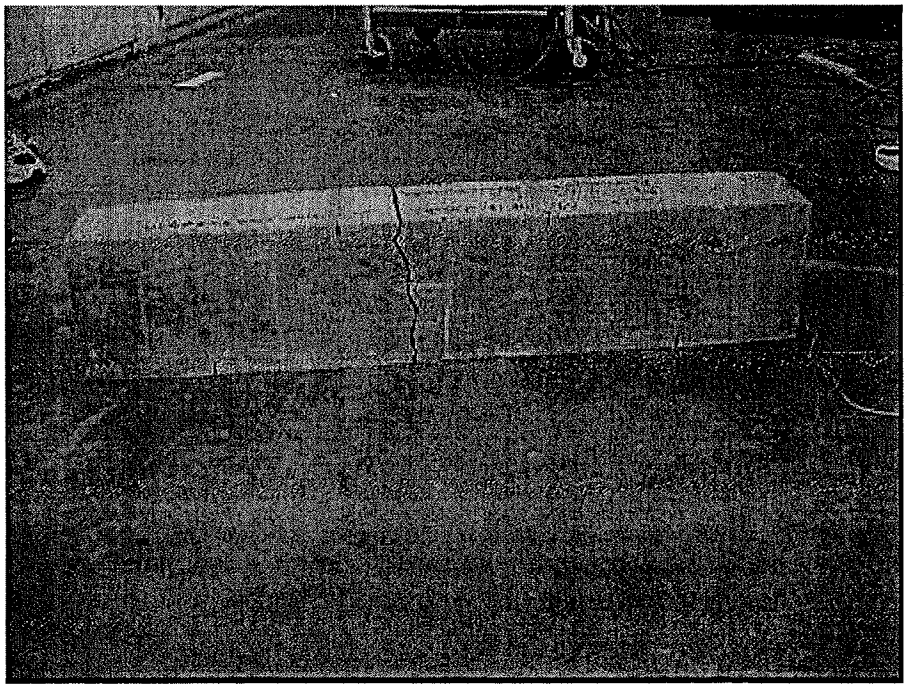

Photo 22: Failed BRC-1 beam (after testing).

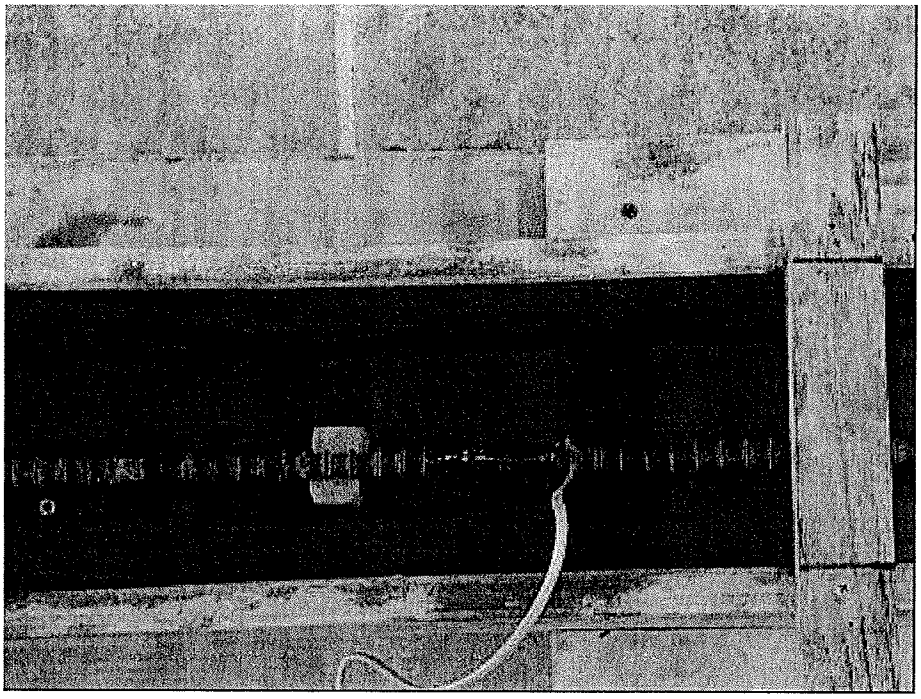

Photo 23: BRC –3 beam with single corrugated bar with a strain gauge.

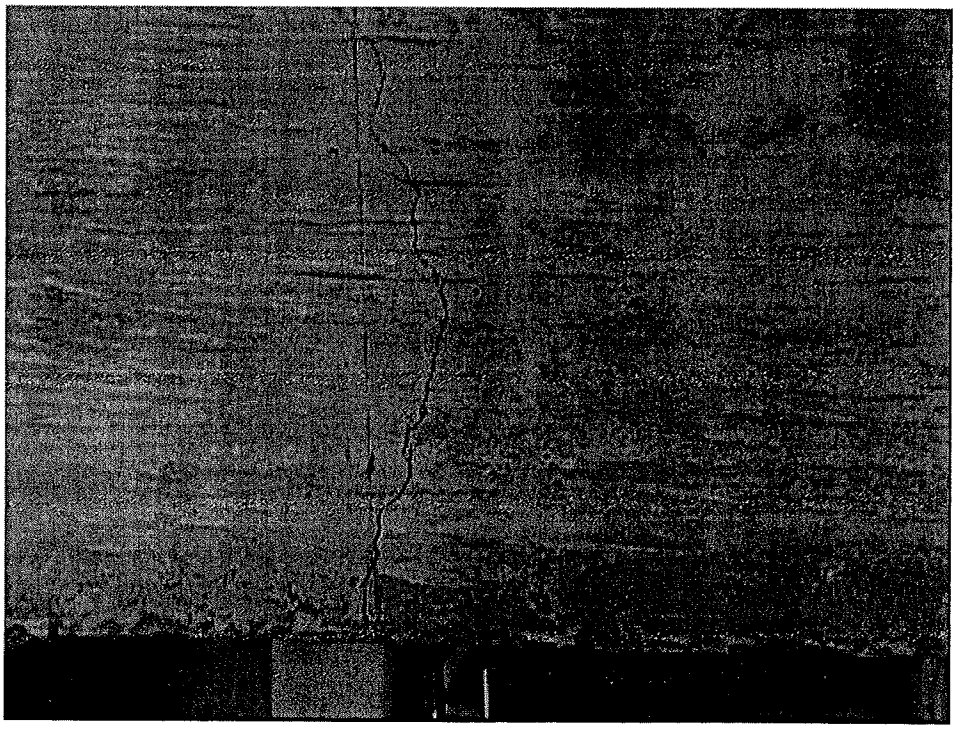

Photo 24: First flexural crack of concrete at the center of the BRC-3 beam, the LVDT's for measuring deflections can also be seen.

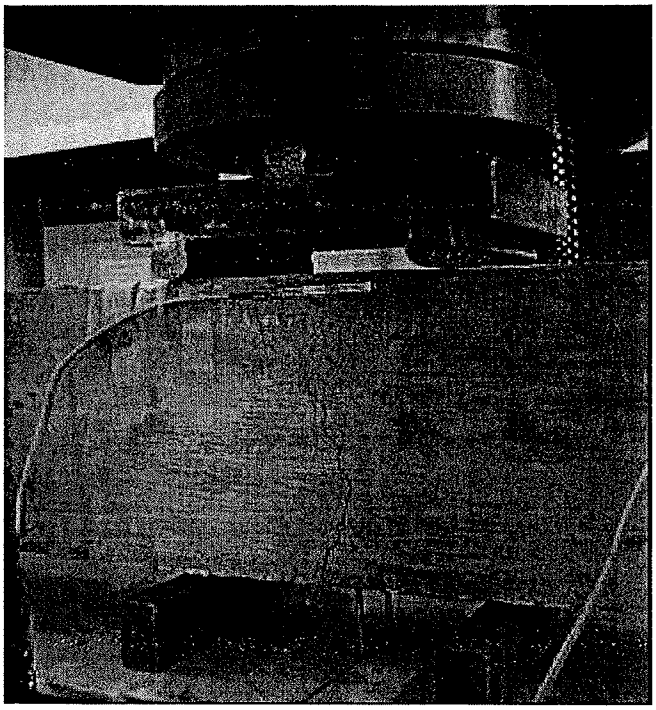

Photo 25: Another view of the flexural crack of concrete in the BRC –3 beam. Strain gauge can also be seen in the photograph.

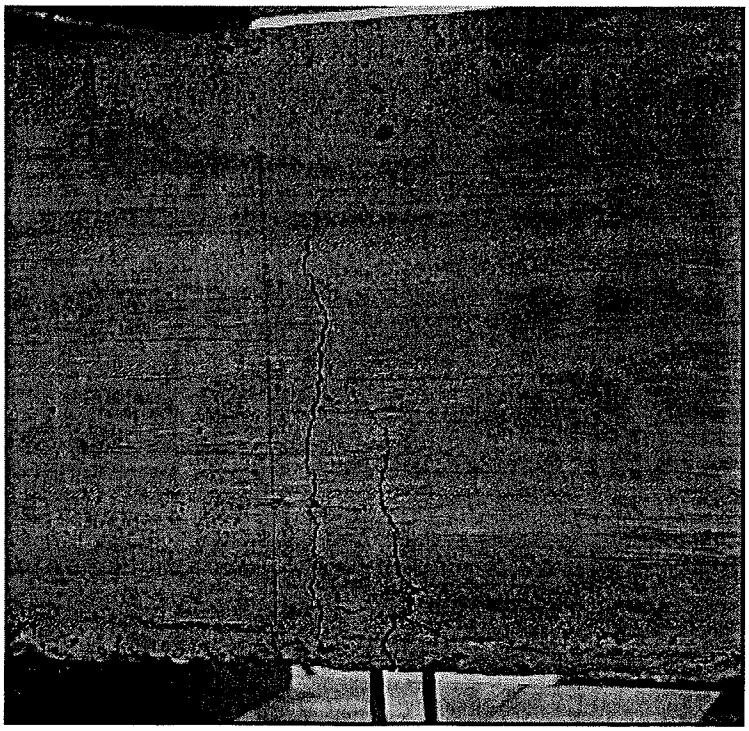

Photo 26: Flexural cracks on the other side of the BRC –3 beam.

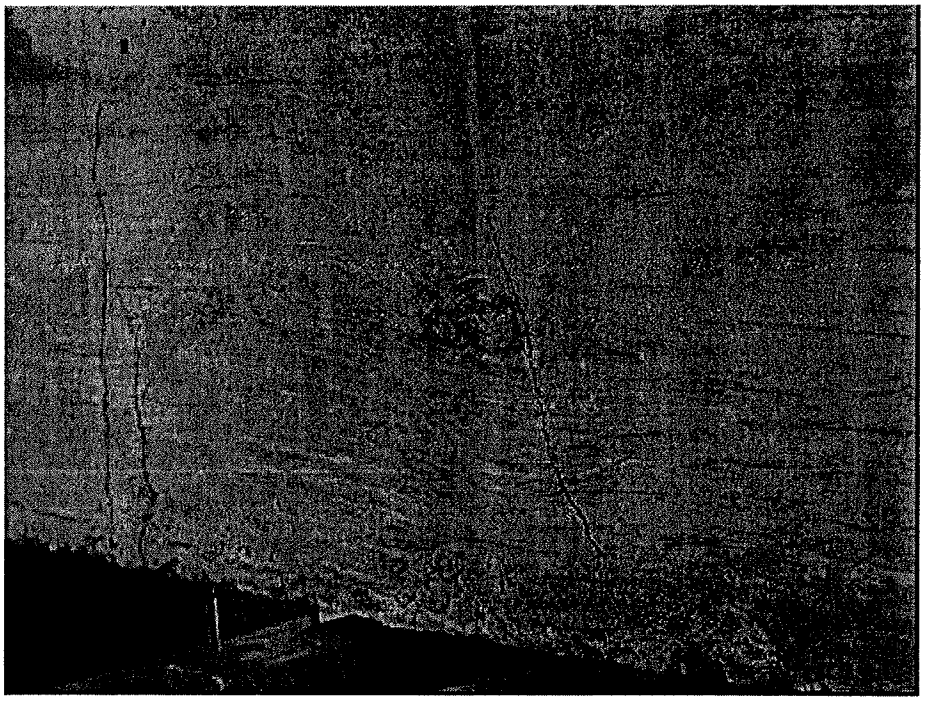

Photo 27: Flexural and shear cracks in the BRC –3 beam.

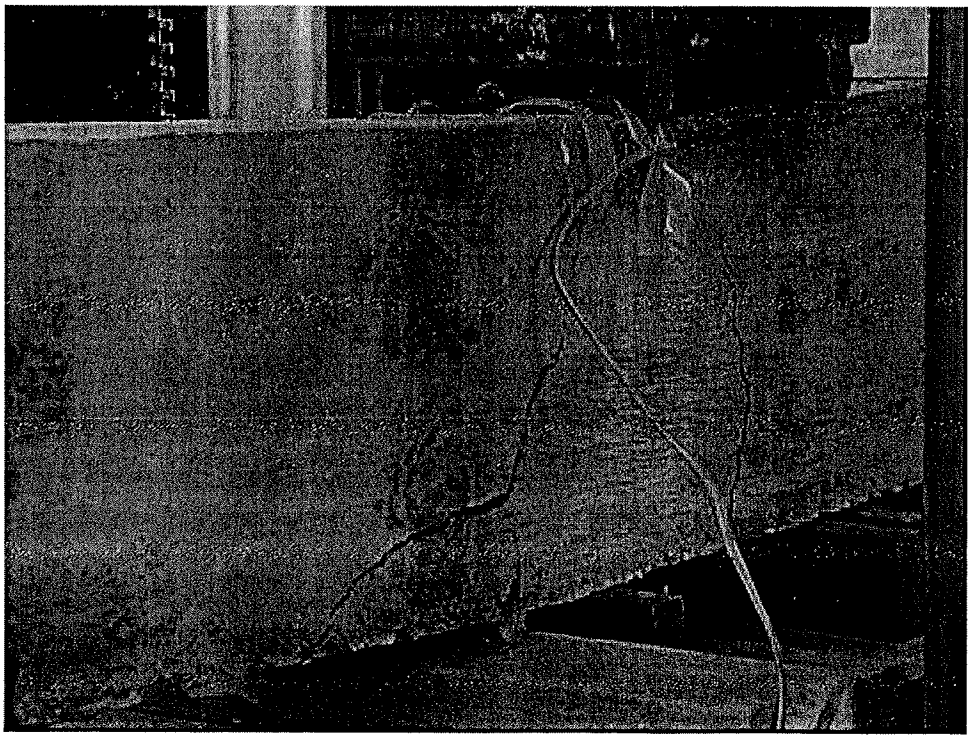

Photo 28: Close up of the shear crack in the BRC –3 beam.

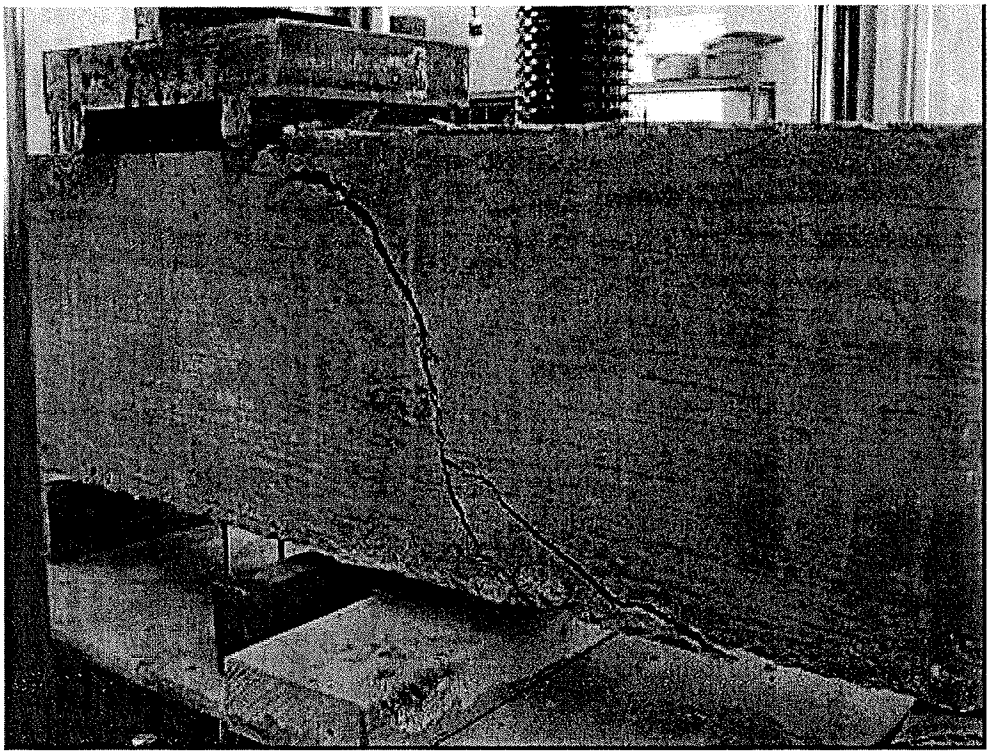

Photo 29: Shear crack on the other side of the BRC –3 beam.

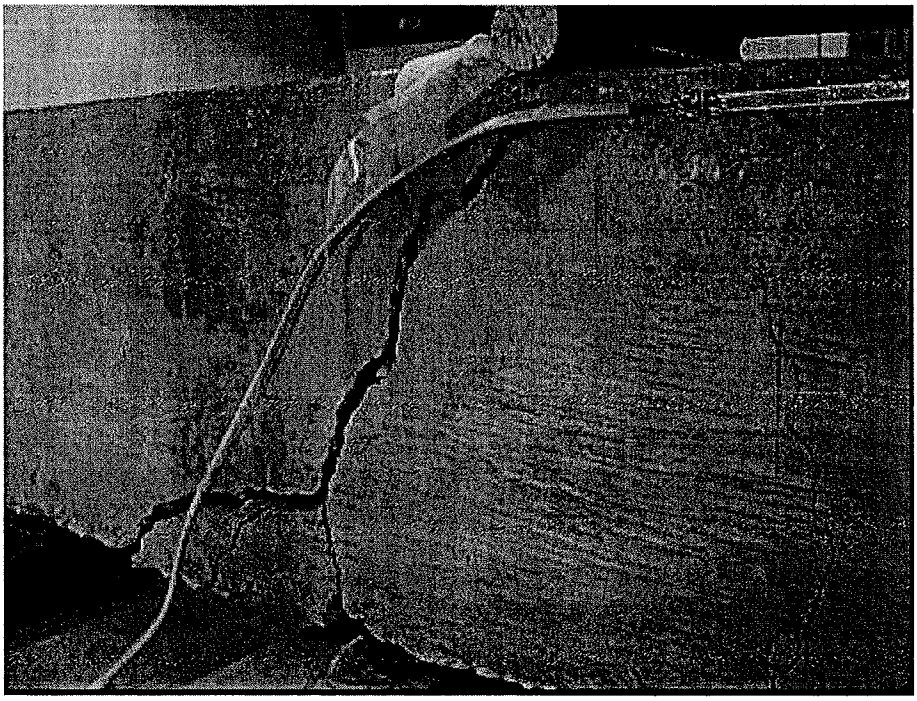

Photo 30: BRC –3 beam at failure, the photograph shows that the beam failed by primary flexural failure and secondary shear failure.

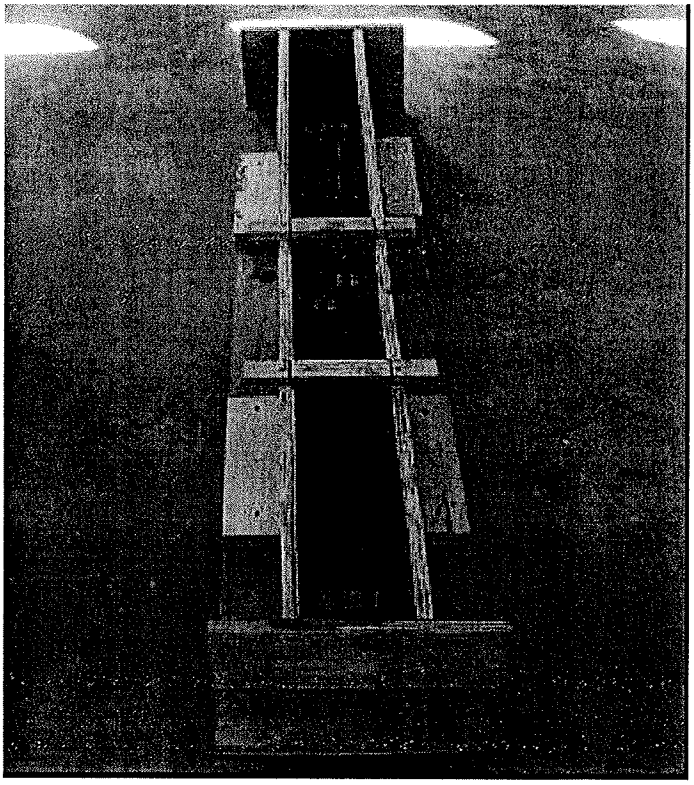

Photo 31: BRC –4 beam with two lab twisted cables. Each twisted cable was made by twisting three individual wires of 0.19 inch in diameter in the lab.

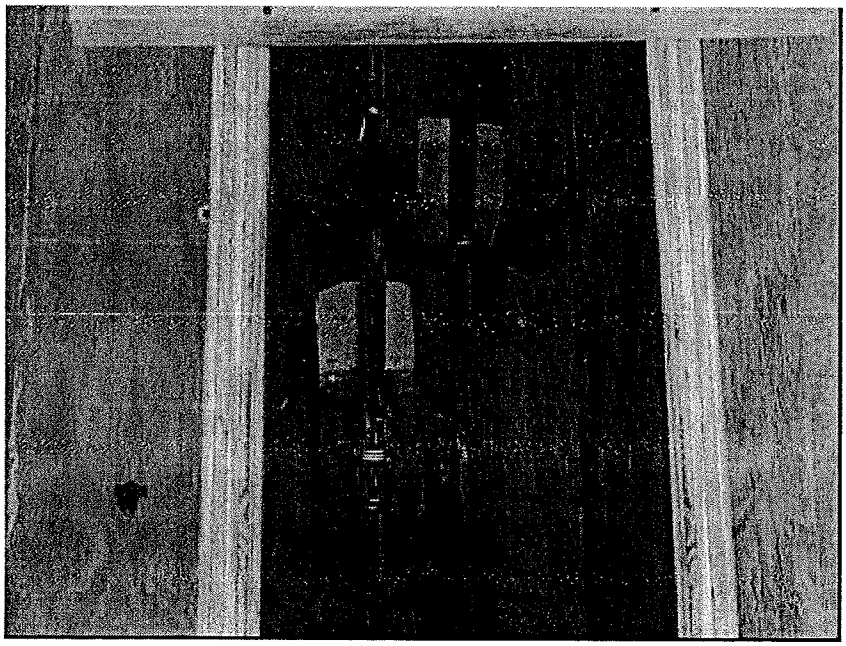

Photo 32: BRC –4 beam with two lab twisted cables, the bars are held in position by ties, and with cover blocks.

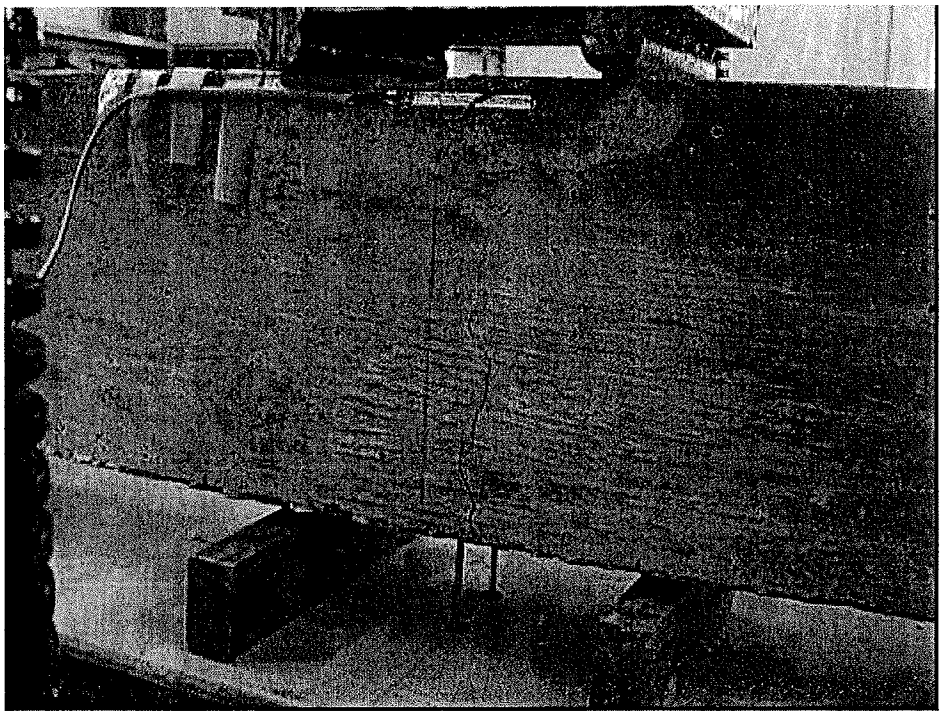

Photo 33: View of the flexural crack in the BRC –4 beam.

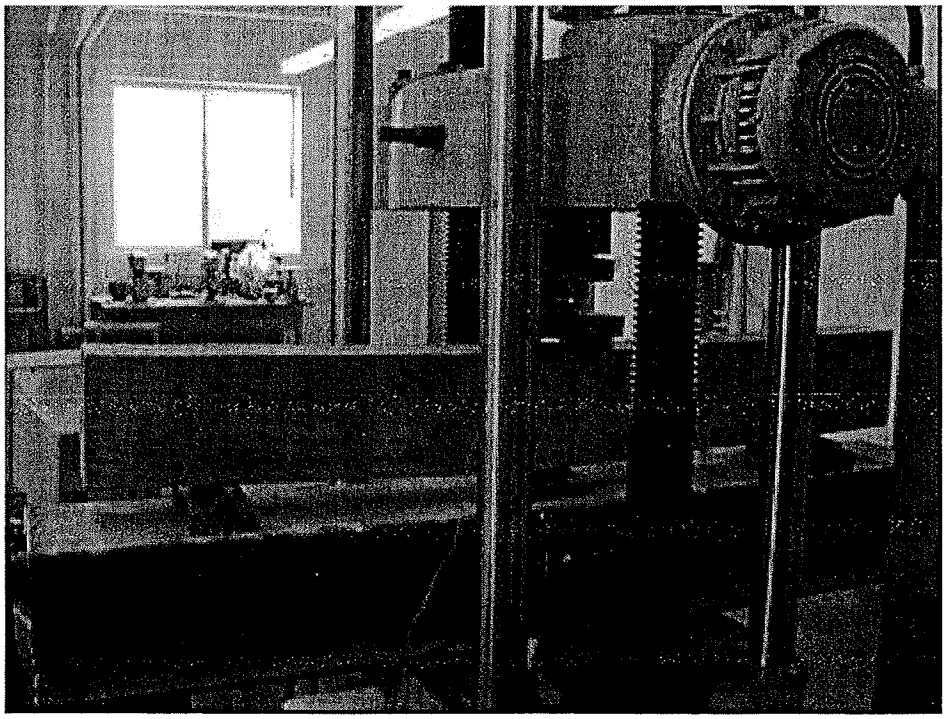

Photo 34: Deflected BRC–4 beam with flexural crack, still carrying load.

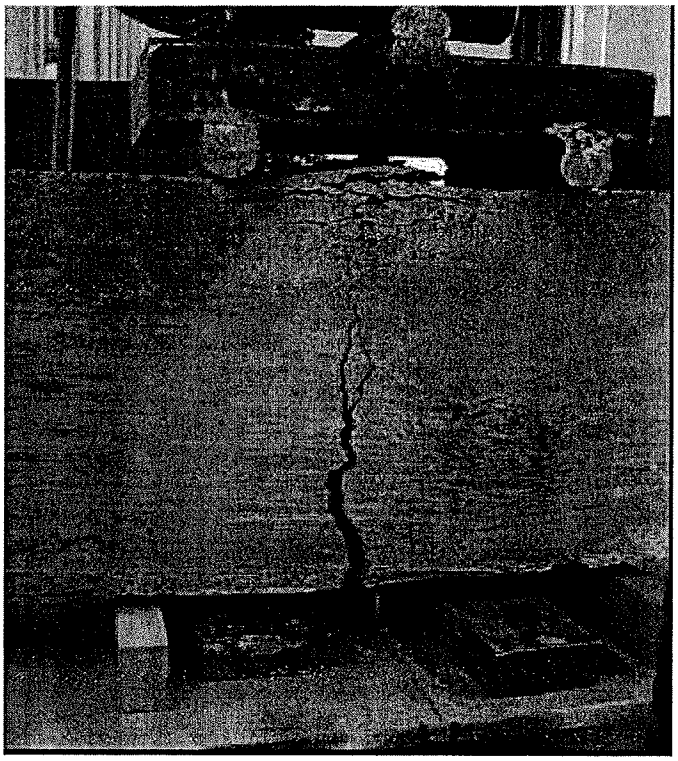

Photo 35: Close up of the flexural crack and crushing of the concrete in the BRC –4 beam.

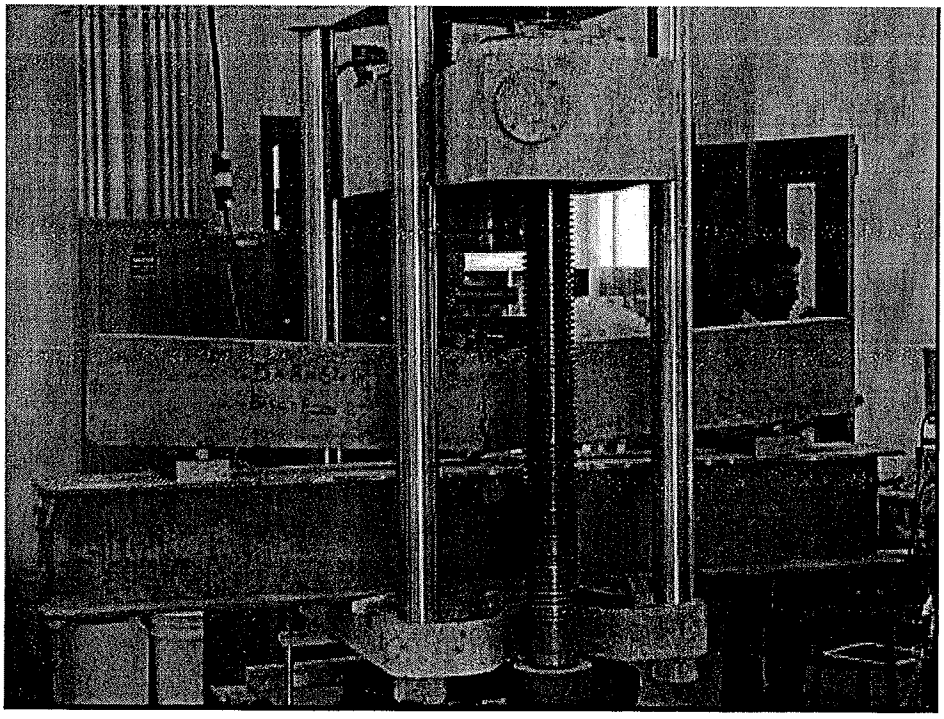

Photo 36: BRC–4 beam, at failure. The beam failed purely in flexure.

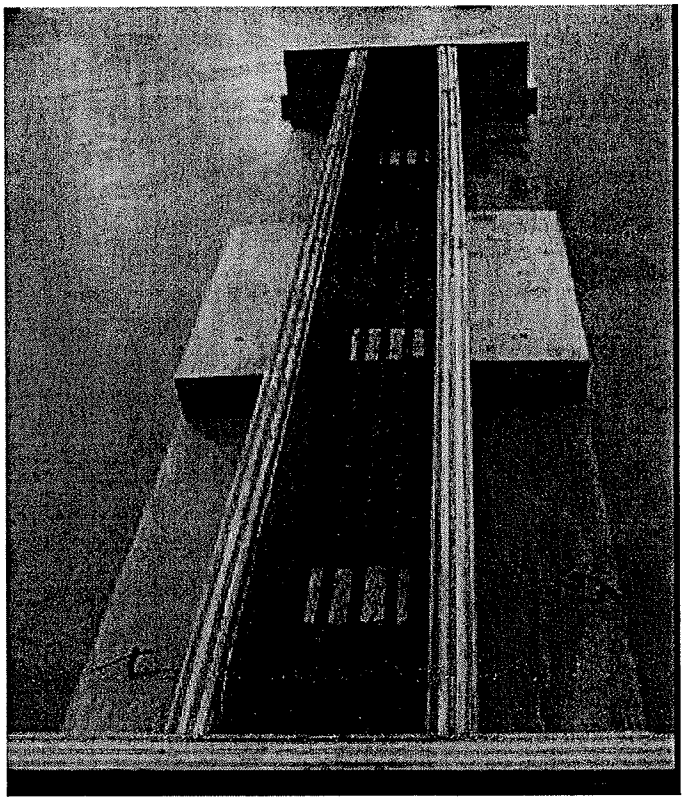

Photo 37: BRC–5 beam with three twisted cables ready for casting.

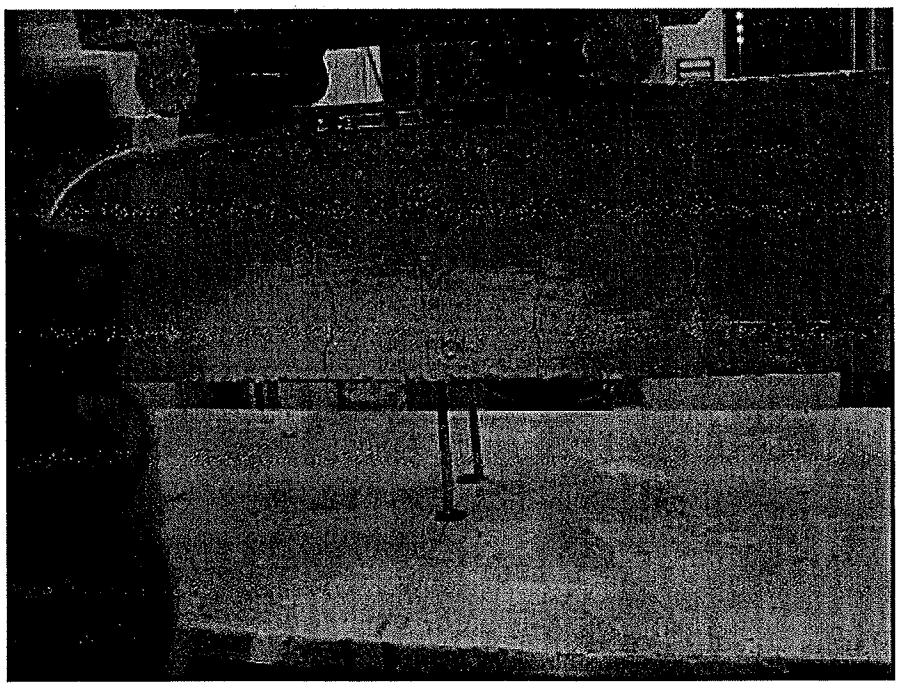

Photo 38: BRC–5 beam with flexural cracks. The picture also shows the loading arrangement, strain gauges and the LVDT's.

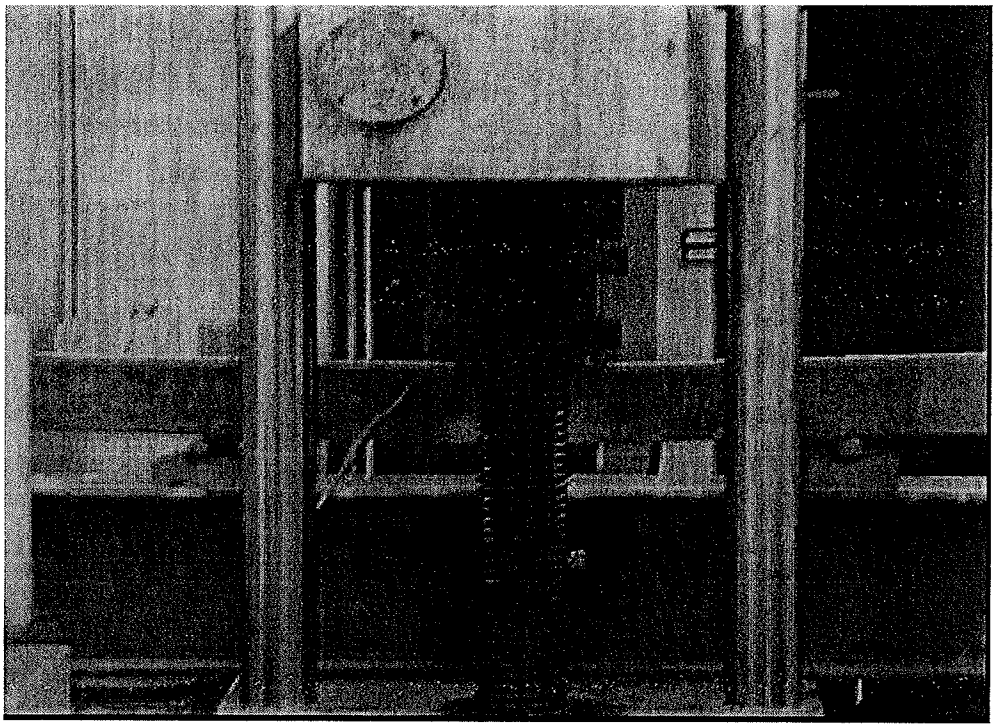

Photo 39: The deflected BRC–5 beam still carrying load.

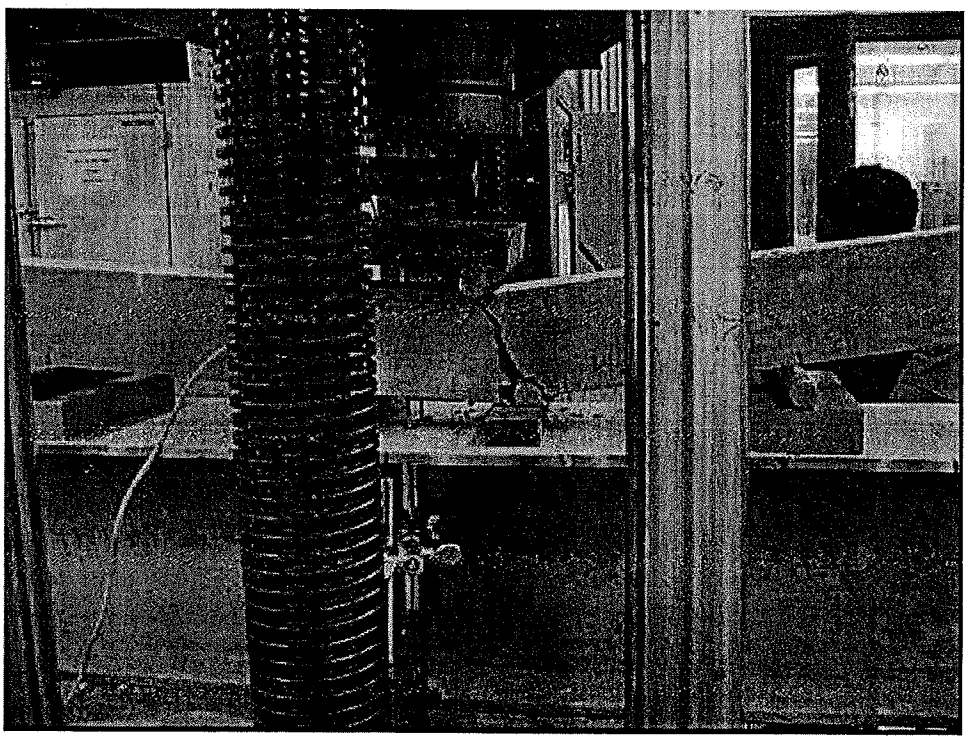

Photo 40: BRC–5 beam at failure, the beam failed primarily in flexure and secondarily in shear.

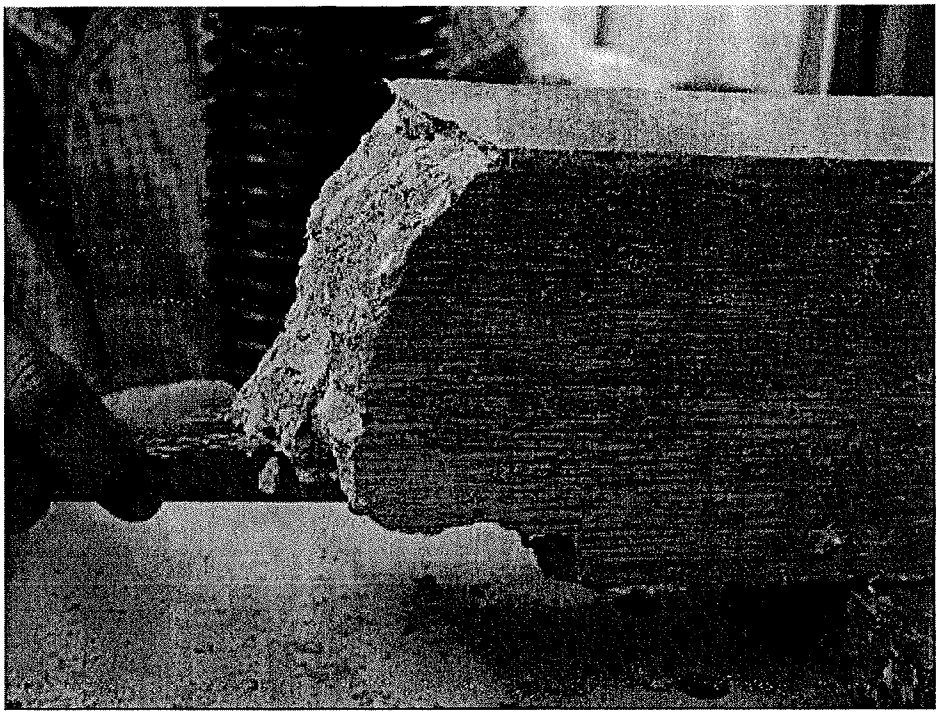

Photo 41: Fractured basalt cables, the cables had split into two indicating that there was a good bond between the concrete and the cable.

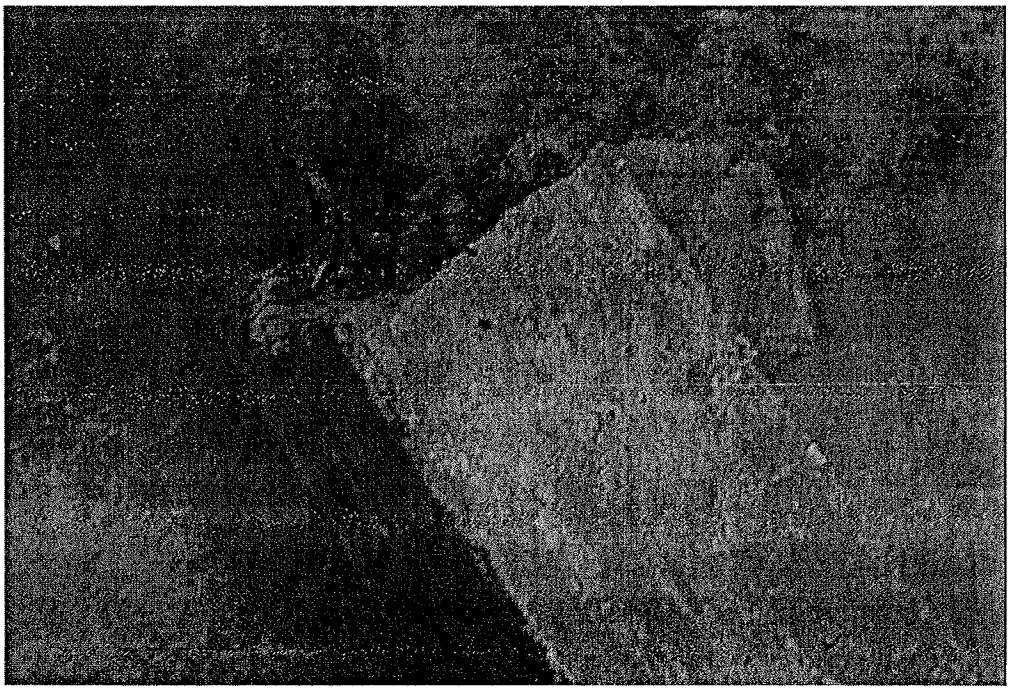

Photo 42: Another view of the failed basalt cables.

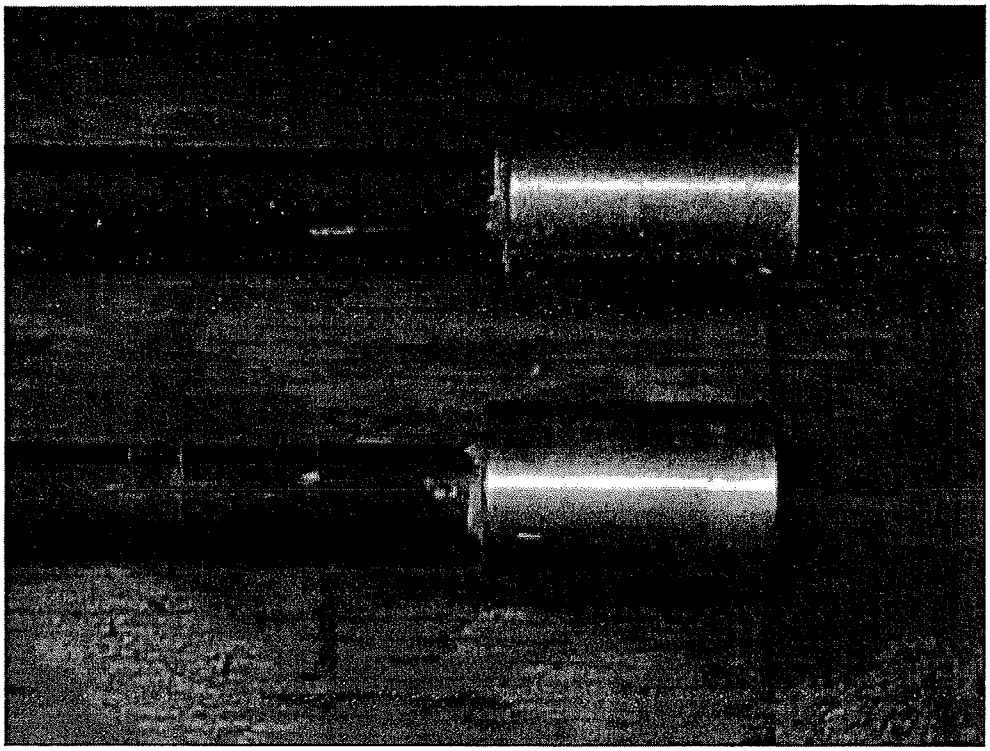

Photo 43: Close-up of the basalt rods with Fe-Mn-Ni anchors, one on each end of the bar for the BRC–6 beam. The anchors are smart alloys, which were provided to improve the bond strength.

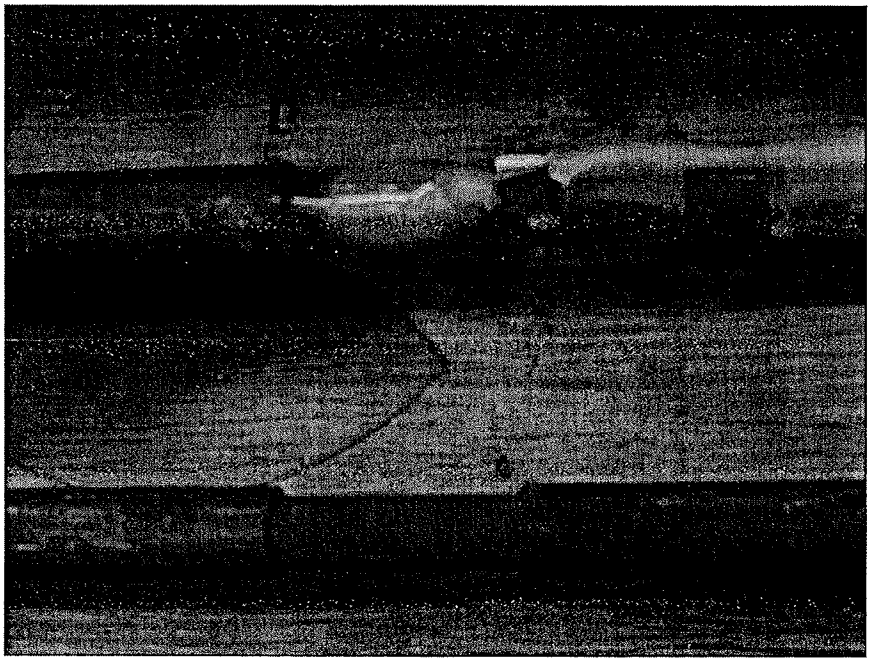

Photo 44: Strain gauge fixed to the basalt rods on the slots. Two slots were provided in each bar to improve the bond strength. The strain gauge was covered by epoxy to protect it from damages while casting the beam.

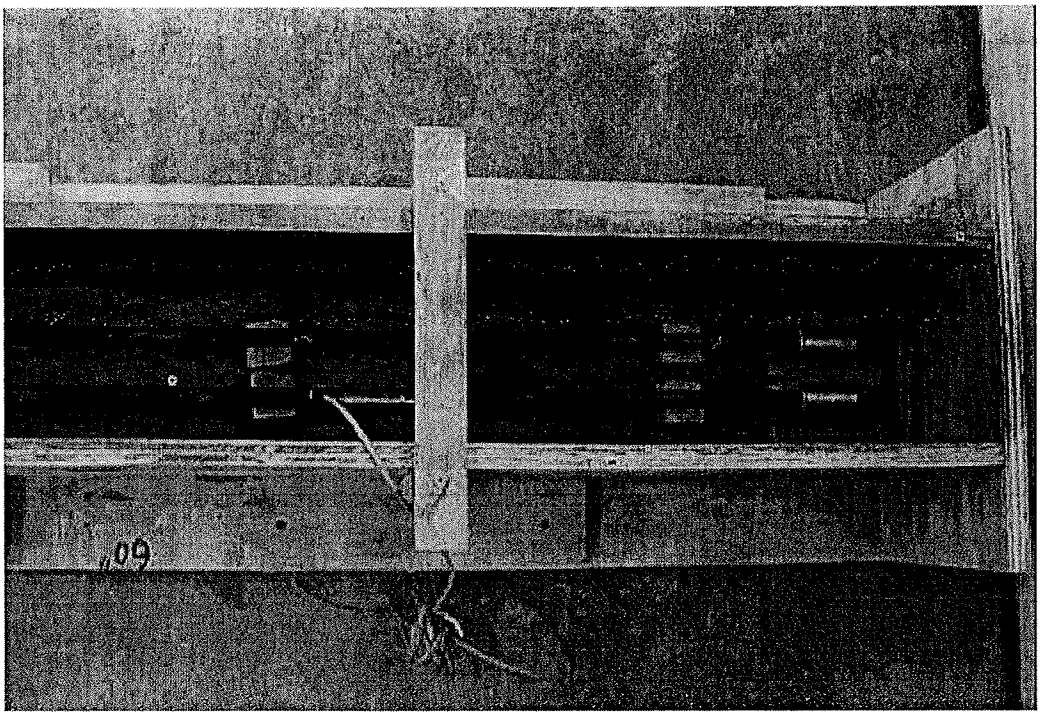

Photo 45: BRC–6 beam with basalt rods, fixed with Fe-Mn-Ni anchors and strain gauge, ready for casting.

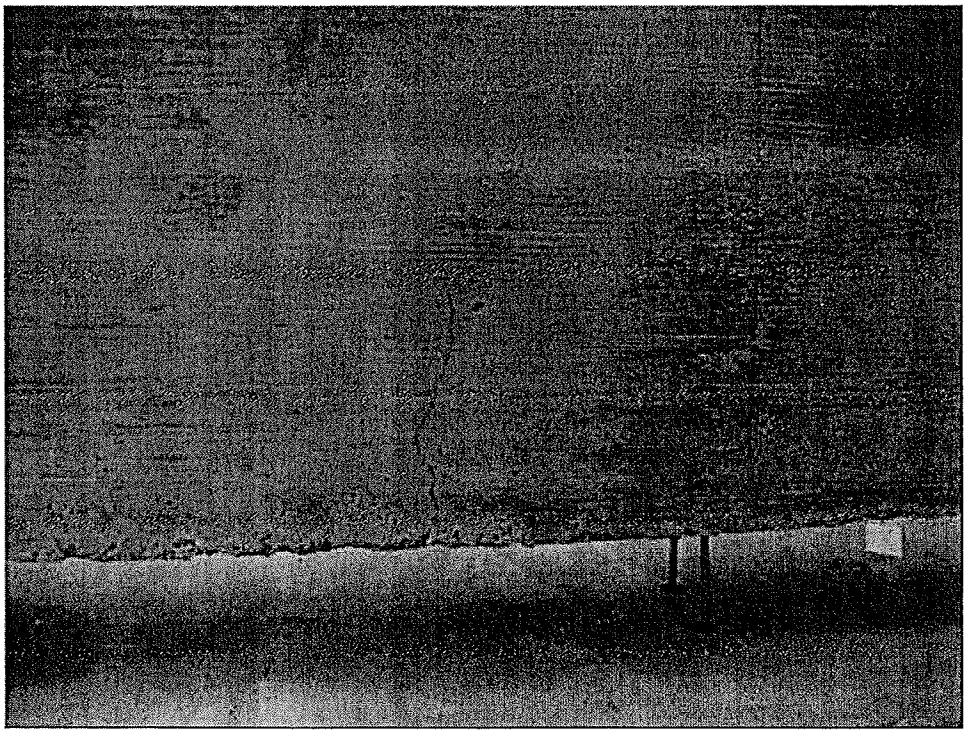

Photo 46: BRC–6 beam with flexural crack. LVDT's are also seen.

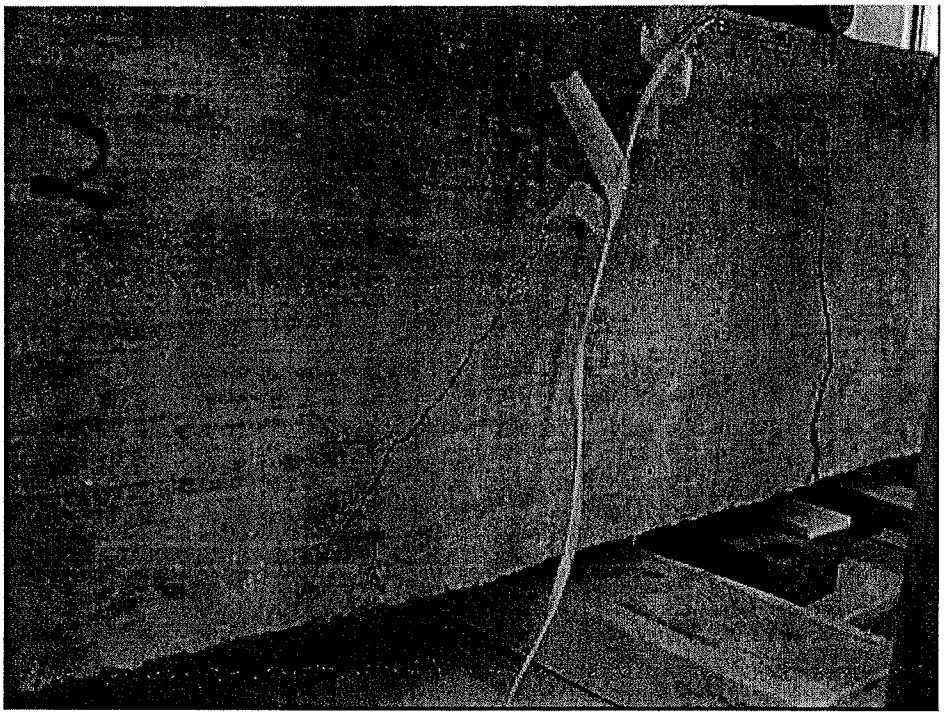

Photo 47: Another view of the BRC–6 beam with flexural and shear cracks.

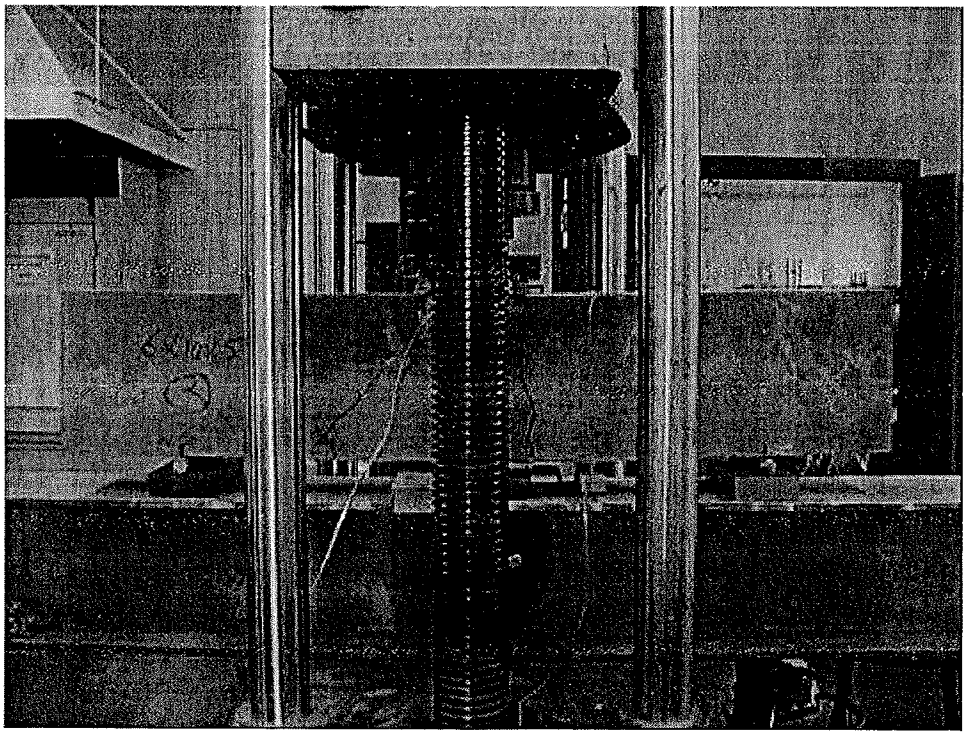

Photo 48: Deflected BRC–6 beam with flexural and shear cracks still carrying load.

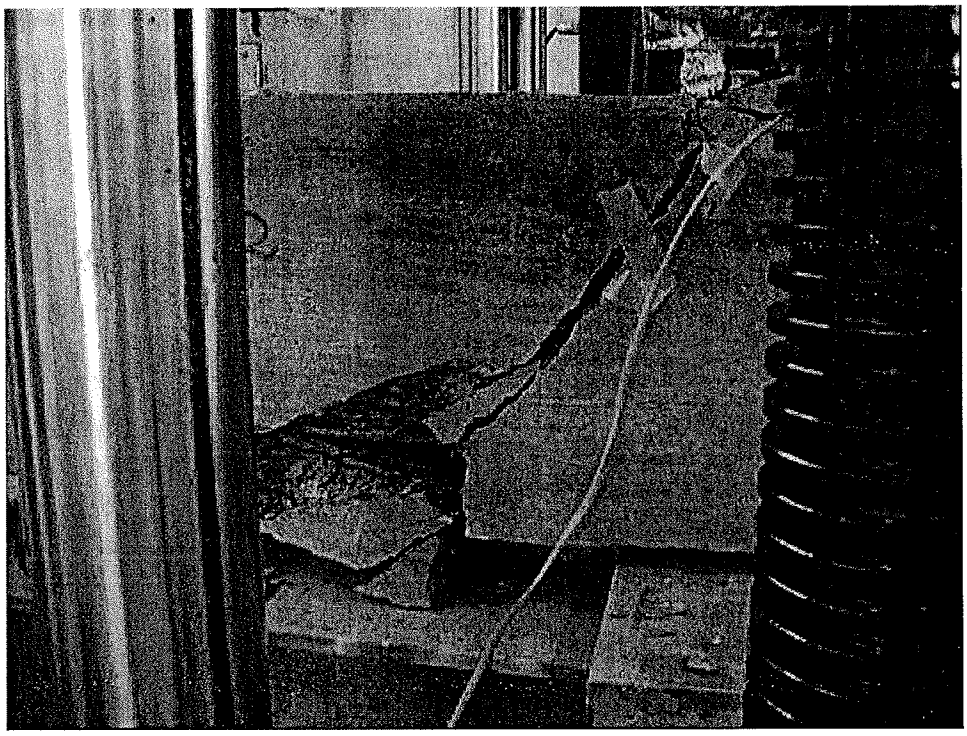

Photo 49: BRC–6 beam at failure. The close-up of the shear crack and the basalt rod are also visible.

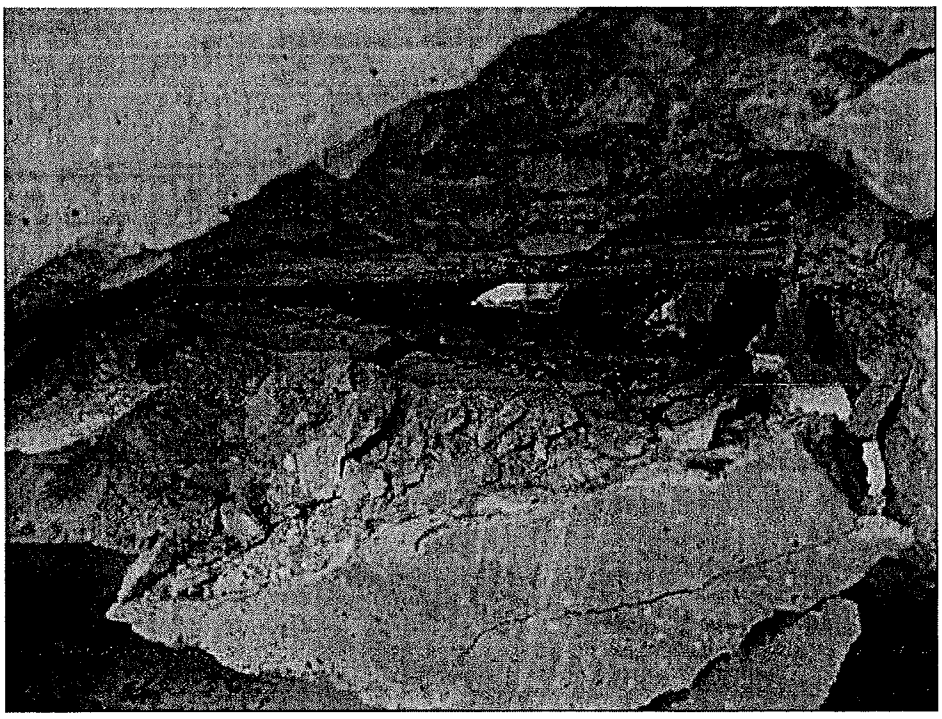

Photo 50: Close-up of the crack. The rod impressions in the concrete shows that the rod did not slip.

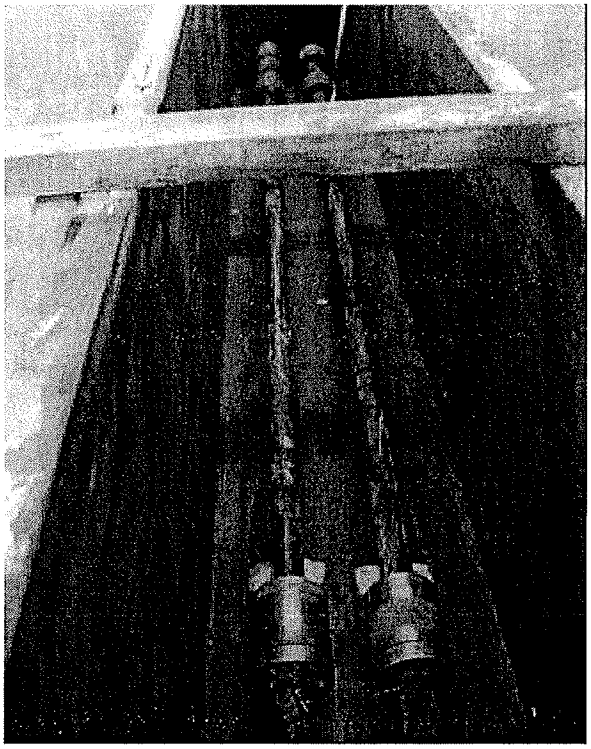

Photo 51: The basalt rods with TiNi (50/50) anchors for the BRC–7 beam. The bars were held in position by concrete cover and ties. Two slots (visible in the picture) were provided in each rod to improve the bond strength

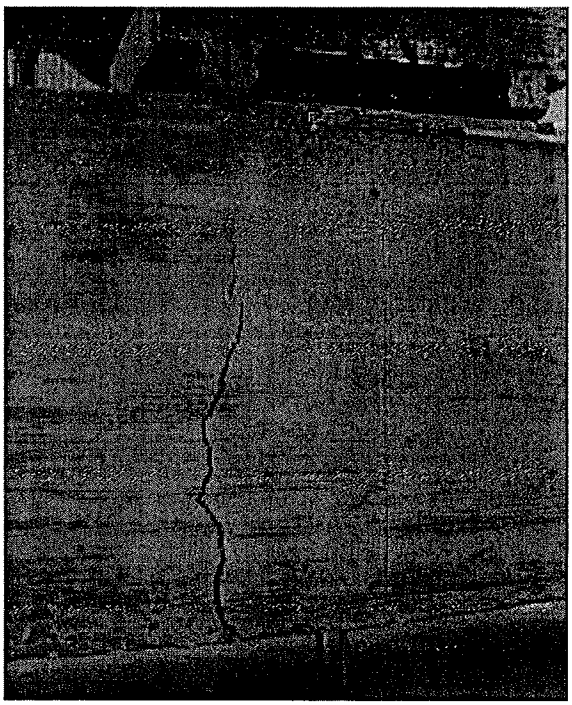

Photo 52: BRC–7 beam with flexural crack (first crack). The picture also shows the strain gauges fixed at the top of the concrete beam (compression side).

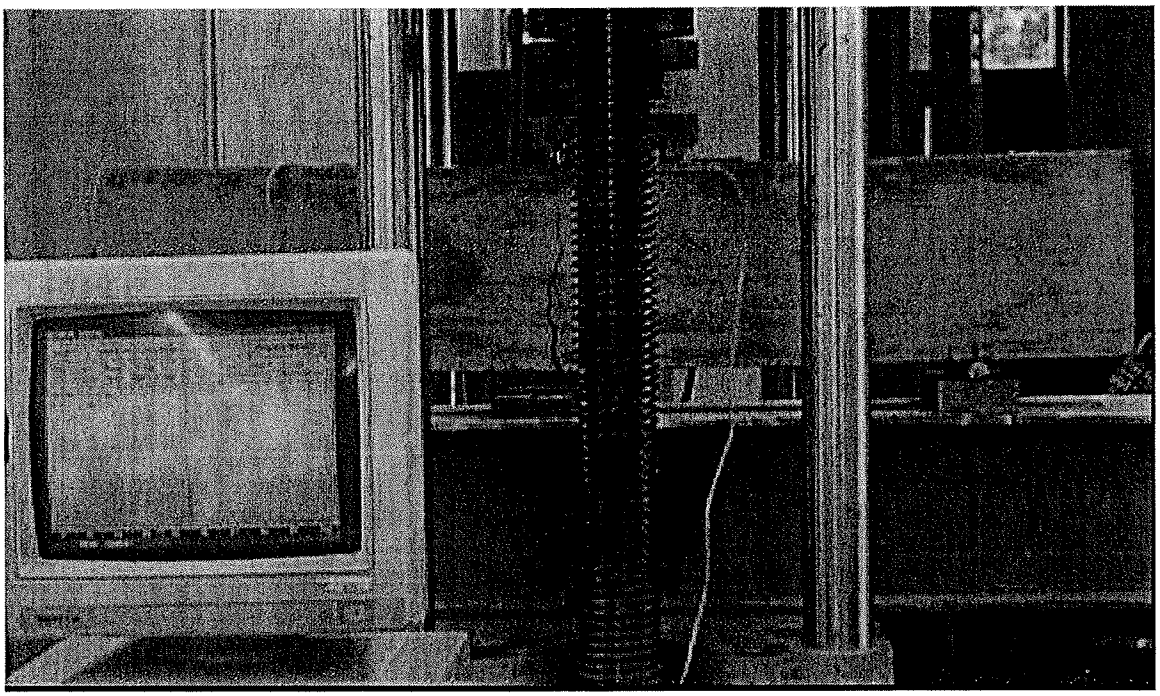

Photo 53: Deflected BRC–7 beam with flexural crack still carrying load. The MEGADAC data acquisition system for recording strain readings is also seen.

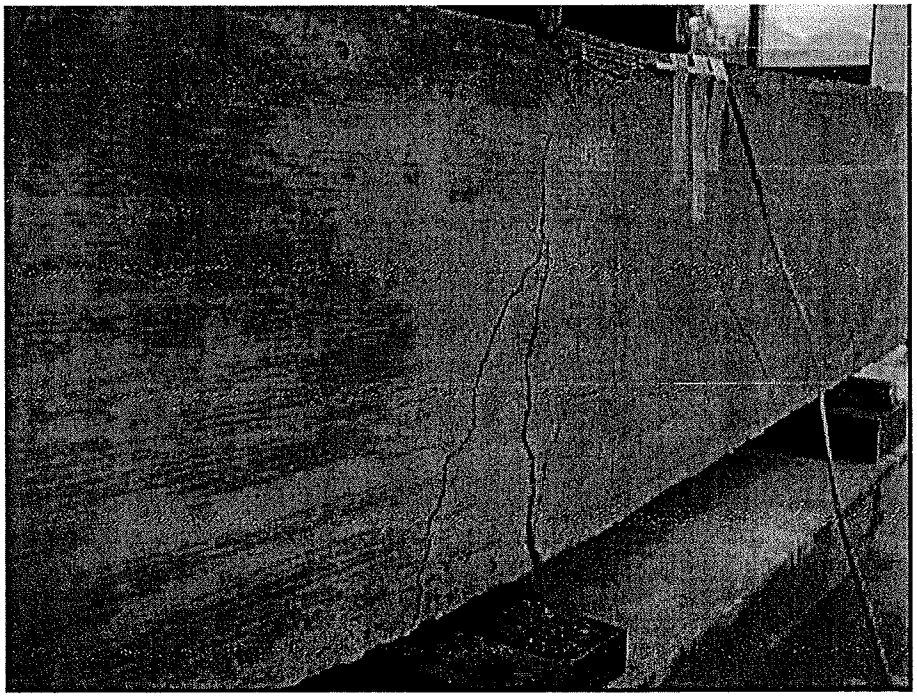

Photo 54: BRC–7 beam with flexural and shear cracks. The crushing of concrete at the point of loading is also seen.

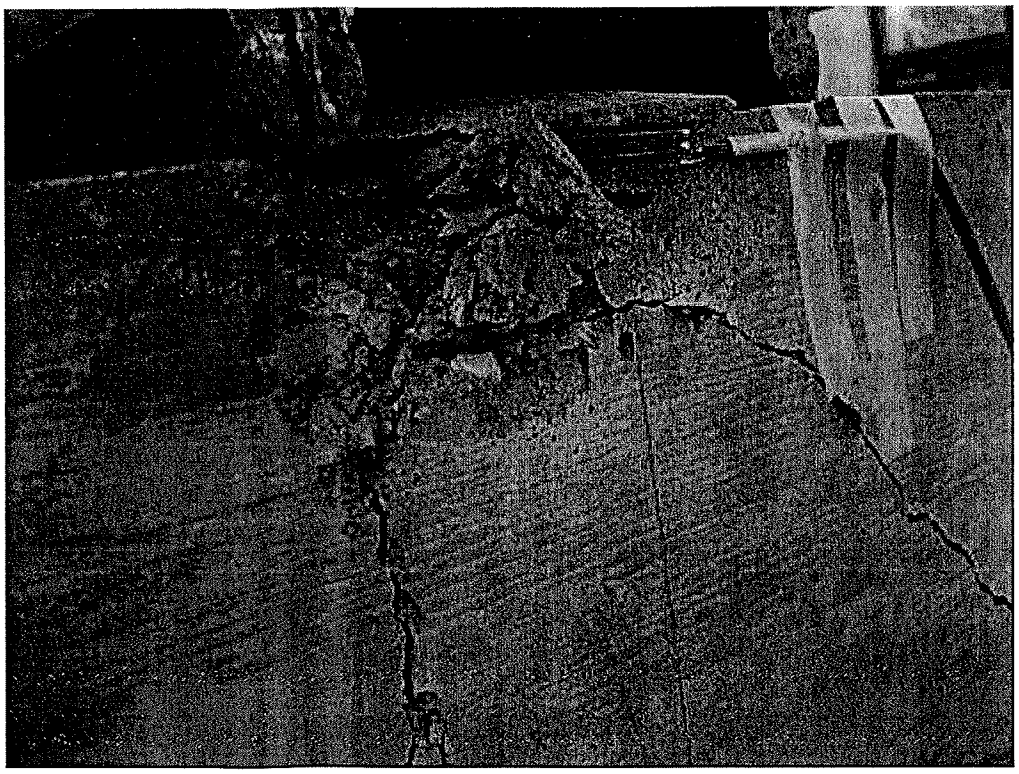

Photo 55: Crushing of concrete at the point of loading.

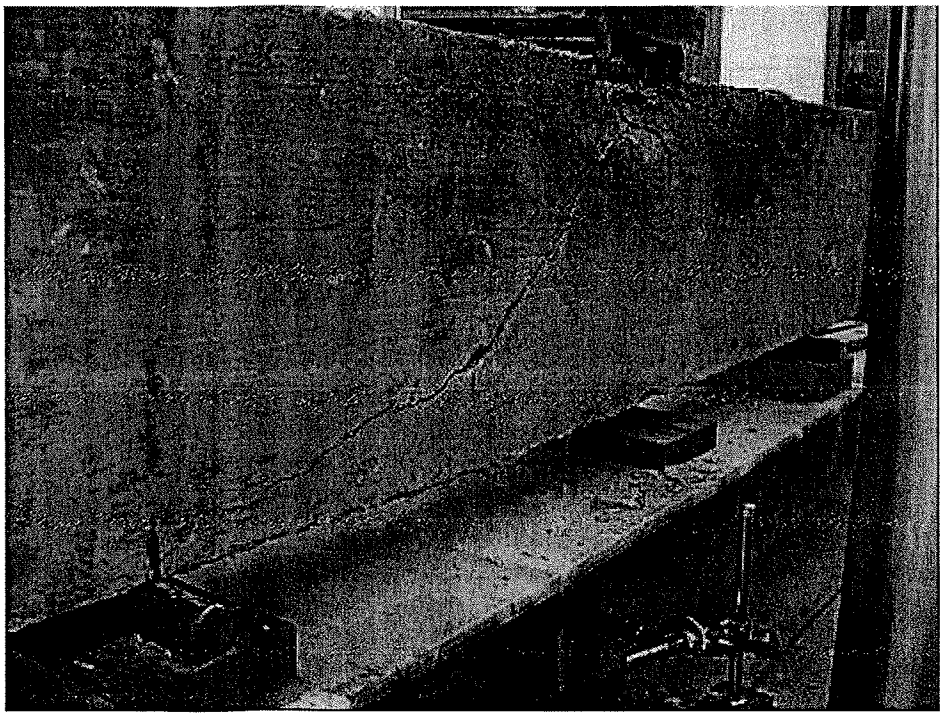

Photo 56: Shear crack in the BRC–7 beam with rods fixed with smart alloys anchors. The beam had failed primarily in flexure and secondarily in shear.